N. De Bruyn

Application of extreme value theory for the assessment of turret moored floating structures

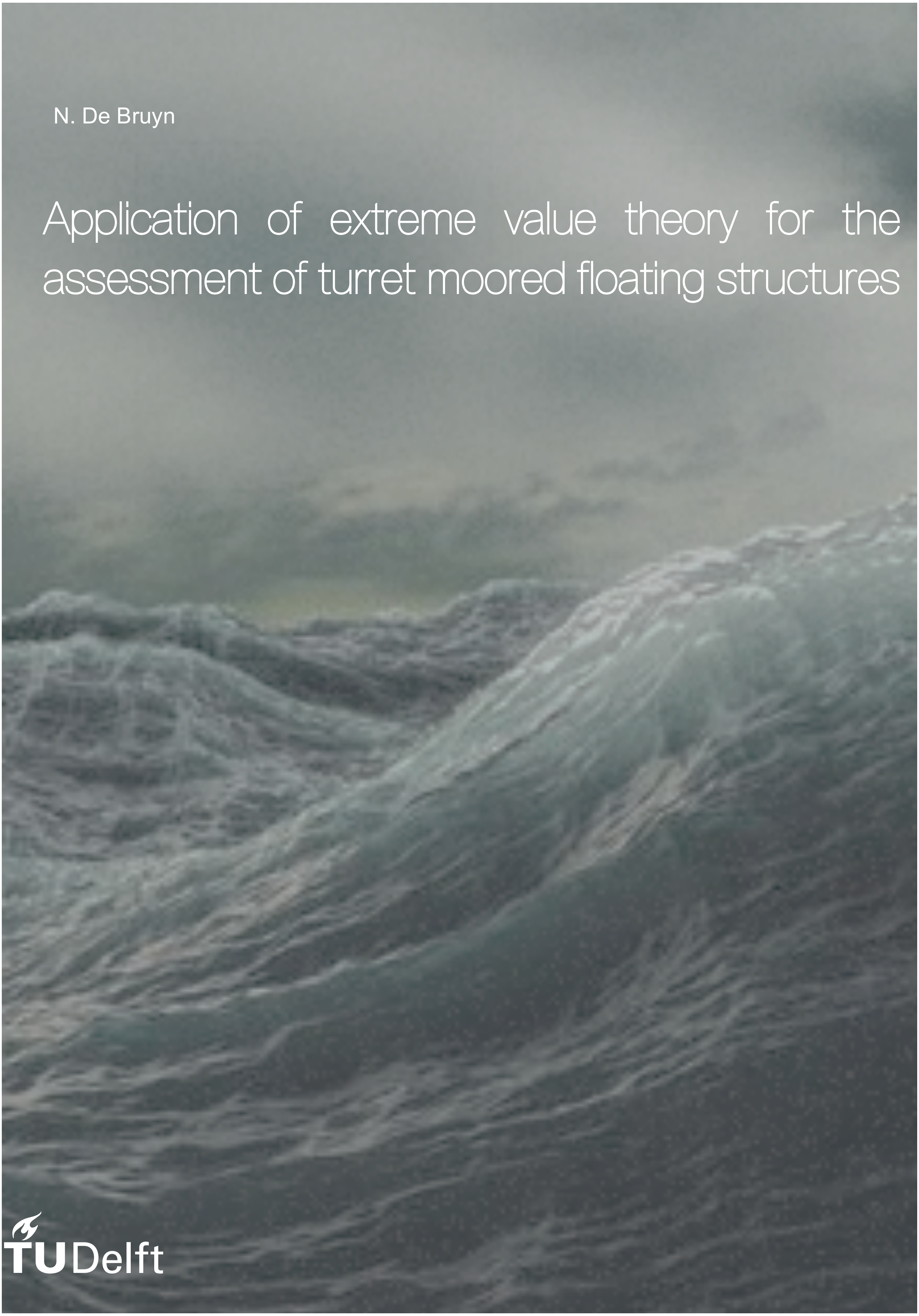

TU Delft

Application of extreme value theory for the assessment of turret moored floating structures

Thesis
In partial fulfilment of the requirements for the degree Master of Science (MSc.)

Committee

prof. dr. ir. R.H.M. Huijsmans	Delft University of Technology
prof. dr. ir. P.H.A.J.M. van Gelder	Delft University of Technology
dr. ir. A. Romeijn	Delft University of Technology
ir. R. Leeuwenburgh	Bluewater Energy Services B.V.

Nathan De Bruyn (4114272)

Master Offshore & Dredging Engineering: Floating Offshore Structures

Acknowledgements

First I would like to thank Bluewater to give me the opportunity and the resources to work on an assignment, that has the potential to be used in future design. It was a great motivational factor to know that my work will probably contribute to the design methodology used by Bluewater in the future.

Further I would like to thank Richard van Leeuwenburgh, Terry van Rossum and the other colleagues of the “mooring and subsea department” for the advice on the subject and the guidance on using the simulation software package Dynfloat.

I would also want to thank the committee for the steering and guidance during the interim evaluations and individual meetings.

At last I want to thank my family, who supported me during my entire study.

Abstract

In the design of mooring systems, it is a common practice to use a 100-year design environment to calculate extreme responses. Statistical inference is executed on the environmental data to produce a 100-year environment. This 100-year environment is then simulated to calculate the loads that occur when the vessel is under the influence of the 100-year environment. An alternative for this method is response based design. In response based design, measurements with a 3-hour interval of the environment over a long period of time are used to simulate the behaviour of the FPSO. The simulation provides a data-set of dominant loads for the mooring system over the time period. With extreme value theory the tail of this data is fitted on a distribution. With this distribution a 100-year extrapolation can be made that result in the 100-year extreme loads. This could result in a more realistic value of the extrapolated loads.

In (Oostra 2015) this method is applied for a specific case and extrapolated for one load parameter (Line tensions). In this thesis it will be studied if response based design can be used as a general tool to calculate reliable 100-year return levels for the dominant load parameters. This resulted in the following research question;

"Is it possible to apply extreme value theory in an efficient way during the design stage with the use of hindcast data for the assessment of mooring configurations?

First a method reconstruction is done to check the reproducibility of the applied methods and get a clear insight in the methodology. The three important steps in response based design are studied. First the raw data is filtered and prepared as an input for simulations. Secondly the simulations are performed. These are the response models which are the link between the environmental data and the loads. At last the post-processing is carried out where the data-set of dominant loads is fitted to a distribution and extrapolated. It can be concluded that these three steps do not lead to large differences in results compared to the traditional assessment.

The second step was to prove the robustness of the methodology. First an alternative simulation method is proposed to limit the needed computer resources. This alternative uses a quasi-dynamic simulation method. To prove the robustness of the methodology a parameter study is done. In this parameter study the extrapolations of several cases with variations in input parameters are studied. Most cases gave reliable extrapolations. An exception is the 3X3 mooring system which has a significant difference in mooring system stiffness for in-line and in-between-line translations. It is also noted that the accuracy of the fit depends on the arbitrary decisions made by the user during the process.

To limit these arbitrary decisions, the possibility of using a Generalized Extreme Value (GEV) distribution is studied. Monthly and annual load data is fitted to a GEV distribution. This resulted in reasonable extrapolations and passed all goodness-of-fit tests for the annual data. In comparison with the conventional method the extrapolations where approximately 30% lower. The monthly data didn't result in a reliable fit. To produce reliable extrapolations with monthly data, time dependent parameters need to be included to compensate for the seasonal variations.

The final step was a case study. In this case study extrapolations for all dominant load parameters for a 3X3 mooring configuration are obtained. Four variations of the mooring system are studied. For all four variations good extrapolations are produced. It can be concluded that the performance of the methodology isn't influenced by the individual mooring line make-up. For four out of five dominant load parameters reliable extrapolations are obtained. Extrapolations for the horizontal offset are less reliable due to the difference between in-line and in-between line stiffness. This problem can be coped with if directionality is included. To include directionality, the mooring configuration is divided into several sections. For these sections 100-year return levels are calculated individually.

The overall conclusion is that it is possible, for an experienced user, to efficiently produce reliable 100-year extrapolations for four out of five dominant load parameters with straightforward extreme value theory in a design stage. For horizontal offset it is also possible to produce reliable extrapolations if more complex methods like directionality are included.

Table of Contents

List of figures

List of tables

1 Introduction

Classification society requires that the design of a mooring system for long-term application like FPSO's is based on not less than a 100-year recurrence interval of the environmental conditions (DNV.GL 2015). The common practice in the industry is to create a 100-year maximum for all different environmental parameters. The combination of all of these 100-year environmental parameters forms the design conditions. This is a misinterpretation of the reality and could lead to an overestimation of the 100-year loads on the mooring system, to deal with this more detailed assessments are performed to derive associated wind, wave and current. In this thesis a complete different approach for this method will be presented. This alternative is response based design, extrapolation of measured or simulated loads on the mooring system will be executed with the use of extreme value theory. This is studied by (Oostra 2015) for one specific case and one load parameter.

The results of this study were promising but are only studied for one specific case. In this report it will be studied if it is possible to apply response based design for all dominant load parameters and for various design choices. Also the robustness of the method, and an alternative distribution will be studied.

This will lead to conclusions about the possibility of using extreme value theory in a design stage to produce reliable and realistic 100-year return levels.

First the previous work will be studied. In this chapter the theory behind response based design will be presented. The simulation method will also be discussed.

Secondly the research question is presented and a method reconstruction and validation will be done, this to assure that the applied methods are without errors.

The third part will include a robustness study to check if the methodology is applicable for multiple load parameters and various environmental conditions and still produce reliable extrapolations.

The fourth chapter concerns the case study which is executed. In this case study different mooring system designs are studied for a 3X3 mooring configuration. This gives the possibility to study the influence of different design choices on the methodology.

The final part of this thesis includes the overall conclusions and the recommendations for further studies around the use of response based approach in mooring design.

2 Research question

A research question is formulated after thorough analysis of the work done by (Oostra 2015), (Tromans et Vanderschuren 1995) and (Battjes 1979).

This previous work discusses the potential of the response based approach to incorporate the environment in a more elegant way. (Tromans et Vanderschuren 1995) present two alternatives to use response based methods in the calculation of extreme return levels. The first is a complex method to produce a more realistic 100-year environment by including joint statistics of all environmental variables and the other is to apply extreme value theory on load responses as studied in (Oostra 2015). In this technique statistical inference is performed on load data and not on environmental data.

This as a possible alternative and verification method for the conservative methodology that is a common practice in the industry. Considering the needs of Bluewater for a helpful tool that can be used in an efficient way during the design stage to calculate reliable return periods for load data oriented for single point mooring systems. The research question is formulated as follows.

"Is it possible to apply extreme value theory in an efficient way during the design stage with the use of hindcasted metocean data for the assessment of mooring configurations?"

3 Study of previous work

In this chapter a review of the work on the subject of response based design will be discussed. A part of this chapter will be an overview of the methodology proposed by (Oostra 2015), another part will be a description off the underlying theory. Primary a review of metocean practices will be given and secondly a general overview of the proposed methodology with conclusions made, and some recommendations.

3.1 Metocean data

The definition of 'metocean' according to the society of petroleum engineers is:

"A contraction of the words 'meteorology' and 'oceanology' referring to the wave, wind and current conditions that affect offshore operations."

In essence metocean data for a specific place gives a detailed description of the environment at that specific place including wave, wind and current data. This data can be used to define the design parameters to assure long-term resilience of offshore structures. In the ideal case one would have multiple years of site measured metocean data to validate and supplement a long-term metocean time-trace. Due to cost intensity of such site measurements and limited time-windows to perform studies, experts usually resort to only a very limited time frame of site measurements. Sometimes only metocean time traces constructed by numerical modelling are available.

The metocean numerical model consist out of three smaller models forming together a composed model which delivers a full description of the ocean environment. These three models are an atmospheric- and wind-model, a wind-wave model, and a current model. Metocean models can be used to forecast ocean environment as well to hindcast the environment. In hindcast models, measurements of the real environment are used as boundaries for the model. In essence the model will use these as reference points to hindcast the waves, wind and current. In this way the reliability of the hindcasts is improved. Based on these hindcasts, 100-year return levels can be calculated to be used in engineering.

The accuracy of the results from these models highly depends on the performance of the model. This is covered comprehensively by (Oostra 2015). In this thesis the metocean data will only be used as an input parameter. The correctness of this data will influence the final calculated values. It is important that the available data is of high quality to be sure that the calculated responses are reliable representations of the reality.

3.1.1 Conclusions metocean practices

The main conclusions to be considered when metocean data is used to calculate extreme return levels are listed below (Oostra 2015).

- Metocean data could be more suitable to extreme events if the focus was on extremes and not on a broad representation of the environment.
- Some events are missed out by models (polar lows, cyclone events...).
- Unquantifiable risk of accumulated error (model 2 uses results of model 1).
- Model performance need to be verified for the extremes, not for the bulk of data.
- Models work within boundaries. This fills the holes in our understanding of the real phenomena behind the environment.
- IID (independent and identically distributed) assumption is incorrect.
- Data is validated in a decoupled manner (wave steepness (combination of wave height and period) is important).
- Directionality and reliability of extrapolations are underexposed.
- Length of time traces is to short (30 years of data for 10000-year extrapolations).

3.1.2 Recommendations Metocean practices

In this section recommendations presented in (Oostra 2015) are listed.

- There is information coming from metocean models that is not supplied in metocean reports that could be very valuable in engineering design. Examples of which are, more detailed information during extreme events, but also the information on spreading, directionality and wave-grouping are good examples.
- More effort should be put in verification of metocean models for wave-height and –period at the same moment. This combination (wave steepness) is very important in engineering design.
- In validation and verification of metocean data more focus should be put on the extremes.
- Though directional measurements are scarce, validating model performance in a few characteristic geographical locations would considerably increase the trust we can put in the directional information supplied with extremes.
- More research on how scatter indices of the separate models and methods influence the extrapolated extremes would greatly enhance our understanding why in specific regions there are more failure cases than in others.

3.2 Response based approach

In this section a methodology will be presented that makes use of fitting response data to a generalized Pareto distribution (GPD) to extrapolate extreme return levels. To calculate an extreme return level with the proposed methodology (Oostra 2015) 3 steps need to be taken. First pre-processing to analyse the environment and to select the environmental data that will lead to extreme events. Secondly the simulation, in this step the environmental data will be used as an input in a simulation model to generate responses (loads). Finally, these responses can be fitted on a distribution and extreme return levels can be calculated. These three steps will be discussed in the following paragraphs. Also a general introduction of response based design will be given.

3.2.1 Introduction

(Tromans et Vanderschuren 1995) The conventional method to obtain extreme load events is to fit hindcast series to a distribution and extrapolate this to obtain a design sea-state. With this sea-state the extreme loads can be calculated with a response model. With this method, to calculate extreme return levels, the influence of the present environmental conditions on the uncertainty of the extreme wave of a sea-state is neglected. An alternative to this method is response based design. In response based design two categories can be seen. The first are responses that are produced, with a load/response model, from metocean data over the total period of the hindcast. This produced set of loads can then be fitted to a distribution and extrapolated for the wanted return level. The second (Coles et Tawn 1994) is a complex method of performing joint statistics of all metocean variables to obtain a design sea-state. This design sea-state is a better representation of the reality and will results in a more reliable extrapolation.

The conventional method will lead to an over estimation of the return level because it is assumed that extreme wind, extreme wave and extreme current occur at the same moment and come from the same direction. The first category of response based design, fitting responses to a distribution, will be used in this thesis.

Instead of performing statistical inference on metocean data to use these to develop the relevant design cases, we will calculate responses from raw metocean data and perform statistical inference on this to obtain 100-year extreme events. The steps of the applied method are listed below.

- Metocean data is obtained from measurements with 3 hourly intervals.
- defining high Hs threshold that results in a I.I.D (Independent and Identically Distributed) data set
- using environmental parameters above threshold in the load/response model (Dynfloat)
- fit response values to a Generalized Pareto Distribution
- set a second threshold above where the parameters become stable
- verification of the distribution (visual comparison, bootstrap, goodness-of-fit)
- extrapolation to the required return period

The conventional method results in more conservative extrapolations; the proposed method will give a better representation of the reality.

3.2.2 Pre-processing

Pre-processing includes all steps needed to select the appropriate environmental data that can be used as an input for the response model.

The 5-month analysis

Because it is impossible to simulate all sea-states that are measured for a hindcast (5-50 years) we need to make a selection of the hindcast data which is responsible for the high loads that are in the tail of the distribution. To achieve this, we need to get a good insight in the environmental phenomena that results in the highest loads. A period of 5 arbitrary winter months is modelled and analysed (Oostra 2015). With this information a data selection scheme could be developed to reduce the need of computational resources while assuring that all phenomena, resulting in high maximum average line tensions, are included.

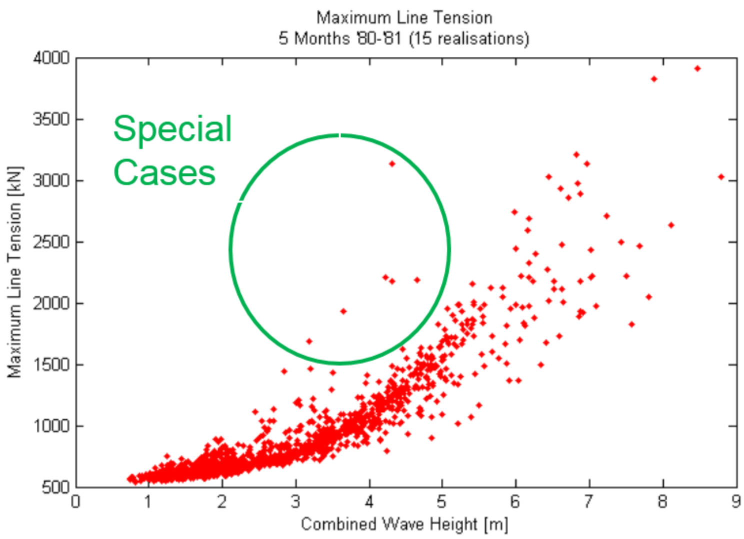

Figure 3-1 AVG MAX LT versus wave-heights for 5-month analysis (Oostra 2015)

In Figure 3-1 two groups can be identified. These two groups result in maximum line tensions above approximately 2000 kN. First the group with wave heights higher then 6,5m. Here the wave height is the governing phenomena behind the high line tensions. The second group consist out of some special cases. In these special cases the wave height is not the governing phenomenon that results in high line tensions. (Oostra 2015) concluded that the phenomena governing the special cases are:

- Sea-states with considerable angles between wind and waves, resulting in an angle between equilibrium-heading and waves. (directional-cases)
- Sea-states with two wave systems, resulting in an angle between equilibrium-heading and the dominant wave-system. (swell-cases)

Besides these two phenomena wave-steepness is also something to be considered. It doesn't come forward in the analysis but, waves with a short period can result in higher loads in comparison with sea-states with waves of the same height but with a longer period.

3.2.3 Selection and realization of sea states from 30yr Pierce Field hindcast

The information gathered in the previous section (Oostra 2015) produced 2 main data sets. These two datasets are again divided into two sub datasets with some differences between them. This results in 4 individual datasets.

Threshold selection is one of the most important steps in the process of finding a 100-year return level. After a 5-month analysis several wave-height thresholds are applied and it is checked if these thresholds "catch" the max LT events defined in the previous section. Some special cases that aren't included by the threshold are manually added to the set of data to improve the set and to be sure that all MAX load events are included.

The first main dataset (I.I) is created from the metocean data by setting a threshold value of 5,5m, for dataset I.I this resulted in 441 sea-states with a combined wave height of 5,5m or higher. To ensure that these 441 sea-states are IID (independent and identically distributed, ie. originating from well separated storms) a separation time of at least 48 hours is required. In essence the highest wave in a timespan of 48 hours is selected and the remaining data is removed from the set.

Because this dataset doesn't include the special cases under the set threshold of 5,5m, a new threshold is set on 4 m. The storms that have a wave height between 5.5 and 4m and fulfil the following criteria are added to the first dataset. this resulted in a dataset (I.II). There are 757 sea-states with a wave height between 4m and 5.5m.

- Sea states with more than one wave system (waves and swell)
- Sea states with an angle of at least 15 degrees between equilibrium-heading and Wind or Wind-sea

This results in 78 sea-states that can be added by the sea-states from the 5,5m threshold resulting in dataset I.II that consist out of (441+78) 519 sea-states which can be modelled.

The second main dataset (II) is formed by first setting a threshold of 6,5m. This results into 743 sea-states. Other than with the first data set, not only the highest wave in a 48-hour time span is selected but all the 743 sea-states are modelled in 10 realizations and the sea-state that results in the highest MAX LT in a storm cluster is selected. A storm cluster is defined as a series of consecutive measurements that are above the set threshold. This resulted in 196 entries as input for the response model.

For dataset II-refined the same method is applied on the data but now with 20 realizations instead of 10 this gives a more accurate estimate of the AVG MAX LT. In Figure 3-2 a visual representation of the selection procedure is given.

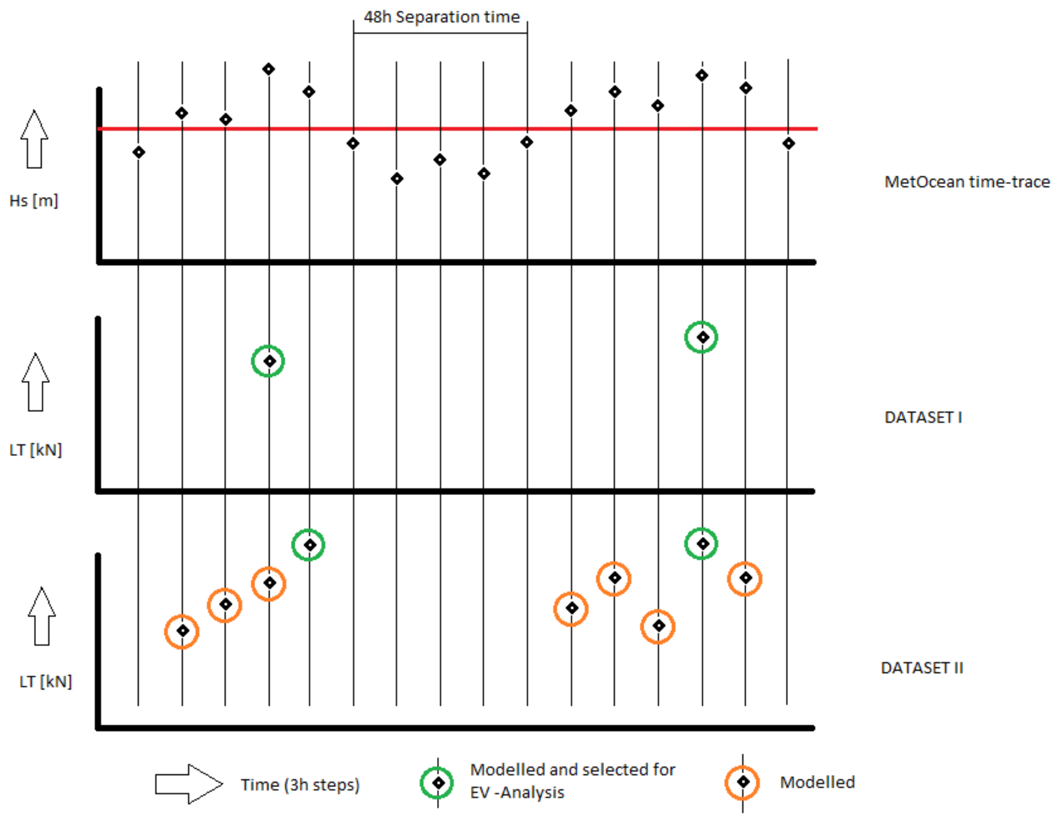

Figure 3-2 Visual representation of the selection procedure (Oostra 2015)

3.2.4 Simulation

The simulation is executed with Dynfloat. Dynfloat is a time domain simulation program that analyses the dynamic behaviour of a moored FPSO in an ocean environment. In this section the input will be discussed for the dynamical model, the numerical model itself and the output.

Input

The input of the Dynfloat model is the description of the modelled system. This system consists out of the environment and the vessel.

The general environmental parameters are the water depth and the density of the water on the specific location. These are constant parameters which do not change during the simulation. The changing environmental parameters are the wind, wave, and current conditions. For wind and waves the height/speed is given, as well as the direction. For the current, a current-profile is given to incorporate the variable current speed in relation to the water depth.

In Dynfloat the variable environmental conditions can be provided as a spectrum or as a time-trace. In this thesis the variable environment will be provided as a time-trace. This time-traces are hindcasts of environmental data with a 3-hour interval. The environmental data follows directly from metocean data.

The other input parameters are the vessel and the mooring characteristics. In Figure 3-3 an overview of the general ship data that needs to be provided is given. The wind-areas and radii of inertia are calculated with empirical equations that can be found in the Dynfloat manual (Marin 2008) .

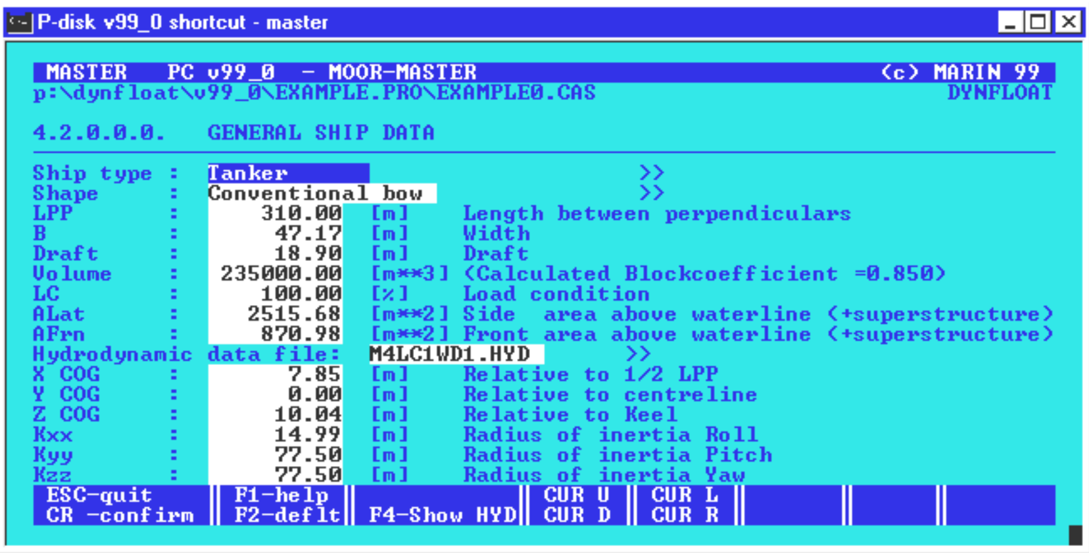

Figure 3-3 General ship data

The hydrodynamic data file (. HYD) is a file that describes the wave frequency vessel motions and low frequency wave drift forces. This file is the result of diffraction calculations for the specific vessel for a specific water depth.

The specifications of the mooring system include a description of the mooring type. This can be a turret mooring or a spread mooring. Each line segment of a mooring leg is defined individually. Figure 3-4 is an example of the description of a mooring leg from anchor to fairlead. In this example the mooring line is build up out of 5 individual mooring line segments.

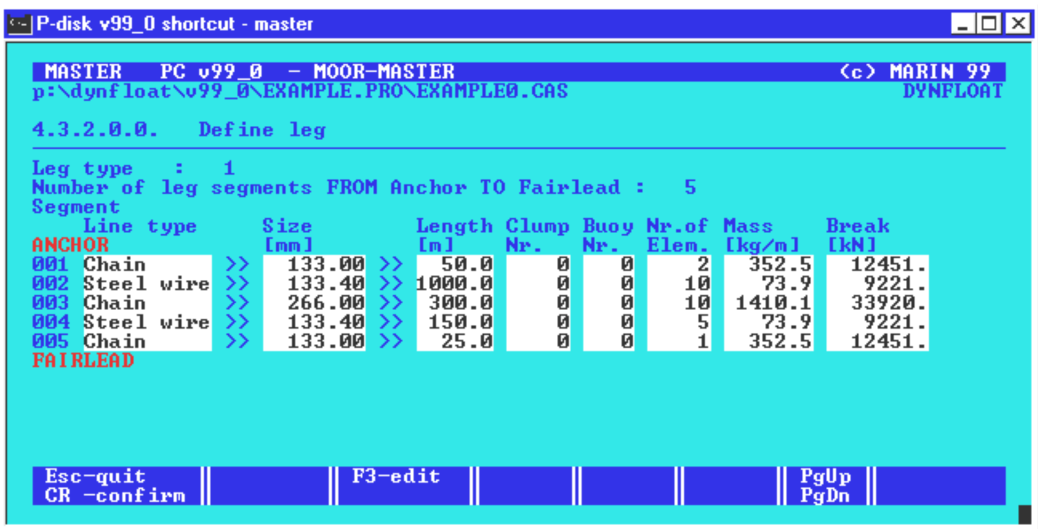

Figure 3-4 Mooring leg

The last input step is to specify the location of the fairlead and the allocation angle of the mooring legs. Also the pre-tension in the mooring lines is specified.

Numerical model

In Dynfloat coupled analysis is used to calculate the dynamic loads in the mooring system, the wave frequency and low frequency vessel motions. A block diagram of this coupling is given in Figure 3-5.

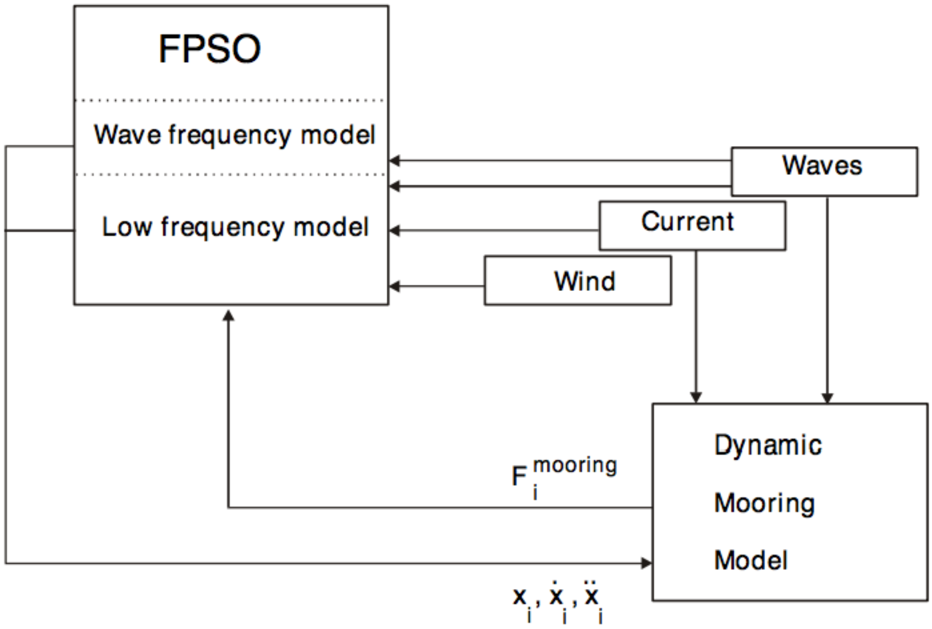

Figure 3-5 Numerical model (Marin 2008)

In Dynfloat, simulations can be done in two different ways. First a traditional way where the low frequency motions are determined using only static-force displacement characteristics of the mooring system (a non-linear spring). This method is called the quasi-dynamic simulation.

The second method is a fully coupled calculation where the dynamic loads in the mooring system are the result of combined wave and low frequency motions that are determined for each time-step during the simulation. In this way not only a restoring force is provided by the mooring system, also damping and inertia loads are applied on the vessel.

The coupled dynamic analysis is preferred if an environment with significant large water depth is analysed. In deep water with long line lengths and high line weights the influence of, mooring system damping on the low frequency motions, mooring line dynamics due to vessel velocities and accelerations, and direct current loads on the mooring lines are of bigger importance in comparison with shallow water.

Output

Four output files are created in Dynfloat. The first output file a .STA file gives an overview of the input parameters and gives the static results of the system. The static load table for a single mooring line and for the complete mooring system and the total forces for the equilibrium position.

The second output file is a .PLT file, this file contains the forces following from the environmental conditions. These forces are the total mean environmental surge and sway forces, static load curves, and the moment around the turret axis as function of the vessel heading.

The third output file is a .OUT file this file describes the drift forces resulting from the environmental conditions. Mean drift forces from waves wind and current; mean wind, wave and current forces in the starting position; the mean environmental forces during the simulation and the mean displacements of the vessel during the simulation.

The final output file is a .RES file, this file describes the time-traces for all parameters: wave height, CoG (Centre of Gravity) translations, vessel rotations, mooring loads, wind loads, low frequency damping loads, wave drift loads, the total environmental loads, the turret forces, mooring line loads and the reference point translations. With these output values all input is created that can be used for post-processing.

3.2.5 Post-processing

In the post-processing part of the method, the output generated with the simulation will be fitted on an extreme value distribution. With this distribution, return levels for a desired return period can be calculated.

Fitting realizations to a Generalized Pareto Distribution

To fit the data to the generalized Pareto distribution (GPD) the extreme value procedure described by (S. Coles 2001) is used. Equation 3-1 describes the GPD.

$$\lim_{u \to x_F} P\left\{\frac{X-u}{g(u)} \leq x \middle| X > u\right\} = \begin{cases} 1 - e^{-\frac{(x-\mu)}{\sigma}} & for\ \xi = 0, x > 0 \\ 1 - \left(1 + \frac{\xi(x-\mu)}{\sigma}\right)^{\frac{-1}{\xi}} & for\ \xi \neq 0, 1 + \xi\frac{(x-\mu)}{\sigma}, x > 0 \end{cases}$$

Equation 3-1 General Pareto Distribution (GPD)

With X a random variable with continuous distribution function F, x_F being the endpoint of F ($x_F \leq +\infty$) such that $F(x_F) = 1$ and $F(x) < 1$ for $x < x_F$. Where variable $\frac{X-u}{g(u)}$ is a scaled excess and scale parameter δ dispenses the necessity to have prior knowledge of function g. This means that (conditionally on an observation being high enough), the probabilistic behaviour can be described by the Generalized Pareto Distribution function. The scale- ($\tilde{\sigma}$) and shape-parameters (ξ) of the GPD for the POT (Peak Over Threshold) describe the distribution for a given set of empirical data.

First the parameters of the distribution need to be estimated. Parameter estimation is done by maximum likelihood (Dekking, et al. 2005) . The values $y_1, \ldots, y_k$ are the k excesse above a threshold u. for $\xi \neq 0$ the log-likelihood function (Equation 3-2) is described below.

$$l(\sigma, \xi) = -k\ log\sigma - \left(1 + \frac{1}{\xi}\right) \sum_{i=1}^{k} \log\left(1 + \frac{\xi y_i}{\sigma}\right)$$

Equation 3-2 Log-likelihood function for parameter estimation

If this equation is maximized for a range of threshold values a plot can be made that illustrates the chosen threshold vs de parameter estimation for that threshold. This plot can be seen in Figure 3-6. The point where the plot becomes stable will be used as the threshold chosen for the final distribution. The empirical data behind this stable point can be represented by the same GPD fit parameters. In the example this threshold will be 2900kN.

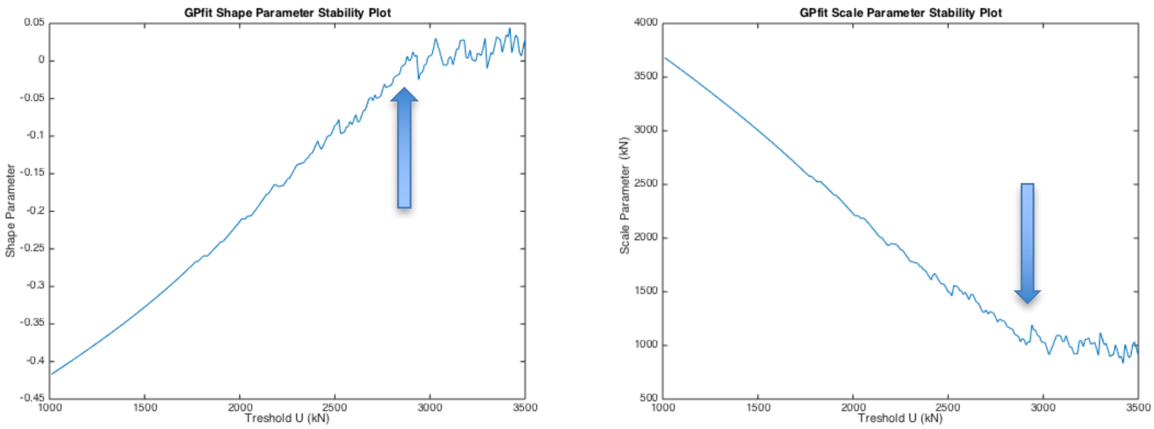

Figure 3-6 Parameter stability

After this step the distribution, with the corresponding fit parameters, is known describing the initial extreme load data the best. To check that the distribution is actually a good representation of the reality, some goodness-of-fit tests needs to be done.

There are a couple methods to assess the goodness-of-fit of the distribution to the empirical data. The tests underpin a claim of the form “the empirical distribution of the data matches a certain theoretical distribution”. This can be checked visually and numerically. The two numerical test are the Chi-squared goodness-of-fit test and the Kolmogorov Smirnov test (Klemens 2009).

The chi-squared test statistic is the sum of the squared deviations between the empirical and the expected values. The conclusion can be made that the empirical data fits the distribution if this sum is lower or the same as the critical value of the chi-squared distribution for a chosen significance level. The critical value of the chi-squared statistic is based on the degrees of freedom (amount of data points -1) and the chosen significance level (Moore 1976). The chi-squared test is highly dependable on sample size, so if the sample sizes increases absolute differences become a smaller proportion of the expected value. This can result in the acceptance of a fit to a distribution while there are significant statistical errors.

The Kolmogorov Smirnov test method is based on the cumulative distribution function. The Kolmogorov test statistic is the maximum of all vertical distances between the cumulative distribution functions of the empirical and theoretical distribution. If this statistic exceeds the 1-α quantile, the distribution is rejected for the significance level α. (Massey 1951)

Three visual methods are presented. The first two are visual comparisons of the empirical data and the distribution. In the first method the theoretical distribution density function is compared with histograms of the empirical data. In the second method both the cumulative distribution functions are compared. If the distribution is a good representation of the empirical data, both curves will be close to each other.

The third method of visual comparison is a quantile-quantile plot of the parameter estimates from bootstraps of the empirical data. The parameter estimates are normal distributed by definition. If the quantiles of the estimates are plotted to the standard normal quantiles a straight line is observed if the the parameter estimates show asymptotically standard normal behaviour. If this is the case it can be concluded that the distribution parameters are stable and are a good representation of the empirical data.

Results and comparison to conventional method

If the GPD is a good representation of the empirical data, a return level can be calculated for a desired return period N (100, 1000,... year). With Equation 3-3 the N-year return period can be calculated. This equation uses the fit parameters of the GPD.

$$z_u = u + \frac{\sigma}{\xi}\left[\left(N * n_y * \xi_u\right)^{\xi} - 1\right]$$

Equation 3-3 N-year return period value

In which u is the treshold value, σ the GPD scale parameter, ξ the GPD shape parameter, N the return year, n_y the number of observations in a year and ξ_u the probability of a threshold exceedance for an arbitrary observation. The results obtained in (Oostra 2015) for the different datasets are listed in Table 3-1.

The BES (Bluewater Energy Services) mooring analysis design value is calculated by the convenient practice that is used within the offshore industry. With this practice first a design environment is created, For every individual environmental parameter (wind, waves, current) a 100-year extreme is extrapolated. For the 100-year environments different combinations of associated wind, waves and current are obtained. The dynamical behaviour of the FPSO is then simulated for the 100-year extreme environments to find the 100-year return period of the maximum line tension. Besides the maximum line tensions other parameters of interest are calculated in this simulation such as horizontal turret load, offset, etc. In (Oostra 2015) the focus is set on the 100-year maximum line tension. The 100-year maximum line tensions originating from the proposed method are then compared with the results from the conventional method for the various data sets.

	100-year RP MAX LT	Difference	Method	Characteristics
BES Mooring-Analysis	10094 kN	-	LT based on 100-year RP environment	AVG MAX of 25 realisations with random seed
Extreme value analysis DATASET I.I	7015 kN	-30.5%	Based on 100-year RP MAX LT extrapolation	GPD-fit to LT data of max Hs sea-state of storm clusters (10 realisations)
Extreme value analysis DATASET I.II	7244 kN	-28.2%		
Extreme value analysis DATASET II	9390 kN	-6.97%		GPD-fit to max LT event of entire storm (10 realisations)
Extreme value analysis DATASET II - Refined tail	9707 kN	-3.83%		Same but with 25 realisations

Table 3-1 100-year Return level MAX LT for different methods

Reliability and sensitivity

The reliability of the extrapolation is presented in two ways. First the 95% confidence interval of the shape and scale parameter as seen in Figure 3-7. And the secondly the sensitivity of combined parameters. In this method the scatter plots (Figure 3-8) for the parameters and return period are presented. The spread of these plots illustrates the variability of the relation between both parameters.

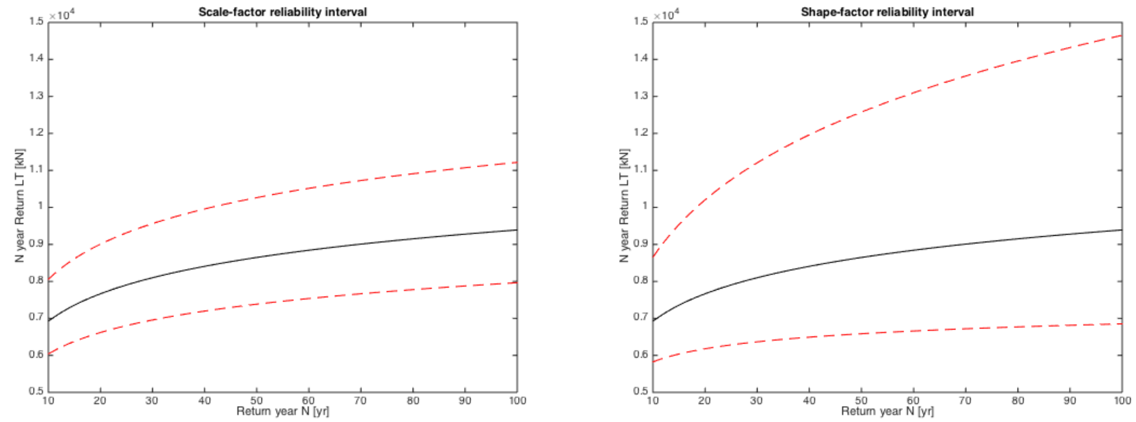

Figure 3-7 95% confidence interval shape and scale parameter dataset II (Oostra 2015)

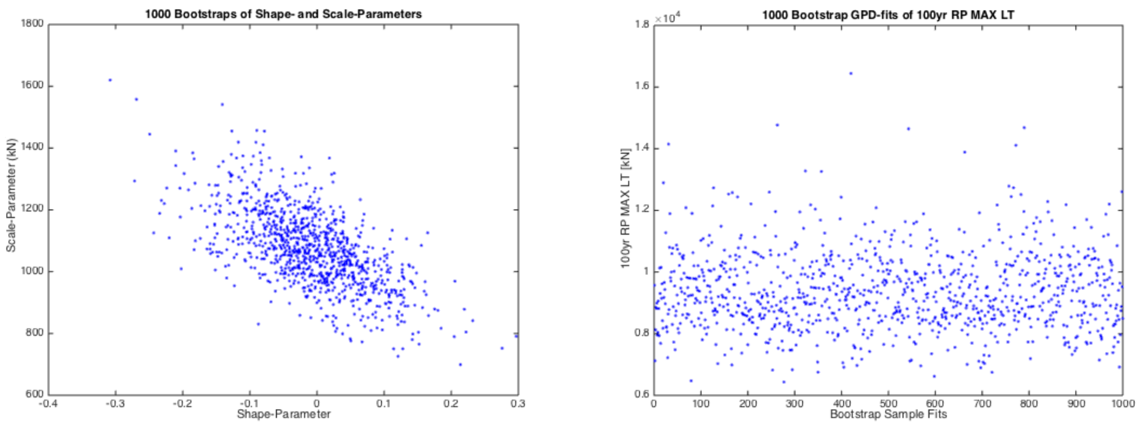

Figure 3-8 Sensitivity of combined parameters based on 1000 bootstraps of dataset II (Oostra 2015)

3.2.6 Conclusions on response based approach

Conclusions made after the work of (Oostra 2015) about the presented method are listed below.

- Very strong coherence between the empirical and fitted data for both the PDF and CDF. This results in a good fit for MAX LT data with the GPD.
- Focusing on a threshold with only max Hs is not sufficient.
- The steepest waves that often lead to the highest tensions often occur in the run-up or decay of a storm.
- The environment is much more confused during the build up and decay of a storm. In those situation there can be a misalignment between the FPSO and the environment leading to higher tensions.
- The reliability of an extrapolation is improved when more realizations of an entry are made. A realization of 25 different seeds will result in a higher quality fit compared to a set of data that is simulated with less seeds.

3.2.7 Recommendations response based approach

Recommendations that are made after the work of (Oostra 2015) are listed below.

- The proposed method should be applied to other locations, configurations and loading conditions to prove robustness.
- Applying a more sophisticated threshold mechanism is recommended.
- This algorithm could be made more sophisticated by implementing code to trigger on joint occurrence between wave-height and other parameters, like wave-steepness.
- The method proposed does not account for possible asymmetry of a mooring-system layout or the asymmetric excitation (directionality) of the environment. Since the lines are oriented in a certain direction it would be more elegant to develop a dataset for every line and superpose the extrapolation to an omni-directional extreme.
- For future improvement more research could be done on how trustworthy true reliability intervals for the extrapolated line tensions could be calculated.

4 Method reconstruction and validation

A method reconstruction and validation is an important step to check the reproducibility of the applied methods and to get a clear insight in the methods applied. The method reconstruction will consist out of a reconstruction of the pre-processing, simulations and post-processing methods.

4.1 Pre-processing

The pre-processing methods are the link between the raw metocean data and the input data provided into the simulations, which will be performed with Dynfloat. The pre-processing consists out of three large parts.

First the data is read from the raw data excel file, secondly a data set is created in Matlab following the rules (section 3.2.2) of the different datasets, as final step case numbers are given and the processed data is written into an excel file.

The different preprocessing steps are checked and evaluated by comparing the raw data and the final processed data file manually. It is checked if the separation time is respected, the threshold is correct and that the given case numbers are logical and unique.

The reconstruction of the pre processing methods resulted in an improvement of the "Matlab" script that selected the sea states above a certain threshold. The script separates entire storm clusters above the selected threshold.

For dataset I the maximum wave height for each cluster is selected to form together the input for EV (Extreme Value) analysis. In the first script the separation time of 48 hours was not included properly. This is now changed so that the dataset can be seen as IID.

4.2 Simulations

The validation of a simulation program like Dynfloat would be complicated and out of the scope of this thesis. Dynfloat is a program developed by MARIN (Marin 2015) over several years. The focus on validation of the simulation part of the process is to fully understands what is calculated with Dynfloat and how this is calculated. The chosen way to prove this is to recreate the static-load part of simulation made in Dynfloat in an analytical way.

For further work on the limitations for the applied extreme value theory in the design of mooring systems it is important to focus on the line characteristics and restoring curves and less on the hydromechanical behavior of the vessel itself. The first step is to set up a test case.

The test case is a simplified model, based on the Bluewater FPSO 'Haewene Brim' . This simplified model can be seen in Figure 4-1. The model consists out of a barge moored by 2 mooring lines in a 2D way. All the parameters used as input for the Dynfloat simulation and the analytical calculation can be found in Appendix I this is the .OUT file created by Dynfloat.

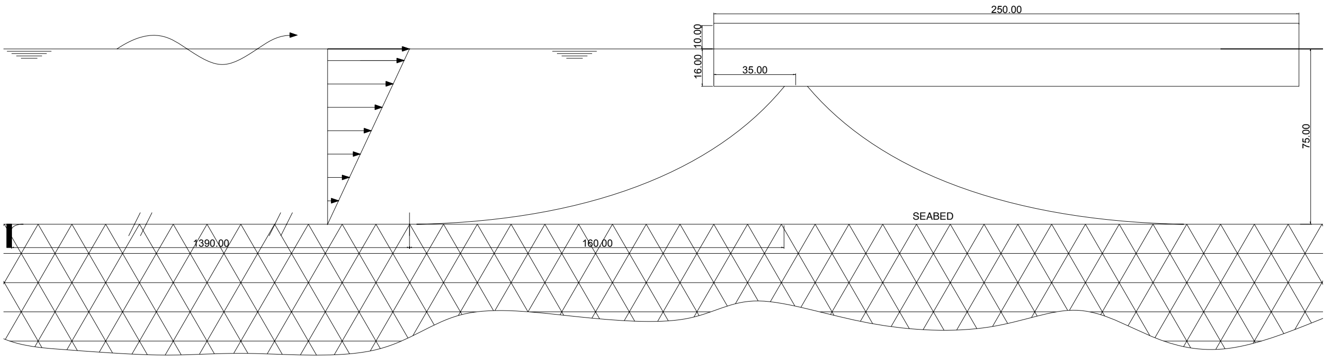

Figure 4-1 Illustration of the model used for method reconstruction

For the validation of the mooring line characteristics and restoring curves a free-decay test is completed on the one hand in Dynfloat and on the other hand in an analytical way. First the simulation in Dynfloat will be discussed and subsequently the analytical method, thereafter the validation of the simulation will be discussed.

A free-decay test is performed in Dynfloat with a surge offset in a quasi-dynamic manner. In this test the model has an initial offset of 20m and will be released for 10000 seconds without the influence of any environmental forces (no wind, no current, no waves). An overview of the input parameters can be found in Appendix I.

The results of the Dynfloat simulation (free decay) can be seen in Figure 4-2.

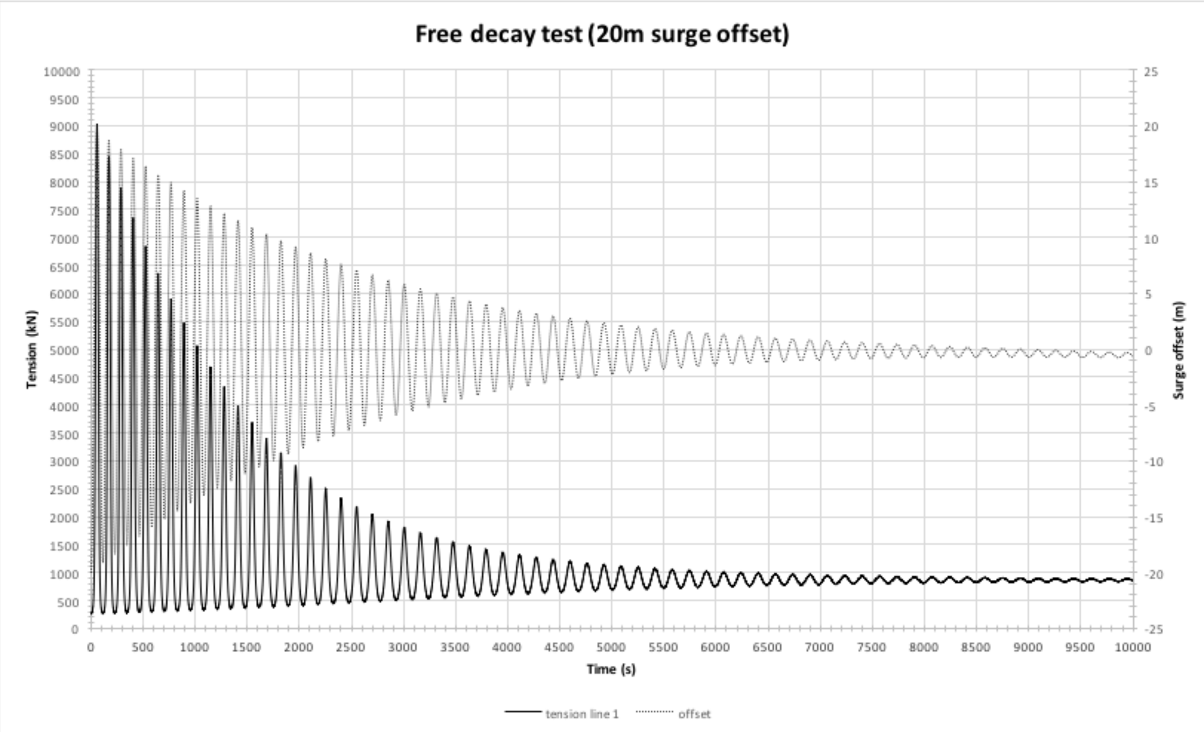

Figure 4-2 Dynfloat simulation

In the above time-traces, the offset of the model and the tension in line 1 can be seen for each time step during the simulation. If these two parameters (offset and line tension) are plotted the restoring curve of the mooring line can be found. This restoring curve can be compared with the restoring curve calculated in an analytical way. This comparison can be found at the end of this section where the conclusions concerning the validation of the simulation will be presented.

For the calculation of the restoring curve in an analytical way, catenary equations with some adaptions specific for analyzing mooring systems are used. The 'standard' catenary equations focusses on free hanging chain between two points. This free hanging chain can be described by the following catenary equation Equation 4-1.

$$y = a\cosh\left(\frac{x}{a}\right) = \frac{a}{2}\left(e^{\frac{x}{a}} + e^{\frac{-x}{a}}\right)$$

Equation 4-1 Catenary equation

In this equation x and y are the coordinates in a Cartesian system and 'a' is a uniform scaling factor. Changing this factor will change the angle between the catenary chain and the horizontal at the points where the chain is suspended.

The output of the analytical calculations consists out of two parts first there is an illustration (Figure 4-3) of the mooring line at a certain offset, and a restoring curve that can be compared with the restoring curve computed by Dynfloat.

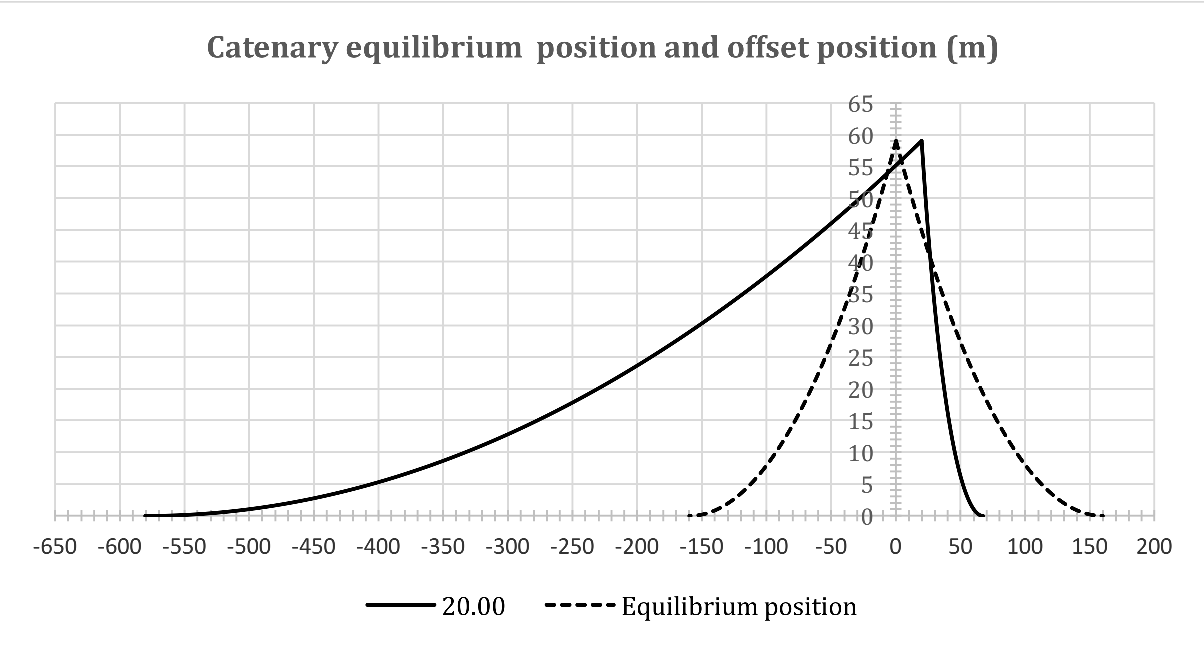

Figure 4-3 Illustration mooring lines

Figure 4-3 illustrates the catenary curve of mooring line 1 and 2, for the equilibrium position (offset 0m and tension in line 1 is the same as the tension in line 2) and the start position for the free-decay test (offset 20m). The illustration only shows the part of the mooring line that doesn't touches the seabed. From this illustration the suspended length and the catenary curve for both mooring lines can be derived.

The results are presented in Figure 4-4. This figure plots the tension in line 1 for a given offset, calculated analytical and simulated by Dynfloat. Further the tension in line 2 and the total horizontal tension is calculated analytical for a given offset.

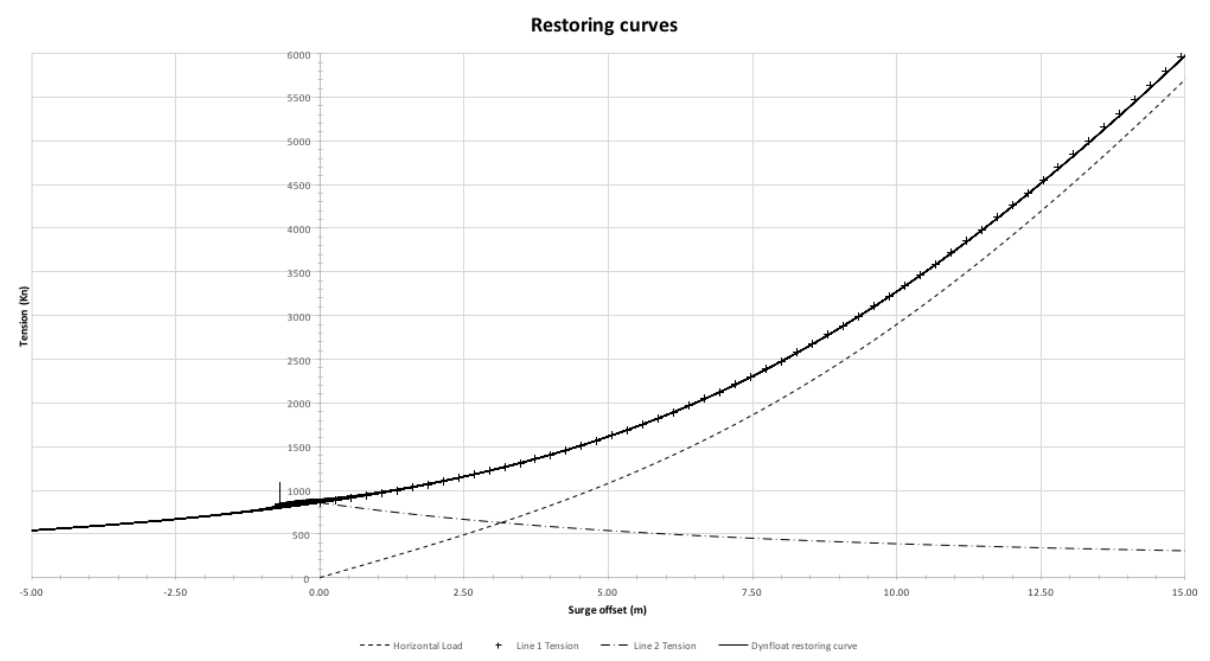

Figure 4-4 Restoring curve analytical and Dynfloat

In Figure 4-4 it can be seen that the restoring curve for line 1, analytically calculated and simulated by Dynfloat, are collinear with some shift above an offset of 12.5m. This error is small if it is compared to the overall fit. It can be concluded that the calculations made by Dynfloat in a free-decay test are in line with the expectations based on the analytical calculations.

4.3 Post-processing

The post-processing methodology exists out of Matlab scripts that fit a set of load data to a generalized Pareto distribution and give its 100-year return level with its corresponding reliability intervals. Also some goodness-of-fit tests are produced.

To check if the simulation data is processed correctly to fit a GPD (Generalized Pareto Distribution) and obtain a reliable extrapolation, a dataset of 10000 points is drawn from an existing GPD fit with the parameters presented in Table 4-1. Drawing the dataset from an existing GPD will ensure that the post-processed set of data can be represented by a GPD, with the condition that the amount of data points is large enough.

u	2500
σ	1000
ζ	0.03

Table 4-1 Input parameters GPD data set

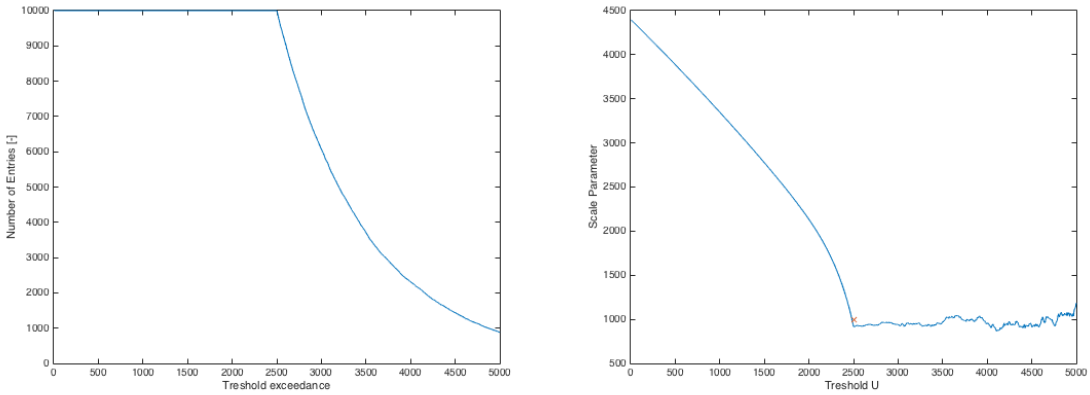

Figure 4-5 Number of EV entries and scale parameter stability

The objective is, that with this method it can be proven that when an infinite amount of points is drawn, the GPD fit calculated by the post-processing script will be exactly the same as the initial GPD fit. The distribution parameters are chosen close to the parameters obtained in (Oostra 2015).

In Figure 4-5 the number of EV entries are plotted for a certain threshold. Since the original GPD has a threshold of 2500, all data points are above this threshold and the fit of the scale parameter becomes stable above 2500 as expected from the input parameters. The data is processed for a threshold of 2500 and fitted on a GPD.

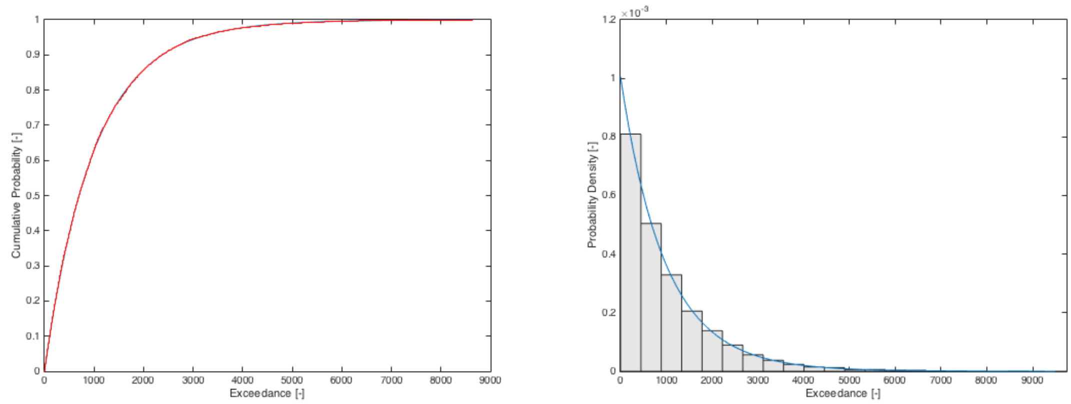

Figure 4-6 Fitted GPD function comparison between fitted data and empirical data

Figure 4-6 shows that the fitted data and original GPD are collinear. It can be concluded that the post-processing scripts produce a reliable GPD fit for a set of data if the tail of this data is actually GPD distributed.

4.4 Conclusions method reconstruction

It can be concluded that the three tested parts in the overall method; pre-processing, simulation and post-processing will not lead to deviating results. For the simulation part only the static loading parts are checked. This to get a good notion of the static calculations used in Dynfloat. A comprehensive check of the dynamic calculation implemented in Dynfloat would be an extensive job which is out of the scope of this thesis.

5 Prove robustness

The importance of proving the robustness of the proposed method follows directly from the research question of this thesis. The research question states that the proposed methodology needs to be applicable in an efficient way to calculate 100-year return levels for various parameters and various vessel-and environmental characteristics. To use a methodology in an efficient way it is important that all the steps taken, starting from a metocean time trace to a final extrapolation, are without errors and are applicable under all circumstances. This chapter describes the steps taken to prove the robustness of the proposed methodology. First the simulation method is discussed after that a parameter study is done to check the robustness for different design situations. As a final step the possibility of fitting the data with an alternative distribution is checked.

5.1 Simulation method

The simulation method used in (Oostra 2015) is a fully dynamic simulation in Dynfloat (Marin 2015). This is a proven simulation package used for years in the offshore industry. The disadvantage of fully dynamic simulation method is the high demand of computational resources. This high demand on computational resources reduces the usability of the method in a design stage, because in a design stage it is important that multiple mooring configurations can be proved in an efficient way. The time needed to simulate a 3-hour time trace is 15 minutes. On average 1000 cases need to be simulated, so the time needed to perform an entire fully dynamic analysis is in the order of weeks. This is too time consuming for use as an efficient tool in a design phase. In this section it will be discussed if it is possible to simulate the time traces in a less time consuming quasi dynamic manner instead of the fully dynamic method.

The difference between a fully dynamic analysis in Dynfloat is the way the mooring lines are simulated. When the cases are simulated dynamically the mooring line forces are calculated with mooring line damping included. When the cases are simulated quasi-dynamic the mooring line forces are based on the interpolation of static load curves. In (Marin 2008) it is recommended to use Quasi-dynamic analysis when the expected influence of mooring line dynamics is small. (Huse 1986) concludes that the drag forces on the mooring lines represent a large part of the total surge and sway damping of the system. Surge amplitude reductions of 20 to 25 percent are possible. These reductions have a large influence on the mooring line peak loads. The line damping forces will be compensated by including added vessel damping to the quasi-dynamic model. These damping values will be calculated with the results of a free decay test in subsection 5.1.1.

In (Johanning, Smith et Wolfram 2006) and in (Fontaine, et al. 2013) it is concluded that a highly dynamic system with several degrees of freedom can be simulated with quasi-dynamic calculations. The quasi-dynamic method can be used in a design process to produce an estimate of suitable line characteristics (materials, dimensions,...), which can then be analysed later with more advanced methods. As stated in the research question the goal of the methodology is to create a "less time consuming" tool that can be used in a design stage.

In the following subsections the added damping values to compensate for the mooring line damping will be calculated by performing a free decay test in surge direction. Also the difference between the extrapolation of a quasi-dynamic and the full dynamic analysis will be compared to see if the simplification of the reality still results in reliable extrapolations.

5.1.1 Free decay test

The damping of moored floating structures is build up out of 4 parts (Triantafyllou, Yue et Tein 1994). This is wave drift damping that is proportional to the square of the wave height and a function of the ambient wave frequency (Wichers et van Sluijs 1979).

The second part of the total damping is the wind induced damping. This damping is a function of the square of the wind speed and the dimensions of the vessel.

The third is the current and viscous flow damping. These are the drag and lift forces acting on the vessel. The last damping force are the mooring line induced damping forces. These forces are the forces that are not included when the simulations are done in a quasi-dynamic manner. These damping forces will be discussed in the next paragraph.

There are several contributing factors to the mooring line induced damping. (Brown, Lyons et Lin 1995). These are:

- Hydrodynamic damping; This is induced by motions of the vessel that result in a displacement of the top of the mooring line. This displacement will induce a transverse motion of the mooring line. The corresponding damping transverse drag force represents a dissipation of energy and can be used to calculate the damping force. Due to this effect the influence of hydrodynamic mooring line damping increases if the water depth increases (and so the free hanging mooring line length). When environments with large water depths are studied a more in depth study needs to be done on how to compensate for mooring line dynamics in the simulation using the quasi-dynamic method.
- Vortex induced vibrations; If a steady flow passes a mooring line a vortex can be formed behind it. If the forces induced by this vortex are close to the Strouhal frequency resonant response can occur in the mooring line and in-line drag will increase. This effect is more important for wire lines and can be neglected for chain mooring.
- Line internal damping; This damping is the result of frictional forces in the chain or wire.
- Damping caused by sea-bed interaction; Displacement of the mooring line will induce frictional forces between the sea-bed and the mooring line.

To determine the total damping that is induced by the mooring system, a free decay test for the surge motion is performed. In this test we assumed a symmetrical mooring system (8X1) as close as possible to the installed mooring system. A solution for the mooring line damping added in surge direction is found by simulating a free-decay test dynamically and secondly quasi-dynamically with several added damping values to the vessel. The damping value corresponding to the best performing quasi-dynamic simulation shall be used for the quasi-dynamic calculations.

Figure 5-1 illustrates the dynamic free-decay test and the quasi-dynamic with variations. The final estimation of the added damping in surge direction is 450 kN/s^2.

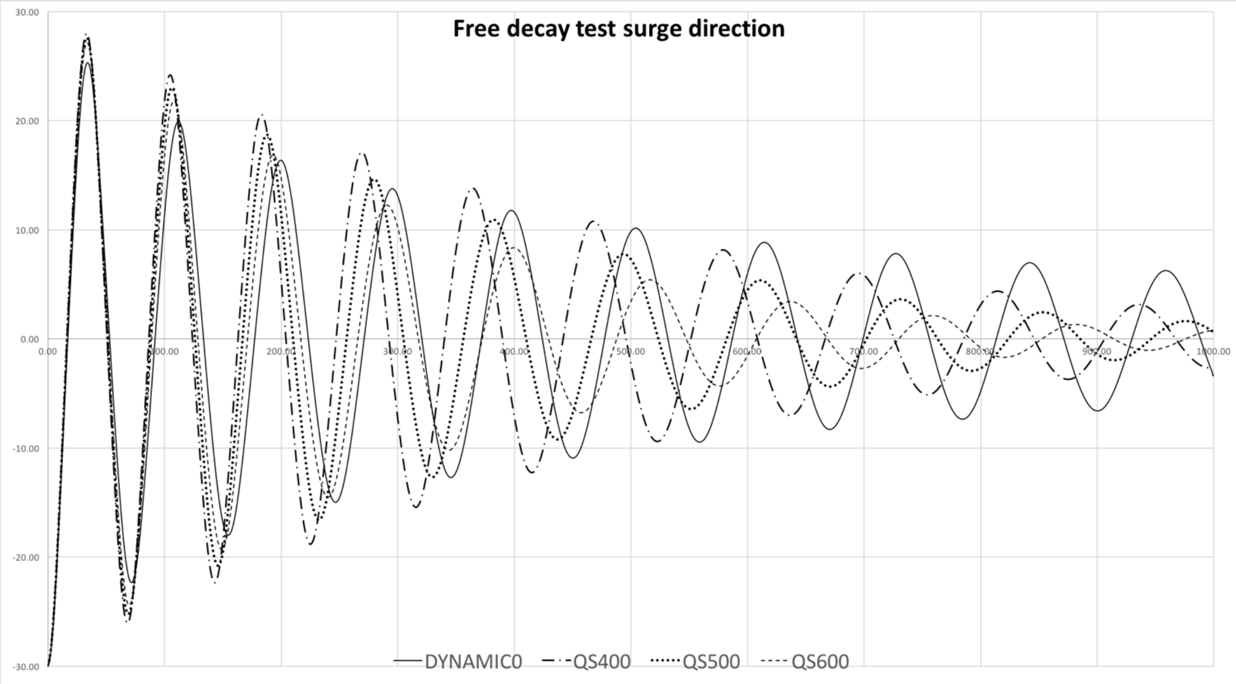

Figure 5-1 Free decay test in surge

If this result is compared to the literature (J. Wichers 2013), it can be concluded that this value is a realistic surge damping induced by the mooring system for a FPSO.

Since we assumed a symmetrical mooring system, the damping factor from the mooring system for sway is the same as for surge. This is 450kN/s^2.

The equivalent yaw damping amidships to compensate for the mooring line induced sway damping acting on the turret is calculated with Equation 5-1 (the International Organization for Standardization 2005).

$$C_{Rz} = C_y \frac{1}{3}(a^3 + b^3)/(a + b)$$

Equation 5-1 Linear yaw damping coefficient.

Where

- C_{Rz}= Linear yaw damping coefficient, Nm/(Rad/sec)
- C_y= Linear sway damping, N/(m/sec)
- a= Length of vessel forward turret
- b= length of vessel aft of turret

This results in an added yaw damping of 4.63 * 10^6 Nm/(Rad/sec).

The next step is to compare the dynamic simulation with the quasi-dynamic simulation method with the added damping values included for one, 3-hour time trace (5050108). For the two cases 30 seeds are produced.

Table 5-1 gives the average maximum line tension for the two simulation methods over 30 seeds.

	Average over 30 seeds
Fully dynamic	6683 kN
Quasi-dynamic with yaw damping	6429 kN

Table 5-1 comparison of case 5050108

Case (5050108) is a time trace of the Pierce field environment (83m water depth). As stated before the influence of mooring line damping increases if the water depth increases. For this specific field the results are promising as an alternative method. If fields with larger water depths are studied it is necessary to do more research on the possibilities to use quasi-static calculation methods. A second test is to compare a 30 year dynamic analysis described in (Oostra 2015) with the same analysis done in a quasi-dynamic manner.

5.1.2 30-year comparison

A comparison is made between the dynamic method and the quasi-dynamic method for dataset II and dataset II-refined defined in section 3.2. In Table 5-2 the 100-year extrapolations of the 30-year comparison are presented with the corresponding characteristics for each case.

	Simulation mehod	100-year RP MAX LT	Difference with BES	Characteristics
BES Mooring-Analysis	Dynamic	10094 kN	-	AVG MAX of 25 realisations with random seed
EV analysis DATASET II	Dynamic	9390 kN	-6.97%	GPD-fit to max LT event of entire storm(10 realisations)
EV analysis DATASET II - Refined tail	Dynamic	9707 kN	-3.83%	Same but with 25 realisations
EV analysis DATASET II	Quasi-dynamic	9447 kN	-6.41%	GPD-fit to max LT event of entire storm(10 realisations)
EV analysis DATASET II- Refined tail	Quasi-dynamic	10076 kN	-0.18%	Same but with 25 realisations

Table 5-2 30-year comparison dynamic vs quasi-dynamic

If the quasi-dynamic extrapolations for the hundred year maximum line tension are compared with the 100-year MAXLT from the BES standard method and with the dynamic analysis described in (Oostra 2015), it can be concluded that the quasi-dynamic analysis of both datasets performs good and is within expectations. It can be noted that when less seeds are produced (tail is not refined) the 100-year extrapolation is lower then when the tail is refined. We see this behaviour for both the dynamic and quasi-dynamic analysis.

In Appendix II a visualization of the evolution of the line tension in the time and the restoring curves are presented. These plots illustrate both the dynamic and quasi-dynamic analysis. We can see in the time trace plot the dynamic and quasi-dynamic lines almost lie on each other and that both the restoring curves are collinear.

Based on the these results the conclusion can be made that it is possible to use a quasi-dynamic simulation method to produce a 100-year extrapolation for a 100-year maximum line tension event for shallow water.

5.2 Sensitivity to threshold choice

In the process of fitting response data to a distribution some arbitrary decisions need to be made. The most important choice that needs to be made is the parameter threshold that defines the point where the fit parameters become stable. The data above this point can be fit on a distribution described by the same fit parameters.

This choice is a trade off between the amount of data to produce meaningful inferences and the quality of the fit. In this section the influence of this choice on the fit and the final extrapolation will be discussed. The sensitivity will be illustrated by fitting a set of response data to a distribution for 3 different thresholds.

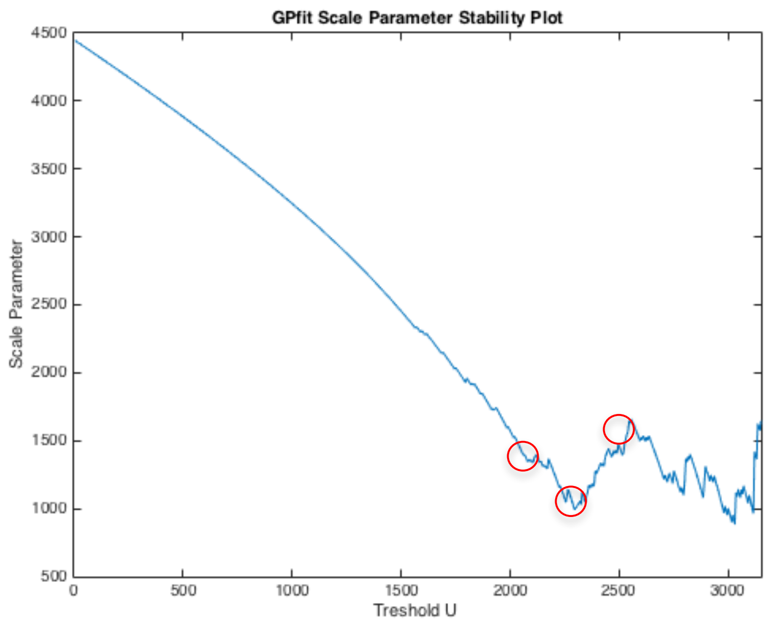

Figure 5-2 Threshold choice scale parameter

In Figure 5-2 three possible points can be identified as possible thresholds for parameter stability. These points are circled in the illustration around (2100 kN, 2300kN, 2450 kN).

Threshold U (kN)	2100	2300	2450
σ (kN)	1324	1151	1368
ζ	-0.0147	0.0638	-0.0308
N (year)	100	100	100
n_y	2920	2920	2920
ζ_u	0.0020	0.0018	0.0015
100-year return level (kN)	10143	11165	10023
Chi-squared test	accepted	accepted	accepted
Kolmogorov-Smirnov test	accepted	accepted	accepted

Table 5-3 Influence of parameters choice on final extrapolations

In Table 5-3 it can be seen that all three distributions with different threshold values pass the goodness-of-fit tests. All of the above distributions also passed the visual checks and can be represented by the Generalized Pareto distribution.

It can be concluded that all the above distributions are good representations of the response data. If the final extrapolations are studied it can be remarked that there is a difference of 10% between the distribution with a threshold of 2100 kN and the one with a threshold value of 2300 kN. While both distributions represent the same underlying data and are both accepted visually and numerically, they have different 100-year extrapolations.

This difference shows the sensitivity of the final extrapolation to the threshold choice. It is of importance that the user of the methodology takes this sensitivity in consideration when applying the methodology.

5.3 Parameter study

A parameter study will be used to examine the sensitivity to variations in extrapolated load parameters and input parameters.

In the previous work the methodology is applied for 1 set of input parameters. The extrapolation is executed for 1 load parameter (maximum line tension). For this specific case the methodology proved itself to be able to produce reliable 100-year extrapolations. The global characteristics of this case are listed below.

- ship: Haewene Brim
- mooring configuration: 8X1
- response parameter: line tension
- simulation method: dynamic
- environment: Pierce field

All of the above parameters can be changed. This results in hundreds of combinations that can be studied. If the method preforms good for all combinations the robustness of the methodology is proved. Studying all possible combinations is not possible in the limited time frame of this research project. To gather an idea of the robustness of the method a limited parameter study of the underneath parameters is performed.

- change in mooring configuration
- change in response parameter
- change in environment

For all changes in the listed characteristics the method needs to be robust and must produce reliable extrapolations which can be be used with confidence during a design process.

The dataset that performed the best in the previous work, ie. the data set with the smallest difference to the original Bluewater 100-year return level is selected. This is dataset II-refined (25seeds). This set is made up of the storm events with a combined wave height above 6.5m. All the parameters except the parameter of variation will be kept the same as described in (Oostra 2015).

In this parameter study 8 different cases are simulated. In Table 5-4 the characteristics of the 8 studied cases can be found. The parameter that is changed in comparison with the original case is underlined. The West of Shetland case is a special case. This case includes the environment of the West of Shetlands with the water depth of the Pierce field this is done to keep the vessel and mooring parameters the same and just study the influence of a more severe environment.

Case	Field	Mooring	Loading condition	Seeds	Evaluated MAX Load Event	DATA	Simulation
BASE	Pierce field	8X1	Loaded	25	MAX Line Tension	Dataset II	Dynamic
1	Pierce field	8X1	Loaded	10	MAX Line Tension	Dataset II	Quasi-dynamic
2	Pierce field	8X1	Loaded	25	MAX Line Tension	Dataset II	Quasi-dynamic
3	Pierce field	8X1	Loaded	25	MAX Horizontal Turret Load	Dataset II	Quasi-dynamic
4	Pierce field	3X3	Loaded	25	MAX Line Tension	Dataset II	Quasi-dynamic
5	West of Shetland	8X1	Loaded	25	MAX Line Tension	West of Shetland 8,5m	Quasi-dynamic
6	Pierce field	8X1	Loaded	25	MAX Offset	Dataset II	Quasi-dynamic
7	Pierce field	8X1	Loaded	25	MAX Turret Bending Moment	Dataset II	Quasi-dynamic
8	Pierce field	8X1	Loaded	25	MAX vertical turret load	Dataset II	Quasi-dynamic

Table 5-4 Case characteristics parameter study

5.3.1 Results parameter study

In this section the results of the parameter study will be discussed. Table 5-5 gives an overview of the results for each of the 8 cases.

Case	u (kN)	σ (kN)	ζ (-)	N (years)	n_y (-)	$ζ_u$ (-)	100-year MAX (kN)	Usage Factor
BASE	2900	1031.1	0.0306	100	2920	0.0015	9707	95%
1	2300	1350.4	-0.0808	100	2920	0.0018	8955	88%
2	2100	1324.1	-0.0147	100	2920	0.0020	10143	99%
3	3340	2289.5	-0.0254	100	2920	0.0020	16845	-
4	2450	1282.3	-0.2570	100	2920	0.00047	6029	59%
5	4500	1868.3	-0.0432	100	2920	0.0013	14326	141%
6	12(m)	2.9476 (m)	-0.2136	100	2920	0.0019	22.21 (m)	-
7	8600 (kNm)	3403.2 (kNm)	-0.1570	100	2920	0.0019	22211 (kNm)	-
8	1980	162.8	-0.7616	100	2920	0.0012	2191.4	-

Table 5-5 Results parameter study

In the table we can see the different fit parameters that describe the GPD with it is compliant empirical dataset. The negative value of the shape parameter denotes a physical limit of the extrapolation. This is in reality the break load of the mooring line. In the next columns the return period (N) and the number of observations(n_y) in a year are given. ξ_u is the probability that an observation exceeds a set threshold (u). It can be seen that the values of ξ_u for all cases are close to each other. This means that the amount of data points with stable GPD parameters that are used to fit the tail data to a GPD are approximately the same. So a consistency in the point where the parameters become stable can be observed. The next column gives the 100-year return level of the extrapolated parameter. The last column gives, for the line tension cases, the percentage that the 100-year return level represents of the minimum break load.

The minimum break load (MBL) is the statistical minimum load a mooring line can withstand before it breaks. This value is the same for all cases because the same mooring line components are used for all cases. The MBL for the for the mooring lines is 17,000 kN. A safety factor of 1.67 is used. So for case 1 → $8955kN * 1.67 = 14955k$N this results in a usage factor of 88%. We can see that the base case and case 1 and 2 have mooring lines that are sufficient for the present environmental extremes at the specific field, and that case 4 and 5 have respectively a to heavy and a too light mooring system.

We can conclude that for all parameter variations the proposed methodology performed good. All GPD representations of the different cases are good even if the mooring design doesn't match with the loads that can be expected for a case. All cases fitted reasonably good and all did pass the goodness-of-fit tests. However, some cases performed better then others. From the analysis presented in Appendix III, three statements can be made regarding the less performing cases.

- The methodology performs better when more seeds are produced. This means that if the tail data is simulated by more random wave seeds a better representation of the load data is calculated. For this reason, a minimum of 10 seeds will be used in the successive work in this thesis.
- The performance of the 3X3 mooring configuration is less good in comparison with the the 8X1 mooring configuration. In chapter 6 (case study) the 3X3 mooring configuration will be studied in depth and explanations for this behaviour will be presented.
- It is difficult to fit the vertical turret load data to the GPD distribution. This is the case because the data isn't heavily influenced by the environment. So the vertical turret loads are more linear in proportion to the Hs in comparison with the other loads. This makes it hard to set the threshold visually where the GPD parameters become stable. If it is done correctly the vertical turret load can be represented by a GPD and reliable extrapolations can be calculated.

5.4 GEV distribution

In this section the GEV (Generalized Extreme Value) distribution will be discussed. This distribution can be used as less complicated alternative for the peak–over-threshold (POT) approach. The use of the POT (GPD), requires some experience from the user to evaluate the initial data and set a suitable threshold that considers both the most efficient use of data and the requirement of IID data points. According to (Méndez, et al. 2006) there are three main approaches to model extremes:

1) monthly maxima series (MMS) (GEV),

2) exceedances over large thresholds, and

3) r-largest maxima within a year.

The second approach is the approach proposed by (Oostra 2015) and described throughout this thesis. In this section the first approach (MMS) is presented. This approach will be used to extrapolate a 100-year return period as an alternative for the more complicated peak-over-threshold approach.

5.4.1 Theory

GEV (Generalized Extreme Value distribution) is a distribution of block maxima M_n.

$$M_n = max\{X_1, \dots, X_n\}$$

M_n follows a GEV (S. Coles 2001) distribution for n → ∞ measurements of X. The period of these blocks can be chosen arbitrary as longs as the variables are independent and identically distributed. For the data used in this thesis, blocks of one month and blocks of 1 year were considered. Both block lengths have their advantages. Block lengths of a year will fulfil the requirement of IID (Independent and identically distributed) variables but are a waste of data. Block lengths of 1 month will not meet the requirement of IID variables due to seasonal variations in wave heights and periods which result in seasonal variations in extrapolated load data. For fitting wave data, blocks with a length of 1 month are chosen and for fitting load data, blocks with a length of 1 year are chosen to meet the IID requirement. In subsection 5.4.3 the incorporation of the seasonal variations is discussed.

The generalized extreme value distribution has 3 parameters (S. Coles 2001). (μ $location\ parameter$, σ $scale\ parameter$, ξ $shape\ parameter$ to fit tail-data. The tail data can be fitted with three types of distribution according to the sign of the shape parameter. If there exist sequences of constants $\{\sigma_n > 0\}$ and $\{\mu_n\}$ such that:

$$Pr\left\{\frac{M_n - \mu_n}{\sigma_n} \leq y\right\} \rightarrow G(y) \qquad as\ n \rightarrow \infty$$

Where G is a non-degenerate distribution function, then G belongs to one of the following families:

Gumbel	$\xi = 0$	$G(y) = \exp(-exp\left[-\frac{y-\mu}{\sigma}\right])$
Fréchet	$\xi > 0$	$G(y) = \exp(-\left[1 + \xi(\frac{y-\mu}{\sigma})\right]^{\frac{-1}{\xi}})$
Weibull	$\xi < 0$	$G(y) = \exp(-\left[1 + \xi(\frac{y-\mu}{\sigma})\right]^{\frac{-1}{\xi}})$

For estimating the distribution parameters the maximum likelihood estimation (Mudelsee 2010) method is used. If we assume that the approximation is perfect and the block maxima are GEV distributed, and the block maxima are Fréchet or Weibull distributed ($\xi \neq 0$). Then we can maximize the likelihood function (Equation 5-2) to estimate the three fit parameters.

$$l(\mu, \sigma, \xi) = -m \log \sigma - (1 + \frac{1}{\xi}) \sum_{i=1}^{m} log \left[1 + \xi \left(\frac{z_i - \mu}{\sigma}\right)\right] - \sum_{i=1}^{m} \left[1 + \xi \left(\frac{z_i - \mu}{\sigma}\right)\right]^{\frac{-1}{\xi}}$$

Equation 5-2 Log-likelihood function

provided that:

$$1 + \xi \left(\frac{z_i - \mu}{\sigma}\right) > 0, for\ i = 1, \dots, m$$

This results in the parameters that describe the GEV distribution, that is the best representation of the empirical data. With these parameters the return level z_p for a given return period p can be calculated with Equation 5-3. (Mudelsee 2010)

$$z_p = \mu - \frac{\sigma}{\xi}(1 - (-\log\left(1 - \frac{1}{p}\right))^{-\xi})$$

Equation 5-3 Return level for p blocks

5.4.2 Annual and monthly block maxima

In this chapter three data sets will be fitted to a GEV distribution, consisting out of monthly maximum wave and load data and annual maximum load (line tension) data. Results of the fit for a set of data on a GEV distribution is presented in 5 plots.

First a CDF (Cumulative Distribution Function) plot and a histogram plot of the rate of occurrence of the empirical data is plotted with the GEV distribution function. These plots can be used to evaluate visually how the empirical data fits to the model.

Another method to check the fit is the quantile-quantile plot. (Wilk et Gnanadesikan 1968) The quantiles of two identically distributed variables (empirical data and the distribution) are plotted. This will result in a straight line with slope 1, pointed towards the origin. The use of Q-Q plots is appealing because it is easy to see linear invariance. A Q-Q plot will show the variance between the two distributions the best for tail data, because the quantile is a rapidly changing function in the tails and a slowly changing function for the bulk of data. Therefore, Q-Q plots are a good tool to visually check the fit of the empirical data on the GEV distribution.

A method to check the fit visually comparable to the quantile-quantile plot is the probability plot. In this plot the probability of the empirical data and the distribution are plotted and will result in a straight line if both variables are identically distributed.

The last plot is the return level plot where the return level with its reliability intervals is presented for a certain return period. This return period can be expressed in blocks or in years. The return level is plotted with a 95% confidence interval.

Three data sets are fitted with a GEV distribution. First the monthly maximum wave height data, secondly the overall monthly maximum line tension and finally the annual maximum line tension.

The first fit was used to show the potential of the distribution method for monthly maximum significant wave heights. The fit of the monthly maxima was good and passed the chi-squared test. This resulted in good hope for the fit of the monthly maximum line tensions. The results of the first fit are presented in appendix IV.I.

In the second fit the monthly maximum line tension, regardless in which line they occur, are fitted with a GEV distribution. The empirical data is not GEV distributed, the Q-Q plot and the probability plot do not show a straight line, the chi-square test isn't passed and it can be seen visually in the CDF that the fit between the empirical data and the distribution is not good. The plots can be found in appendix IV.II.

The third dataset consist out of the annual maximum line tensions. This is a trade off between waste of data and the goodness-of-fit. The fit on the model of the annual maximum line tensions seems to be better and passes all goodness-of-fit tests (chi-squared and Kolmogorov Smirnov). The following figures illustrate results of the third fit. Table 5-6 and Table 5-7 summarize the results of the GEV fit.

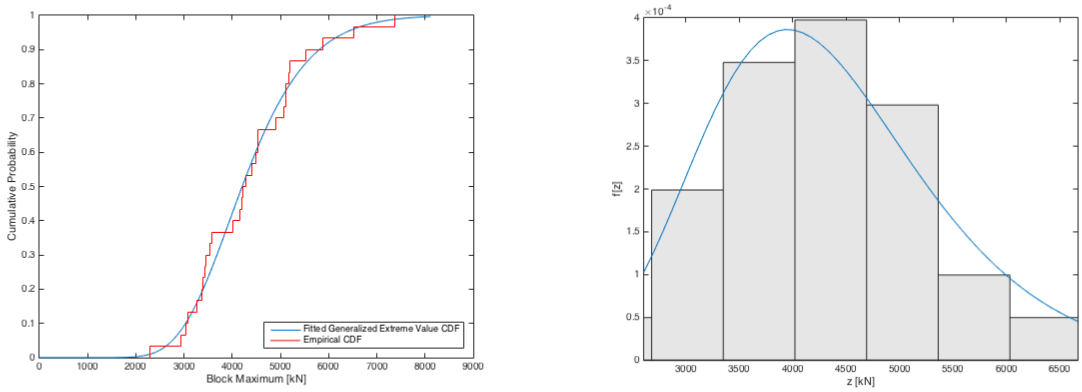

Figure 5-3 Probability distributions annual MAX LT

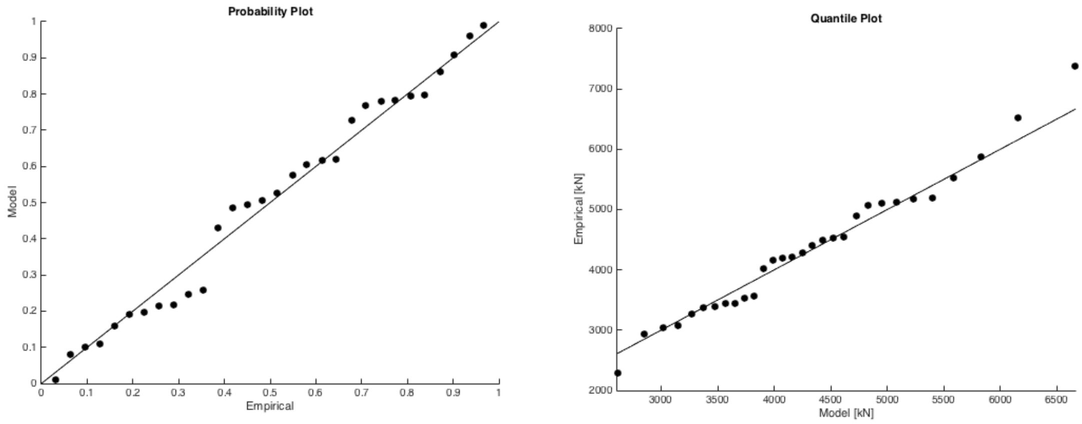

Figure 5-4 Quantile and Probability plot of annual MAX LT model vs empirical

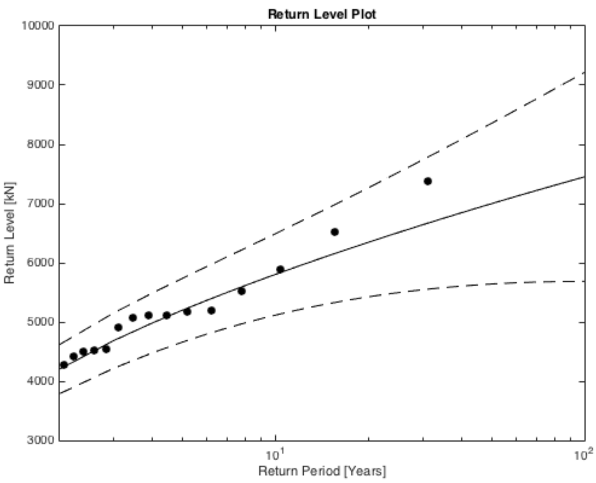

Figure 5-5 Return level plot of annual MAX LT

Case	Field	Mooring	Loading condition	Seeds	Evaluated MAX Load Event	DATA	Simulation
Monthly MAX LT	Pierce field	8X1	Loaded	25	MAX Line Tension	Dataset II	Quasi-dynamic

Table 5-6 Annual MAX LT Input

Case	$\boldsymbol{\mu}$ (kN)	σ (kN)	$\boldsymbol{\xi}$ (-)	N (years)	M (-)	100-year MAX (kN)
Monthly MAX LT	1769.8	667.7	0.1101	100	1	7066.6

Table 5-7 Annual MAX LT GEV results

With these results it can be concluded that a GEV distribution results in a reasonable good fit for monthly maximum wave heights and for annual maximum line tensions. The calculated return periods are low (-30%) in comparison with the classic methodology used by Bluewater and with the extrapolation calculated with a GPD. As a result of the large block the reliability intervals are larger compared to the POT methodology. When blocks with a length of 1 year are chosen only the maximum load of 1 year is considered. This maximum occurs mostly in the same period of year. This raises the question about the influence of seasonal variance for the fit. This will be discussed in the next subsection to see if a good fit can be created with limited waste of data.

5.4.3 Seasonality

In this chapter the influence of monthly seasonal variability of the maximum extrapolated loads will be discussed. Variation of the maximum loads can be seen on different time periods. (Menéndez, et al. 2009) These variations can be harmonics within a year, exponential long-term trend, El Niño covariate, etc. This chapter focusses on the variability that occurs within a year.

For every season of 3 months (winter(1), spring(2), summer(3), autumn(4)) a different fit is made. Figure 5-6 shows the GEV parameters and extrapolations for every season. The resulting plots for every individual season are presented in Appendix V.

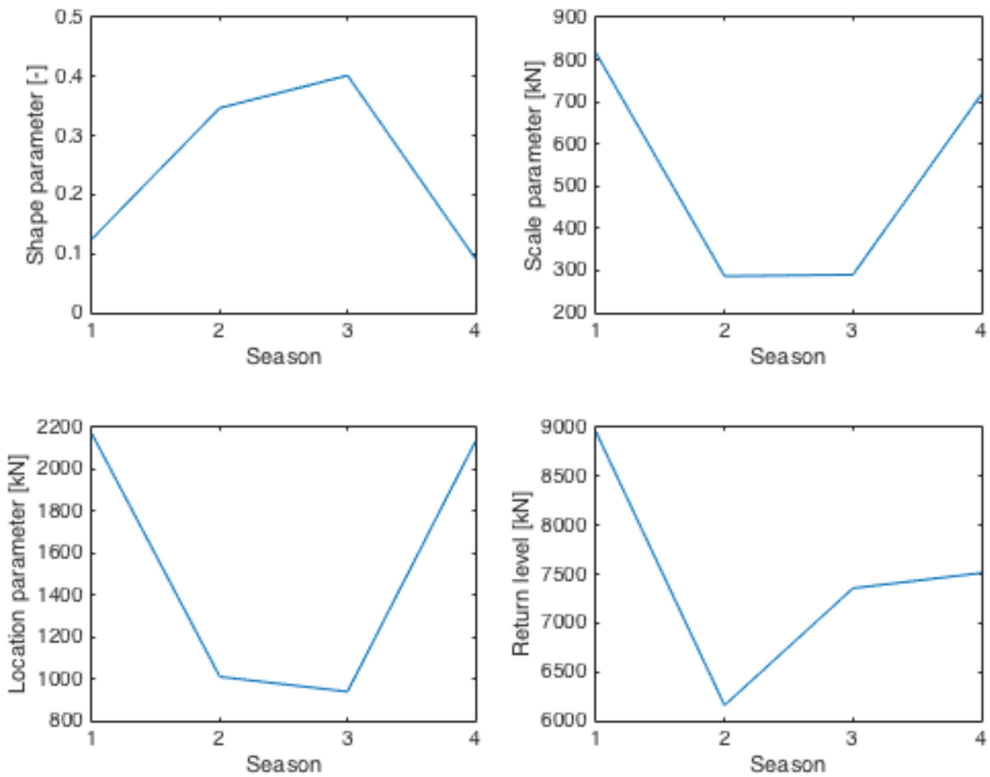

Figure 5-6 Seasonality of GEV parameters and extrapolation

It can be seen that the fits for the winter, spring and autumn are good and reliable. Overall we can see that the process for each season is approximately stationary and only for the summer we can see some non-stationary effects. The writer of this document thinks this non-stationary behaviour can be attributed to the steady and calm sea-state during the summer with some occasional heavy storms. If an entire year is considered, we see some variations between the seasons. As expected the extrapolated loads are the largest in winter and autumn and the lowest in spring and summer. The high extrapolation in the summer is due to the poor fit on the GEV distribution. The data in the summer doesn't really show the behaviour that can be expected for tail data.

This seasonal variation that can be seen within the observation of a year is a non-stationary process that has characteristics that change systematically through time. To cope with these non-stationary processes, it is possible to fit a GEV distribution with time-depend parameters (S. Coles 2001).

5.4.4 Conclusion GEV

The advantages of using the GEV theory are that it is less labour intensive and that arbitrary decisions like choosing a threshold are not necessary. The most important disadvantage of this method is the waste of data. For the annual maximum line tension only 30 data points are used for the extreme value analysis out of a set of almost 90000 measurements.

It is possible to incorporate seasonal effects into the distribution. If this is done it is possible to reduce the block length and so reduce the waste of data, and improve the fit and reliability of the extrapolations. This can be done by using time-depend GEV parameters. Using a time-depend GEV distribution results in a more complex methodology and will cancel out the simplicity of the methodology in comparison with the POT. Therefore, the decision is made to prefer the POT methodology above the GEV methodology. However, the non-stationary GEV methodology has some potential but for use in a design phase the method is to complicated.

5.5 Conclusions robustness

In this section the conclusions about the robustness of the applied method will be presented. First the conclusions about the simulation, secondly the conclusions about the parameter study and finally the conclusions about the possibility to use a GEV distribution.

The reason to prove the robustness of the methodology is to check the influence of change in input parameters on the reliability of the extrapolations calculated with the proposed methodology. In this manner also the influence of the simulation method that produces the data set can be studied.

We can conclude that it is possible to execute the simulations in a quasi-dynamic way. This results in a good approximation of the reality with a small error in comparison with a fully dynamic simulation. A quasi-dynamic simulation doesn't include line dynamics as included in the dynamic method to compensate for this, damping is added to the vessel. These added damping values are calculated by executing a free-decay test. This results in a simulation time which is 10 times shorter, and still produces a reliable extrapolation.

A parameter study is executed to see if it is possible to apply the proposed method on a range of cases with changes made in the environment, mooring configuration, response parameter… . This is possible and from the 8 cases tested, 7 passed all goodness-of-fit tests and passed the visual checks of the distribution fit. Some cases performed less than others. The cases that didn't performed good are:

3X3 cases, these will be studied in depth in chapter 6 and cases where the parameter of interest is the vertical turret load. The reason that it is difficult to represent the vertical turret load with a GPD is because there is a less distinct link between vertical turret load and wave height.

It's a common practice to use a minimum of 10 random wave seeds in the industry to produce reliable 100-year extrapolations. This is a consideration between exactness of the final extrapolation and simulation time. When time is not an issue as much seeds as reasonably possible can be produced to improve the final extrapolation. If time is an issue 10 random wave seeds have to be taken as a minimum to produce reliable extrapolations.

A GEV distribution can provide a good fit for annual and monthly maximum wave data. If load data is represented it is possible to do this with annual data on a GEV distribution. To make better use of the provided data and improve the extrapolation, it is possible to include seasonal variations in the distribution. In this case time-dependent GEV parameters must be used. This is complicated because an equation for the seasonal variations needs to be found, this equation is specific for every parameter. It can be concluded that it is possible to represent the load data with a GEV distribution, but in this thesis the GPD is preferred because it is simple to use in comparison with seasonal GEV distributions.

The final conclusion is that the proposed methodology is robust if the user is familiar with the requirements that need to be fulfilled for the input parameters. At least a simulation with 10 random wave seeds is required, the data set has to be large enough and a high initial threshold is required. The user of the method needs to be experienced to select an appropriate threshold and needs to be familiar with the shortcomings of the method. For example, less reliable extrapolations for vertical turret load.

6 Case Study

To illustrate a mooring design using extreme value theory to extrapolate 100-year return levels for the leading design parameters, a case study is performed. In the case study all conclusions made in the previous chapters will be implemented and an answer to the research question will be formulated.

In section 6.1 the common practice will be discussed. In the following paragraphs the different cases are described. And the results are presented and discussed. In the final paragraphs conclusions will be made.

6.1 Used methodology

Mooring design is based on three fundamental design aspects. First loading conditions and environmental conditions, secondly the analysis methodology and third the design criteria (Silva, et al. 2000).

The environmental conditions are in this case 30 years of metocean data of the Pierce field located in the North Sea 280km east of Aberdeen. The metocean data points are the result of measurements performed with 3 hour intervals. This results in 2920 data points each year.

The second fundamental design aspect is the analysis methodology. Evaluating the proposed methodology, extrapolating 100-year return levels of different design parameters fitted on a generalized Pareto distribution is the main objective of this case study.

The third fundamental design aspects are the design criteria. These are the criteria that result in the limitations of the design of the mooring system. Figure 6-1 illustrates the design parameters and where they act on the vessel.

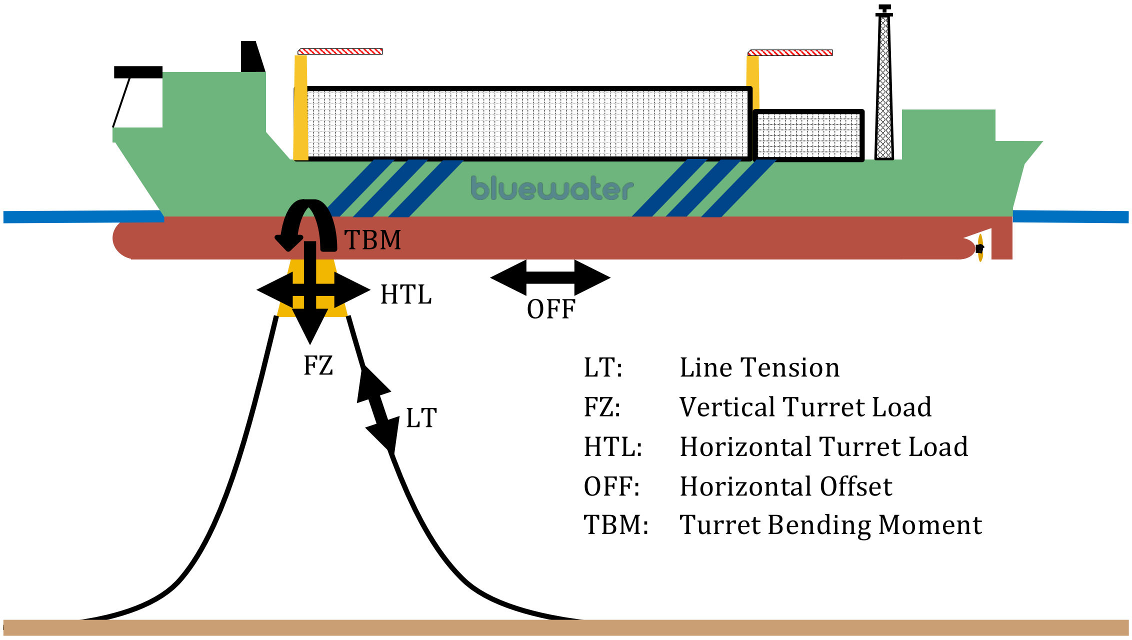

Figure 6-1 Design parameters

The presented design parameters are not all parameters used in the design of mooring systems, but these parameters are the dominant load parameters that directly influence the mooring, turret and riser systems. Five different parameters are identified. First the line tension that will result in the dimensions of the mooring lines, secondly the turret loads divided in horizontal and vertical turret load and the turret bending moment, and finally the horizontal offset or surge/sway motions of the vessel.

6.2 Cases

The case study is focused on the applicability of the proposed methodology for the 5 dominant load parameters. For the mooring lay-out a mooring system with 3 bundles of 3 mooring lines (3X3 clusters) is chosen. The mooring bundles are all separated 120° and the mooring lines within the bundles are separated 5°. The reason that a 3X3 mooring system is used is that it is a common used mooring system so it is likely that it is a design option that needs to be analysed with the proposed methodology in the future. Another reason for using a 3X3 mooring system is the asymmetrical lay-out that will possible expose the limitations of the methodology better then a symmetrical mooring lay-out.

Four mooring design cases are analysed. First the base case. This is an over dimensioned system comparable with the dimensions of a symmetrical 8X1 configuration. Secondly an under dimensioned case, the light case, is evaluated. The two final cases are medium cases with mooring dimensions that are expected to be close to realistic design dimensions. Table 6-1 summarizes the mooring dimensions used for the 4 different cases.

MOORING TYPES		Length	Mass	Diameter	EA	Subm.W.	MBL	Pre-tension Angle	Pre-tension
		m	kg/m	mm	kN	N/m	kN	deg	kN
BASE	Bottom Chain	30	432.2	147	1725000	3686	19089	42	425
	Bottom Wire	700	86.2	152	1609000	682	17000		
	Catenary Chain	575	432.2	147	1725000	3686	19089		
	Upper Wire	70	86.2	152	1609000	682	17000		
LIGHT	Bottom Chain	30	115.5	76	552600	985.3	6001	42	126.8
	Bottom Wire	700	32.5	95	560000	249.2	6043		
	Catenary Chain	575	115.5	76	552600	985.3	6001		
	Upper Wire	70	32.5	95	560000	249.2	6043		
MED1	Bottom Chain	30	259.9	114	1011000	2216.9	12420	42	273
	Bottom Wire	700	65	133.5	1124000	499.3	12129		
	Catenary Chain	575	259.9	114	1011000	2216.9	12420		
	Upper Wire	70	65	133.5	1124000	499.3	12129		
MED2	Bottom Chain	30	220.5	105	904600	1880.7	10754	42	237
	Bottom Wire	700	58.5	127.5	1007000	448.3	10867		
	Catenary Chain	575	220.5	105	904600	1880.7	10754		
	Upper Wire	70	58.5	127.5	1007000	448.3	10867		

Table 6-1 Mooring characteristics for case study

For the base case are besides the 5 dominant load parameters also some directional cases analysed for 2 load parameters, offset and line tension. For each bundle of 3 mooring lines a sector is created of +-60° (120° in total) from the centre of the bundle. These sectors are then analysed individually to calculate the 100-year return level for offset and line tension extrapolated for each individual sector.

6.3 Results

In this paragraph the results of the case study will be presented. Table 6-2 gives an overview of the results of the case study. The table is divided for the 4 cases (base, light, med1, med2) and a separate section for the directional analysed base cases.

	CASE	Threshold (U) [m,kN,kNm]	Scale parameter (σ) [m,kN,kNm]	Shape parameter (ξ) [-]	Return period (N) [yr]	Number of observations each year (n_y) [-]	Probability of exceedance of U (ξ_u) [prob.]	Visual fit Grade (5)	Goodness-of-fit tests [✓ or ✗]	Return level (usage factor) [m,kN,kNm]
BASE	MAX FZ (10)	-1650	31.62	-0.0177	100	2920	3.77e-4	3	✓	-1793
	MAX HTL (10)	5000	1847.3	0.0801	100	2920	7.88e-4	4	✓	17591
	MAX LT (10)	1750	620.84	0.1052	100	2920	15e-4	4	✓	7045 (69%)
	MAX TBM(10)	11000	2552.7	-0.0420	100	2920	11e-4	4	✓	24158
	MAX OFF (10)	13	8.6964	-0.446	100	2920	21e-4	2	✓	31.4
LIGHT	MAX FZ (10)	-540	29.5648	-0.1568	100	2920	8.2e-4	3	✓	-648.7
	MAX HTL (10)	4250	1383.1	0.008	100	2920	14e-4	4	✓	12773
	MAX LT (10)	1750	486.1616	0.0934	100	2920	15e-4	4	✓	5735 (160%)
	MAX TBM (10)	6500	1339.8	-0.0746	100	2920	14e-4	4	✓	12980
	MAX OFF (10)	33	4.3363	-0.2245	100	2920	8.5e-4	3	✓	46.7
MED1	MAX FZ (10)	-645	15.5338	-0.1067	100	2920	6.75e-4	3	✓	-707.7
	MAX HTL (10)	4900	1796.6	0.00066	100	2920	12e-4	3	✓	15392
	MAX LT (10)	1885	650.0594	0.0544	100	2920	17e-4	4	✓	6704 (92%)
	MAX TBM (10)	4600	1329.8	-0.1037	100	2920	18e-4	4	✓	10715
	MAX OFF (10)	30	4.0416	-0.3360	100	2920	9.1e-4	2	✓	40.2
MED2	MAX FZ (10)	-960	29.9653	-0.1997	100	2920	5.9e-4	3	✓	-1057
	MAX HTL (10)	4200	1845.3	-0.0446	100	2920	13e-4	3	✓	13853
	MAX LT (10)	1860	620.8627	0.0796	100	2920	12e-4	3	✓	6513(101%)
	MAX TBM (10)	8000	2210.7	-0.1451	100	2920	15e-4	5	✓	16923
	MAX OFF (10)	28	3.1211	-0.1396	100	2920	5.4e-4	3	✓	39.3
BASE DIRECTIONAL	0°+-60° MAX LT (10)	1400	736.23	0.0020	100	2920	9.5e-4	3	✓	5565 (55%)
	120°+-60° MAX LT (10)	1200	1007.70	-0.4554	100	2920	2.05e-4	2	✓	3070 (30%)
	240°+-60° MAX LT (10)	1700	643.60	0.1011	100	2920	11e-4	4	✓	6690 (66%)
	0°+-60° MAX OFF (10)	11.5	10.46	-0.5496	100	2920	11e-4	2	✓	29.7
	120°+-60° MAX OFF (10)	11	13.95	-0.8338	100	2920	2.17e-4	1	✓	27.2
	240°+-60° MAX OFF (10)	20	3.77	-0.2132	100	2920	5.25e-4	3	✓	31.6

Table 6-2 Overview results case study

The table shows the GPD parameters for the different cases. These parameters describe the GPD that has the best match with empirical data. Further the return period, the number of observations in a year and the probability of exceedance of the threshold U is provided. The visual fit parameter gives a grade out of a maximum of five points. Five points is a near perfect fit and 0 means that there is no match between the fit and the empirical data. Finally, the 100-year return level for the different dominant load parameters is presented.

The cases indicated in red are cases that have the worst fit and the green indicated cases have the best fit. The white cases are all good fits that result in reliable extrapolations. In section 6.4 the results of the case study will be discussed.

6.4 Discussion

The cases can be divided into 2 levels of goodness-of-fit. The first level are the cases that have a good and reliable fit. These are the cases in Table 6-2 coloured white for the good cases and green for the cases that fitted the best. The cases that are coloured red in Table 6-2 have a bad fit and the results are not reliable for use in a design stage. In this chapters the cases that aren't reliable will be discussed and solutions will be presented to improve the performance of the methodology for these specific cases.

The cases that aren't reliable are the directional cases and the cases with maximum horizontal offset as parameter of interest. First the directional cases will be discussed and secondly the cases with maximum offset as a parameter of interest.

After the analysing the results a final design option can be chosen. This design option is the best match between the environment and the mooring configuration. In Table 6-3 the characteristics of the chosen design (med1) will be presented.

Design parameters		**Line mark-up**	Length (m)	Mass (kg/m)	Diameter (m)	EA (kN)	Subm. W. (N/m)	MBL (kN)	Pre-tension angel (deg)	Pre-tension (kN)
Line tension	6704 kN	Bottom Chain	30	259.9	114	1011000	2216.9	12420	42	273
Vertical turret load	-707.7 kN	Bottom Wire	700	65	133.5	1124000	499.3	12129		
Horizontal turret load	15392 kN	Catenary Chain	575	259.9	114	1011000	2216.9	12420		
Turret bending moment	16923 kNm	Upper Wire	70	65	133.5	1124000	499.3	12129		
Offset	40.2 m									
Usage factor	92%									

Table 6-3 Final design characteristics case study

6.4.1 Directional cases

When an environment contains multimodal directional waves the design environment for the vessel will be more severe in comparison with unimodal directional waves. This is due to the steep nonlinear wave groups that occur in multimodal directional wave systems. In (Beal 1991) after a study about the practical value of directional ocean wave spectra, a conclusion is formulated. Critical wave conditions in local areas, based on calculated critical threshold values for wave direction and wave height are an improvement to unimodal descriptions of the ocean climate.

The most severe environmental conditions do not always occur when a storm is at its peak. Before a storm is fully developed large mooring forces already can occur. The reason for this is the poor alignment of the mean wind speed and significant wave height during the build up of a storm. This misalignment can be as large as 60°. Such conditions of already large waves and high wind speeds with a significant misalignment may result in the greatest mooring forces on a single point moored system (Bowers, Morton et Mould 2000).

Dependence of the intensity of the loading with respect to direction was investigated for West Africa by (Fontaine, et al. 2013). It was seen that there is a strong directionality of the environment in this region of the world. To represent the environment in this region analytical models are needed that can represent the directionality of the environment to produce reliable extrapolations. If this is the case for West Africa it can be concluded that it is wise to include directionality for different parts of the world to create a tool that can be used for a broad range of different environments. With this in mind directional cases are included in the case study. Including directionality resulted in some challenges to fit the data to a GPD. Methods on how to deal with these challenges are discussed in the next paragraphs.

If the evolution of the amount of data points throughout the process, from measurements with 3 hour intervals to a final extrapolation is studied, we can see that the amount of data decreases drastically as showed in Figure 6-2.

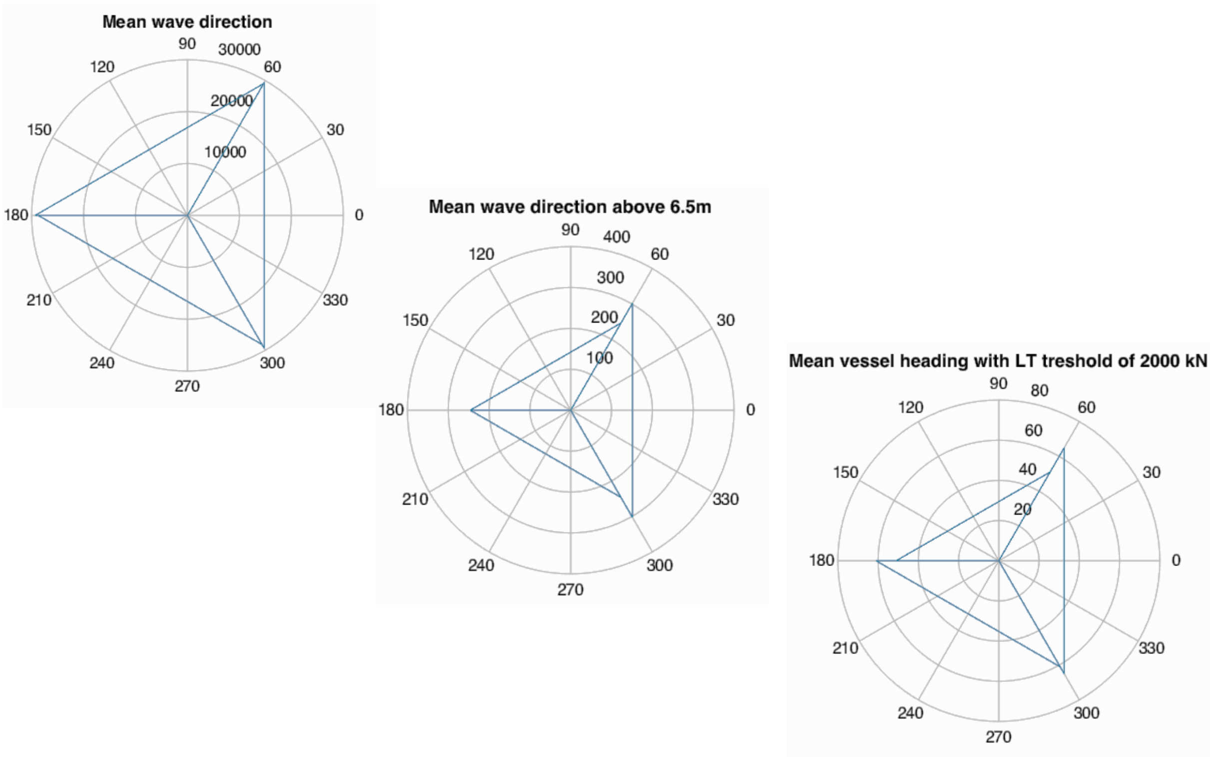

Figure 6-2 Evolution of data points throughout the extreme value analysis

The polar plots are divided in the three directions that are analysed in the case study. These directions are 0°±60°, 120°±60° and 240°±60°. This results in three sectors of 120° each. These sectors are chosen in a trade of between amount of data points for each sector and the requirement of independent identically distributed data points.

The first polar plot shows all measurements. This is 1 data point measured every 3 hours for 30 years resulting in 90000 data points in total and around 30000 for every direction.

The second polar plot shows the remaining data points after a threshold of 6.5m is set for the combined wave height. This results in ± 250 data points for every sector.

The third and last polar plot shows the remaining data points after the threshold (2000kN) is determined where above the GPD parameters are stable. This results in ± 50 data points for every sector that are fitted on a GPD with stable distribution parameters.

According to (S. Coles 2001) if the amount of data is limited it is not possible to make meaningful inferences about the extrapolation and the confidence intervals of that extrapolation. It is necessary to maximize the amount of data points to make reliable conclusions about the extrapolations or apply techniques to improve the reliability of the extrapolation. This can be done in different ways and will be discussed in the following paragraphs.

One method to improve the reliability of the extrapolation is the bootstrap resampling technique as described by (Dave, Li et Reeve 2008).

(Efron et Tibshirani 1998) Bootstrapping is a technique that can be used when a sample size is not large enough for statistical inference. If the underlying distribution of the empirical is known, bootstrapping can be used to account for the misrepresentation caused by the specific sample that is not a good representation of the reality.

If this technique is applied for every sector with sample size N, a bootstrap with sample size N is taken ie. drawing a new sample of size N out of the initial sample. If this procedure is repeated a large number of times, a large number of extrapolations are obtained and these can be used to produce a distribution of the extrapolations. With this distribution, conclusions can be made about the stability of the results. It is not really a way to enlarge the original data set but to improve the estimation of the confidence intervals. The confidence intervals will be narrower compared to the initial extrapolation plot.

Another method to improve the reliability of the extrapolations is to analyse every sector on it is own. So for every sector an analysis of the metocean data will be done to set a combined wave height threshold for every sector. For the dominant storm direction this threshold will be in the neighbourhood of the original threshold and for the other (red coloured cases) the combined wave height threshold will be set lower. This will result in a larger set of data points that can be simulated and fitted on a GPD.

6.4.2 Offset cases

The second type of cases that do not perform well are cases where maximum offset is the extrapolated parameter of interest. First the offset samples are plotted against the significant wave height. This is illustrated in Figure 6-3 for two mooring configurations.

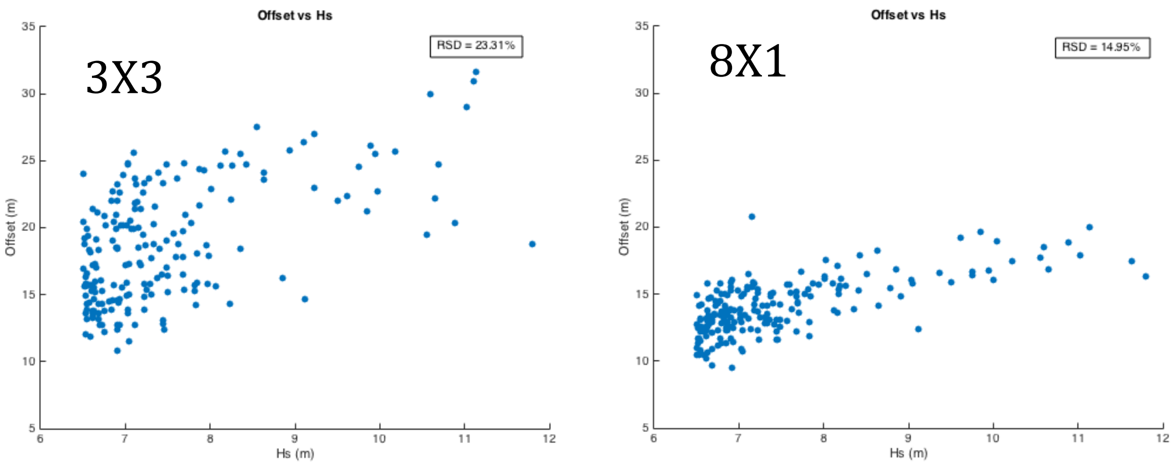

Figure 6-3 Scatter plot of offset vs significant wave height

We can see that the spread of the plot offset vs Hs for the 3X3 mooring configuration is larger than for 8x1 mooring configuration. Also the relative standard deviation (RSD) is given. We expect that the fit to the Generalized Pareto Distribution is better if the spread and so the relative standard deviation is smaller. This is showed in Figure 6-4.

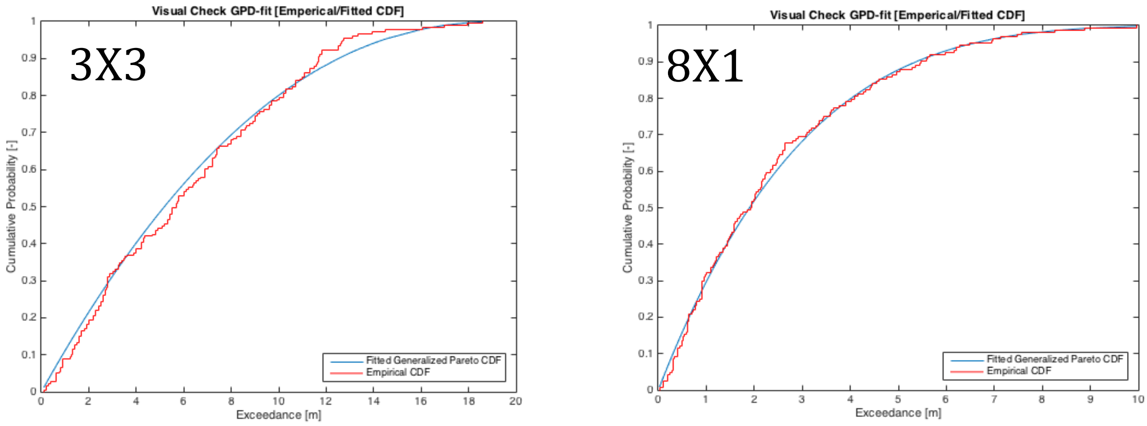

Figure 6-4 Cumulative probability of the empirical data and the GPD distribution

It can be observed that indeed the fit of the data that has a smaller spread does fit better to the GPD than the data with a larger spread. So it can be concluded that the fit to the GPD has a relation to the spread of the data points plotted against the significant wave height.

This spread is the result of the difference in stiffness of the entire mooring system when the vessel experiences a displacement in line with a mooring line bundle (in the direction 180° shifted with the direction bundle of mooring lines) or in between two bundles of mooring lines. Figure 6-5 shows the difference in restoring force for in-line and in between line (line direction + or – 60°) offset for the 3X3 and 8X1 mooring configuration. If the differences for in-line and in-between line tension for the 3X3 mooring configuration are compared with these differences in tensions for the 8X1 mooring configuration it can be seen that restoring force for a certain offset depends on the direction of this offset. For the 8X1 case it can be seen that the restoring force only depends on the offset and not on the direction of this offset. The dependence of the restoring force on the direction of the offset on a 3X3 mooring configuration will induce deviation in the restoring forces. This will have an adverse effect on the fit to the distribution.

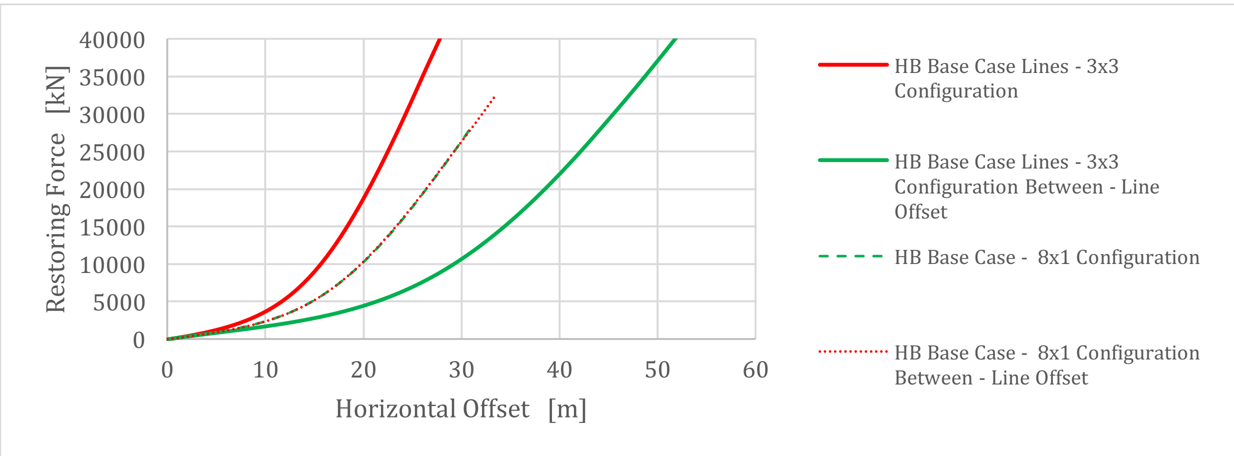

Figure 6-5 Restoring force curves for in-line and in between line offset

To reduce the spread of the data its possible to include directionality. To include directionality the techniques proposed in 6.4.1 need to be applied. As a supplement on the proposed techniques it is also possible to incorporate an automated threshold selection method. This technique, that optimizes the trade off between waste of data and goodness-of-fit cancels out the need of subjective interpretation of plots by users is described by (Thompson, et al. 2008).

Classic threshold is based on empirical selection techniques that require subjective interpretation of plots by users. Thompson proposes an

"automated, simple and computationally inexpensive threshold selection method based on the distribution of the difference of parameter estimates when the threshold is changed". (Thompson, et al. 2008)

The steps taken in the process of automated threshold selection are described by Thompson as follows:

1. "Identify suitable values of equally spaced candidate thresholds $u_1 < u_2 < \cdots < u_n$. We found that setting n= 100 gives good results. We take u1 to be the median and u_n to be the 98% quantile of the data, unless fewer than 100 values exceed this value, in which case u_n is set to the 100th data value in descending order. Our procedure performs well in such circumstances. Less reliable results were obtained from smaller data sets. If u is a suitable threshold, then all differences $\tau_{u_j} - \tau_{u_{j-1}}$ ($\tau_{u_j} = \widehat{\sigma_{u_j}} - \widehat{\xi_{u_j}} u_j$) have an approximate normal distribution with mean 0 provided $u \le u_{j-1} < u_j$. If u is unsuitable, then these differences may not follow a normal distribution. This suggests that a suitably applied test for normality is an effective method to determine u. The Pearson's Chi-square Test is used as a test of goodness-of-fit to establish whether or not the observed differences are consistent with a normal distribution with mean 0; see (Greenwood 1996).

2. Initially, we consider $u = u_1$ and perform the Pearson normality test based on all the differences $\tau_{u2} - \tau_{u1}, \tau_{u3} - \tau_{u2}, \cdots, \tau_{u_n} - \tau_{u_{n-1}}$. If the null hypothesis of normality is not rejected, u is taken to be a suitable threshold. If the null hypothesis is rejected, then we consider $u = u_2$, remove $\tau_{u_2} - \tau_{u_1}$ from the set of differences considered, and repeat the above procedure. We have found from a simulation study that a size 0.2 Pearson normality test generally performs most consistently over a range of normality tests and sizes. Reducing the size of the test has the effect of lowering the chosen threshold.

3. Step 2 is repeated until the Pearson's normality test indicates that the differences are consistent with a normal distribution with mean 0. If this does not happen, u_n is returned with a warning. Our experience is that this latter situation occurs rarely". (Thompson, et al. 2008)

This method improves the confidence intervals of the resulting return period as seen in Figure 6-6. A comparison is made between the method used by (S. Coles 2001) and the method proposed in (Thompson, et al. 2008).

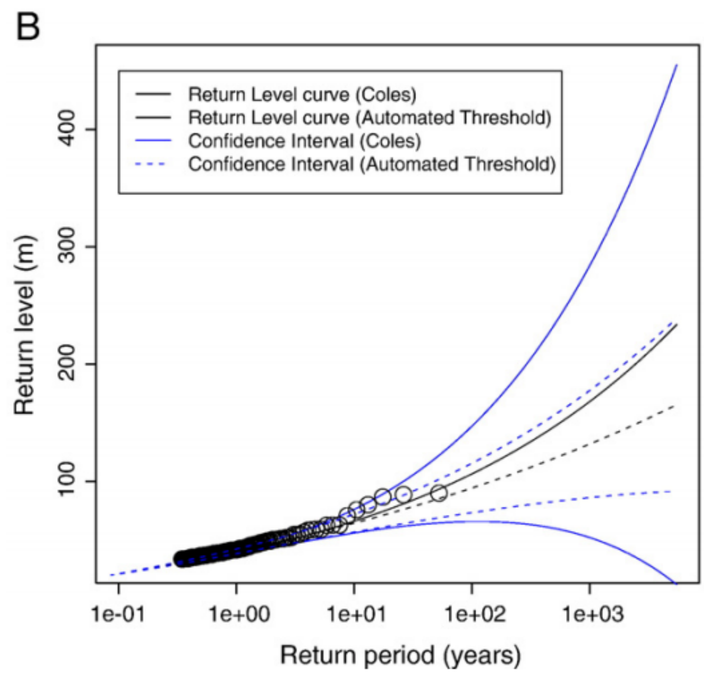

Figure 6-6 Comparison Coles and Automated Threshold

An extension to this method is to make use of directional wave data and not only omnidirectional wave heights. It is clear that wave heights vary over wave direction. Therefore, it makes sense to include directional wave data into the automated threshold selection. The method is comparable with the method that only uses wave heights and is described comprehensive in (Thompson, et al. 2008).

6.5 Conclusions case study

In this section the conclusions based on the analysis of the execution and results of the case study are presented. It can be stated that for four of the five dominant load parameters (line tension, horizontal turret load, vertical turret load and turret bending moment) it is possible to make a reliable omnidirectional extrapolation by fitting the data to a Generalized Pareto Distribution. This can probably be done for different mooring systems besides the studied 3X3 and 8X1 mooring systems. The performance of the methodology isn't influenced by the dimensions of the mooring components. The methodology performed well for the four studied cases (base, light, medium1, medium2).

For one dominant load parameter the methodology didn't perform well. This parameter is maximum horizontal offset. The reason for this is the spreading of the data. For one wave height multiple offset values are measured depending on the direction the waves are coming from in relation to the mooring system. The background behind this phenomenon is the difference in the tension of the mooring system when waves are encountered in line with a mooring line bundle, or in-between two mooring line bundles. The proposed solution is to include directionality and analyse smaller individual sectors, and include an automated threshold selection method to enlarge the sample size when directionality is included.

During the case study some tests are performed to include directionality into the methodology. It can be concluded that it is possible to include directionality to extrapolate load data. Although the fit was representative for the underlying directional data and passed the Chi-square and Kolmogorov goodness-of-fit tests, the quality of the fit was considerable lower then other fits with a larger underlying sample. To improve the quality and reliability of the extrapolation it is possible to incorporate bootstrap resampling techniques to check the stability of the extrapolations and improve the estimation of the confidence intervals. Another way to improve the quality of the fit is to enlarge the sample size by defining a separate threshold. This threshold can also be defined automatically, for every sector after analyses of the metocean data in the specific environment.

7 Conclusions

In this chapter some overall conclusions will be presented about the possibility to apply extreme value theory in an efficient way during a design stage to assess different mooring design choices. The conclusions will be presented following the structure of this thesis. At the end of each chapter the comprehensive conclusions can be found.

For the method reconstruction it can be concluded that the three parts that form the overall method together, perform good and will not be the cause of some deviating results.

A quasi-dynamic simulation method is chosen. The main reason for this is to limit the computational resources that are required for a dynamic analysis. This will improve the possibility to use the methodology in an efficient way in a design process. To compensate for the absence of line damping in the quasi-dynamic approach, linear damping is added to the vessel.

To prove the robustness of the method a parameter study is executed. It can be concluded that for most variations good extrapolation can be made. The most remarkable exception is the case when a mooring system has a large stiffness difference for in-line and in-between-line translations.

An alternative approach is studied for the POT (GPD) method. The GEV distribution can provide a good fit for annual load data. To make better use of the provided data it is possible to incorporate time-depend GEV parameters that takes seasonal variations into account.

In the final part of this thesis a case study is executed to study the applicability of the five dominant load parameters. For a 3X3 mooring configuration it is possible to produce reliable extrapolations for four of the five load parameters with the proposed methodology. These parameters are vertical turret load, horizontal turret load, line tension and turret bending moment. For the fifth parameter (horizontal offset) some adaption of the proposed method can be done. This can be done by including directionality.

The answer to the research question is: It is possible to produce reliable 100-year extrapolations for shallow water by fitting responses from quasi-dynamic simulations of environmental data to a generalized Pareto distribution for the most dominant load parameters, with or without some adaptions to the methodology depending on the mooring lay-out.

8 Recommendation for further work

In this section possible further work will be presented. This further work is mostly focused on improving the methodology and the resulting extrapolations.

8.1 Joint occurrence

In (Oostra 2015) the following conclusions is stated:

"Since only the extrapolations based on dataset II and dataset II-refined are within reasonable distance of the result from the conventional method, the conclusion can be made that focusing on the maximum Hs case within a threshold exceeding period is not sufficient."

This statement says that the best performing dataset is the dataset with a result close to the conventional method. It will be valuable to get a good insight in the differences and dependences to the environmental characteristics between the conventional method of creating a 100-year design environment with associated wind, waves and current and the response based approach.

Analysis of dependence (Fontaine, et al. 2013) and joint probabilities can be done in two steps. The first step is to describe the marginal PDF of the main variables. These are wind, wave and current. The empirical distributions can now be fitted by probability distribution models like GPD or GEV.

The second step described in (Fontaine, et al. 2013) is to analyse the dependence between variables, using three methods:

- "Statistical test of significance of correlation: Bravais–Pearson and Spearman.
- Scatter plot between two variables (X1 and X2) and analysis of main conditional statistical parameters (mean and standard deviation) of one variable versus the other.
- Principal Component Analysis (PCA) that allows for the analysis of dependence between more than two variables. " (Fontaine, et al. 2013)

The dependence analysis resulted in following conclusions:

- "Independence of sub-surface currents versus wind and sea states.
- Independence between sea state systems.
- Independence of wind and swell systems.
- Dependence of wind and wind sea (intensity and direction).
- Dependence of Hs and Tp in every sea state system. " (Fontaine, et al. 2013)

Applying this study will result in a better insight in the sensitivity of both methodologies to variations in the environment on the final extrapolations.

8.2 Climate change

The trend nowadays is to require longer return periods for the assessment of mooring configurations. When longer return periods are required it will be necessary to study the influence of climate change on extreme return levels.

Global warming will result in increased temperature all over the world. This will result in a sea level rise, and probably in an increase of the frequency and severity of extreme events.

8.3 Cancel out arbitrary decisions

The reliability of extreme return levels with the peak-over-threshold approach is highly depending on the engineer using it. It would be an improvement to minimize the influence of the user on the decisions made through the process. It is possible to study the possibility to improve or automate the threshold selection procedure and its influence on the final extrapolations.

8.4 Deep water

In this thesis all calculations are done for the Pierce field with a water depth of 83 meter. It would be valuable that the influence of deep water is studied. For deep water the low frequency damping terms increase considerably, so the mooring line dynamics will become more important.

9 Bibliography

Battjes, J.A. 1979. “Encounter probability of extreme structural response values based on multi-parameter descriptions of the physical environment.” *BOSS conference proceedings.*

Beal, Robert C. 1991. *Directional ocean wave spectra.* Baltimore: The Johns Hopkins University Press.

Bowers, J.A., I.D. Morton, and G.I. Mould. 2000. “Directional statistics of the wind and waves.” *Elsevier* 13-30.

Brown, D. T., G. J. Lyons, and H. M. Lin. 1995. “Advances in Mooring Line Damping.” *Underwater Technology.* Society for Underwater Technology. 5-11.

Coles, Stuart. 2001. *An Introduction to Statistical Modeling of Extreme Values.* London.

Coles, Stuart G., and Jonathan A. Tawn. 1994. “Statistical Methods for Multivariate Extremes: An Application to Structural Design.” *Journal of the Royal Statistical Society. Series C (Applied Statistics)* (Wiley for the Royal Statistical Society) 1-48.

Dave, Simmonds, Ying Li, and Dominic Reeve. 2008. “Quantifying uncertainty in extreme values of design parameters with resampling techniques.” *Ocean engineering* (Elsevier) 35: 1029-1038.

Dekking, F.M., C. Kraaikamp, H.P. Lopuhaä, and L.E. Meester. 2005. *A modern introduction to probability and statistics.* Delft: Springer.

DNV.GL. 2015. *Offshore standard position mooring (DNVGL-OS-E301).* Standard, DNV.GL.

Efron, Bradley, and Robert J. Tibshirani. 1998. *An introduction to the bootstrap.* CRC Press LLC.

Ferreira, J.A., and C. Guedes Soares. 2001. “Modelling bivariate distributions of significant wave height and mean wave period.” *Elsevier.*

Fontaine, E., P. Orsero, A. Ledoux, R. Nerzic, M. Prevosto, and V. Quiniou. 2013. “Reliability analysis and Response Based Design of a moored FPSO in West Africa.” *Structural Safety* (Elsevier) 82-96.

Greenwood, Priscilla E. 1996. *A guide to Chi-Squared Testing.* New York: Wiley & Sons, Inc.

Huse, E. 1986. “Influence of mooring line damping upon rig motions.” *Offshore technology conference.* Houston: Offshore technology conference. 433-438.

Johanning, J., G.H. Smith, and J. Wolfram. 2006. “Mooring design approach for wave energy converters.” *Proc. IMechE.* Edinburgh: Journal Engeneering for the maritime environment. 159-174.

Klemens, Ben. 2009. *Modeling with data (tools and techniques for scientific computing).* Princeton: Princeton university press.

Marin. 2008. *Dynfloat Master.* Manual, Marin, Wageningen: Marin.

—. 2015. *Marin.nl.* Accessed 11 23, 2015. http://www.marin.nl/web/Research-Topics/Mooring-offloading/Mooring-loads.htm.

Massey , Frank J. 1951. "The Kolmogorov-Smirnov Test for Goodness of Fit." *Journal of the American Statistical Association* 68-78.

Méndez, F. J., M. Menéndez, A. Luceno, and I.J. Losada. 2006. "Analyzing Monthly Extreme Sea Levels with a Time-Dependent GEV Model." *Journal of atmospheric and oceanic technology* 24: 894-911.

Menéndez, Melisa, Fernando J. Méndez, Cristina Izaguirre, Alberto Luceño, and Inigo j. Losada. 2009. "The influence of seasonality on estimating return values of significant wave height." *Coastal Engineering* (Elsevier) 56: 211-219.

Moore, David S. 1976. *Chi-Square Tests.* Purdue University.

Mudelsee, Manfred. 2010. *Climate Time Series Analysis.* Hannover: Springer.

Oostra, Kay. 2015. *On the use of hindcasts in SPM design.* Delft.

Silva, R.M.C, J.M. Vasconcellos C.E. Parente, B.P. Jacob, and A.C. Fernandes. 2000. "Review of design criteria for deepwater risers and mooring systems in a multidirectional environment." *Proceedings of the tenth international offshore and polar engineering conference.* Seattle: The international offshore and polar engineers. 8-14.

Stansell, Paul, Julian Wolfram, and Stan Zachary. 2003. "Horizontal asymmetry and steepness distributions for wind-driven ocean waves from severe storms." *Applied ocean research 25* (Elsevier) 137-155.

the International Organization for Standardization. 2005. *ISO 19901-7.* First Edition. Geneva: ISO.

Thompson, Paul, Yuzhi Cai, Dominic Reeve, and Julian Stander. 2008. "Automated threshold selection methods for extreme wave analysis." *Coastal Engineering* (Elsevier).

Triantafyllou, M. S., D. K. P. Yue, and D. Y. S. Tein. 1994. "Damping of moored floating structures." *Offshore technology conference.* Houston: Offshore technology conference. 215-224.

Tromans, Peter S., and Luc Vanderschuren. 1995. "Response Based Design Conditions in the North Sea: Application of a New Method." *OTC 7683.* Houston: Offshore technology conference. 387-398.

Wichers, J. E. W., and M. F. van Sluijs. 1979. "The influence of waves on the low-frequency hydrodynamic coefficients of moored vessels." *Offshore technology conference.* Houston: Offshore technology conference. 2313-2324.

Wichers, Johan. 2013. *Guide to Single Point Moorings.* Delft.

Wilk, M.B., and R. Gnanadesikan. 1968. "Probability plotting methods for the analysis of data." *Biometrika* 55: 1-17.

Appendix I Dynfloat output method reconstruction barge

```
  D Y N F L O A T  v2003_1  Date 2015-11-17  Start Time 11:28
Page :  1


                   General data  and  vessel particulars

                    Review of input


  Project :
  Casename: MRNDBR

                  Case        Description
  Environment :   MRNDBR
  Vessel      :   MRNDBR      Method Reconstruction Barge
  Mooring     :   MRNDBR      Method Reconstruction Barge
  Control     :   MRNDBR
  Output      :   MRNDBR


  Main particulars

  Type of vessel                       : Tanker
  Type of bow                          : Cylindrical  bow
  Length between perpendiculars        :     250.00       [m]
  Moulded breadth                      :      35.00       [m]
  Draft                                :      16.00       [m]
  Displaced moulded volume             :  119000.00    [m**3]
  Mass of vessel                       :  121975.00     [ton]
  Loading condition in % of max. draft :     100.00       [%]

  Projected side  area above waterline :    1773.91    [m**2]
  Projected front area above waterline :     553.43    [m**2]




  D Y N F L O A T  v2003_1  Date 2015-11-17  Start Time 11:28
Page :  2


                   General data  and  vessel particulars

                    Review of input  (Continued)
```

```
  Project :
  Casename: MRNDBR

                  Case        Description
  Environment :   MRNDBR
  Vessel      :   MRNDBR      Method Reconstruction Barge
  Mooring     :   MRNDBR      Method Reconstruction Barge
  Control     :   MRNDBR
  Output      :   MRNDBR
  Hydrodynamic data

  Radius of inertia              (Kxx) :      11.66       [m]
  Radius of inertia              (Kyy) :      62.50       [m]
  Radius of inertia              (Kzz) :      62.50       [m]
  Roll  moment of inertia        (Ixx) :0.16592E+08  [kNm**2]
  Pitch moment of inertia        (Iyy) :0.47646E+09  [kNm**2]
  Yaw   moment of inertia        (Izz) :0.47646E+09  [kNm**2]
  Location of COG wrt midship    (Xcog):       5.00       [m]
  Location of COG wrt centreline (Ycog):       0.00       [m]
  Location of COG wrt keel       (Zcog):       7.50       [m]

  Additional damping for Surge         :       0.00    [kNs/m]
  Additional damping for Sway          :       0.00    [kNs/m]
  Additional damping for Yaw           :       0.00[kNms/rad]

  Wave drift force computation         : full matrix
                                         (WDD coef. for zero
current)

  User supplied hydrodynamic datafile  : M7390100.HYD


  Correction for Z-cog is applied.



  D Y N F L O A T  v2003_1  Date 2015-11-17  Start Time 11:28
Page :  3


                   General data  and  vessel particulars


  Project :
  Casename: MRNDBR

                  Case        Description
  Environment :   MRNDBR
  Vessel      :   MRNDBR      Method Reconstruction Barge
  Mooring     :   MRNDBR      Method Reconstruction Barge
```

```
Control      :   MRNDBR
Output       :   MRNDBR
LF damping model : 1 (acc. J.E.W.Wichers)
Current Force Coefficients : OCIMF data


Wind    Force Coefficients : OCIMF data


Reference points (vessel fixed)

Number           X           Y           Z
                [m]         [m]         [m]

     1       95.00        0.00       -2.50


D Y N F L O A T  v2003_1  Date 2015-11-17  Start Time 11:28
Page :  4

                        Environmental conditions


                    Review of input  (Continued)


Project :
Casename: MRNDBR

                Case        Description
Environment :   MRNDBR
Vessel      :   MRNDBR      Method Reconstruction Barge
Mooring     :   MRNDBR      Method Reconstruction Barge
Control     :   MRNDBR
Output      :   MRNDBR


Water depth                         :      75.00       [m]
Rho Water                           :    1025.00 [kg/m^3]
Rho Air                             :       1.25 [kg/m^3]


Waves

Type of wave spectrum               : No wave


Swell
```

```
  Type of swell spectrum                : No swell


  Wind

  Type of wind                          : Constant speed and
direction

  Wind velocity                         :        0.00    [m/s]
  Wind direction                        :        0.00    [deg]


  Current

  Type of current                       : Constant speed and
direction

  Current velocity                      :        0.00    [m/s]
  Current direction                     :        0.00    [deg]


  D Y N F L O A T  v2003_1  Date 2015-11-17  Start Time 11:28
Page :  5

                         Mooring system data


                      Review of input  (Continued)


  Project :
  Casename: MRNDBR

                Case        Description
  Environment : MRNDBR
  Vessel      : MRNDBR      Method Reconstruction Barge
  Mooring     : MRNDBR      Method Reconstruction Barge
  Control     : MRNDBR
  Output      : MRNDBR


  Design Water depth              :       75.00      [m]
  Design draft                    :       10.00      [m]

  Mooring Type                    : Spread mooring

  Design location (Earth Bound Position of Vessel Keel Point)

  X - coordinate                  :     -95.000     [m]
  Y - coordinate                  :       0.000     [m]
```

```
Heading                        :      0.000   [deg]


Number of (defined) LEGS       :          2


Number of (defined) LEG-types  :          1
Number of (defined) BUOYS      :          0
Number of (defined) CLUMPS     :          0

Anchor allocation              : Pre-Tension Angle & Azimuth Angle
Seabed option                  : Horizontal seabed plane
```


Mooring system data

Review of input (Continued)

```
Project :
Casename: MRNDBR

                Case        Description
Environment :   MRNDBR
Vessel      :   MRNDBR      Method Reconstruction Barge
Mooring     :   MRNDBR      Method Reconstruction Barge
Control     :   MRNDBR
Output      :   MRNDBR
```

Fairlead Coordinates

Line No [-]	X-Coord [m]	Y-Coord [m]	Z-Coord [m]
1	0.000	0.000	0.000
2	0.000	0.000	0.000

Anchor allocation input

Line No [-]	Line Type [-]	PreTension Angle [deg]	Azimuth Angle [deg]
1	1	35.000	180.000
2	1	35.000	0.000

```
  D Y N F L O A T  v2003_1  Date 2015-11-17  Start Time 11:28
Page :  7

                        Mooring system data


                     Review of input  (Continued)


  Project :
  Casename: MRNDBR

                  Case        Description
  Environment :   MRNDBR
  Vessel      :   MRNDBR      Method Reconstruction Barge
  Mooring     :   MRNDBR      Method Reconstruction Barge
  Control     :   MRNDBR
  Output      :   MRNDBR

  Attention !! Mooring legs should be defined from

               ANCHOR up to the FAIRLEAD

  Leg type :  1 Number of segments :   1


  Type of segment                : Chain
  Length                         :    1550.00    [m]

  Mass                           :      352.5 [kg/m]
  Diameter                       :     133.00    [mm]
  Breaking strength              :    14693.6    [kN]
  Elasticity                     :  1297480.0    [kN]
  Weight (submerged)             :     3008.7   [N/m]

  Inertia  Coef.Normal Dir. (CIN):       3.10    [-]
  Inertia  Coef.Tangen.Dir. (CIT):       1.70    [-]
  Drag     Coef.Normal Dir. (CDN):       2.40    [-]
  Drag     Coef.Tangen.Dir. (CDT):       0.80    [-]
  Friction Coef.Normal Dir. (CFN):       0.00    [-]
  Friction Coef.Tangen.Dir. (CFT):       0.00    [-]
  Selected buoy  number          :          0
  Selected clump number          :          0
  Number of elements of segment  :          1
```

```
  D Y N F L O A T  v2003_1  Date 2015-11-17  Start Time 11:28
Page :  8


                        CONTROL data

                    Review of input


  Project :

  Casename: MRNDBR
                Case        Description
  Environment :  MRNDBR
  Vessel      :  MRNDBR      Method Reconstruction Barge
  Mooring     :  MRNDBR      Method Reconstruction Barge
  Control     :  MRNDBR
  Output      :  MRNDBR


  Total simulation time              :    10001.0   [s]
  Start-up time                      :        1.0   [s]
  Max. heading angle                 :      45.00 [deg]
  Start condition                    : User defined (Decay)
  Simulation option                  : Quasi-Static
  Computation option                 :

            Mean envir. forces + equil. configuration+time domain
simulation


  X-start (wrt to design position)    :     -20.00 [m]
  Y-start (wrt to design position)    :       0.00 [m]
  Heading (wrt to design position)    :       0.00 [deg]



  D Y N F L O A T  v2003_1  Date 2015-11-17  Start Time 11:28
Page :  9


                        CONTROL data

                    Review of input
```

Appendix II Comparison between Dynamic and Quasi-dynamic simulation

II.I Time-trace case 5050108 LINE 5 Dynamic and Quasi-Dynamic and a zoomed part of the time-trace

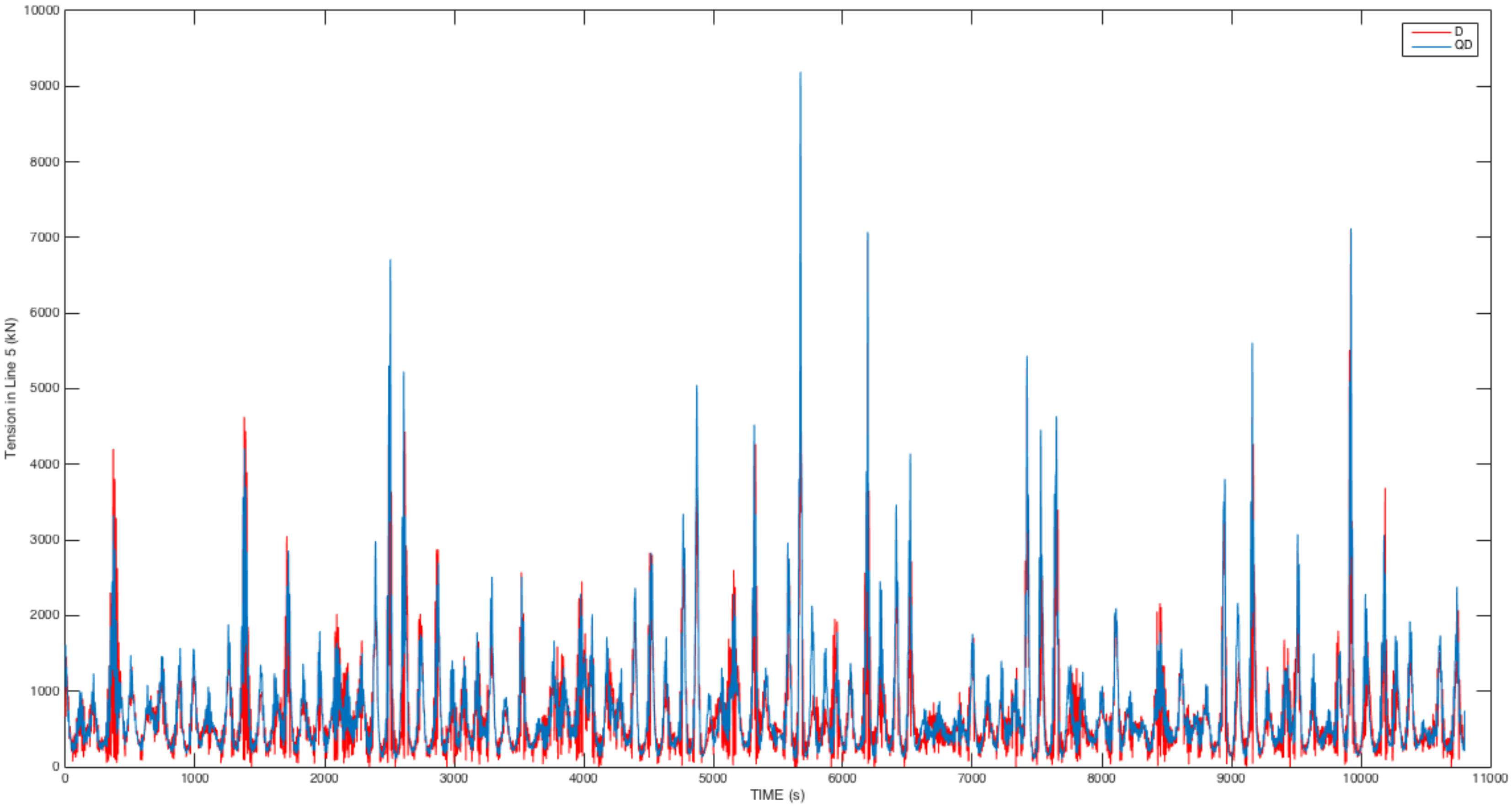

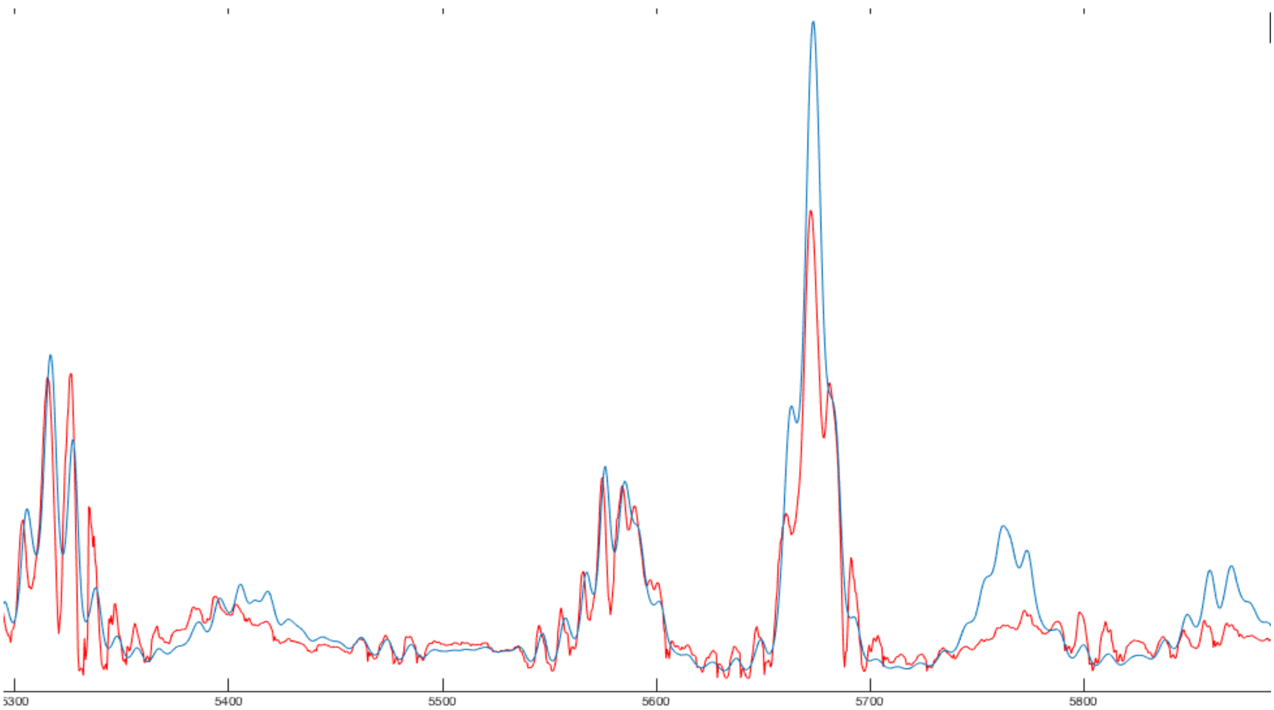

II.II Restoring curve case 5050108 LINE 5 Dynamic and Quasi-Dynamic

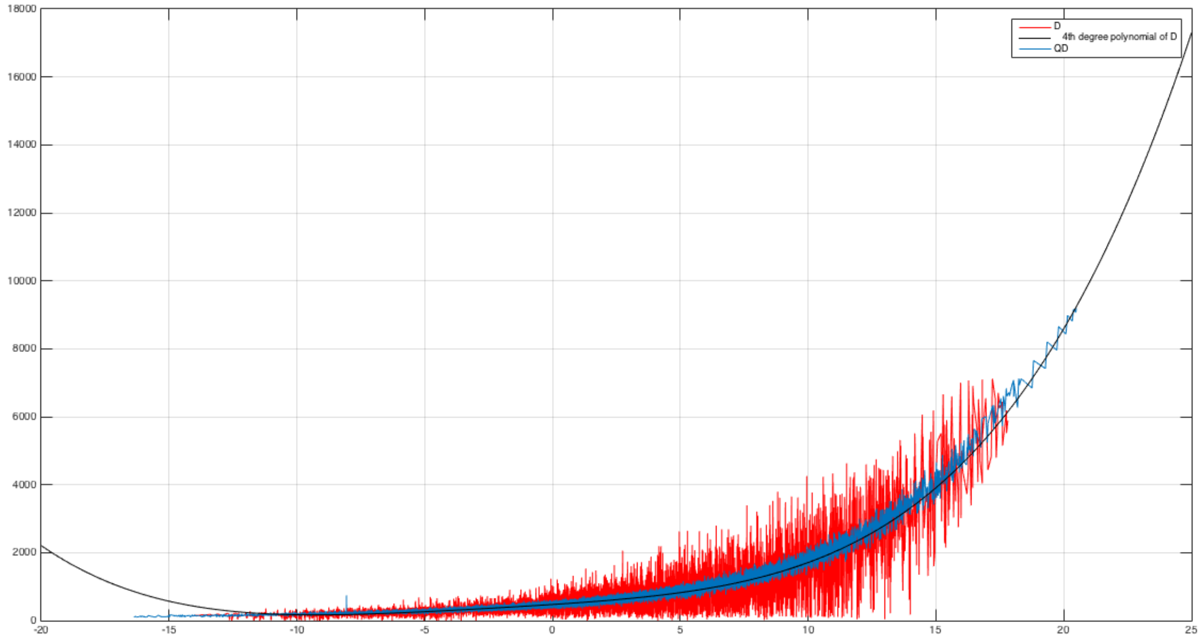

Appendix III Results parameter study

In this appendix all the results obtained in the parameter study are presented. For the 8 different cases a short analysis will be made.

III.I Results dynamic analysis dataset II refined (Oostra 2015)

u [kN]	2900
σ [kN]	1031.1
ζ	0.0306
N	100
n_y	2920
ζ_u	0.0015
100-year MAX LT	9707 kN
100-year MAX LT BES	10094 kN

Test	*Significance level*	*Null-Hypothesis*	*Outcome*	*Simulation method*
Chi-Square	5%	DATASET II - Refined follows GPD	Accepted	Dynamic
Kolmogorov-Smirnov	5%	DATASET II –Refined follows GPD	Accepted	Dynamic

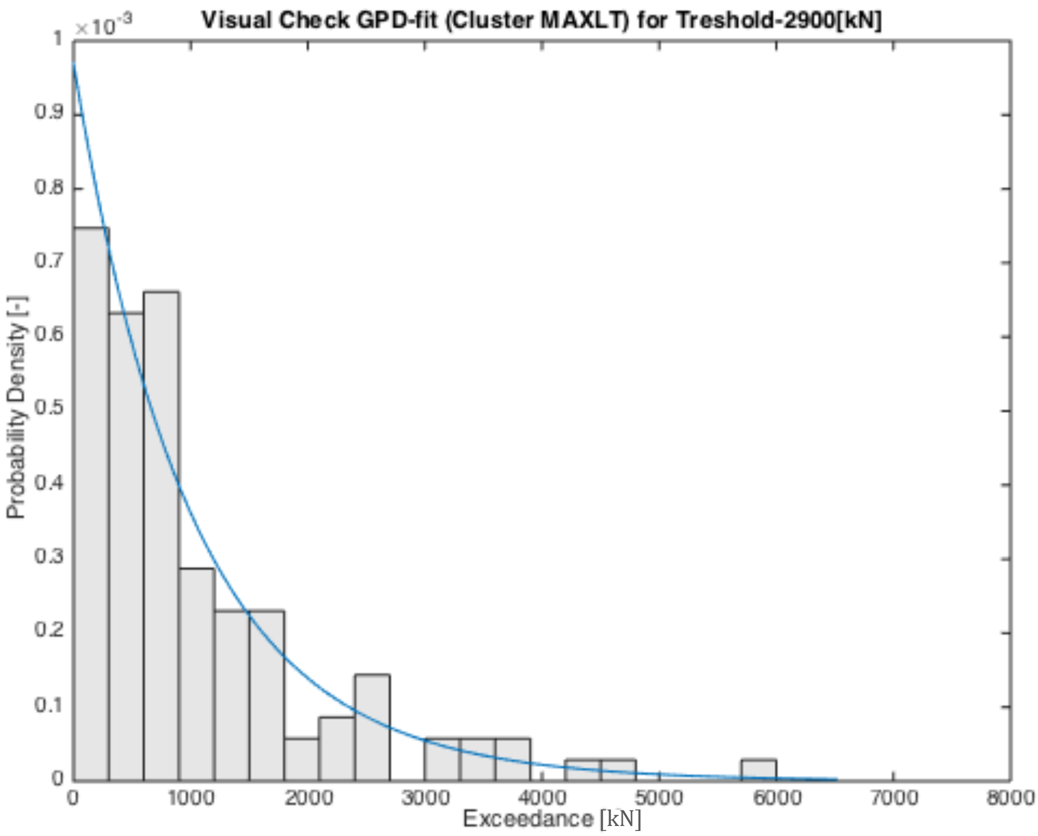

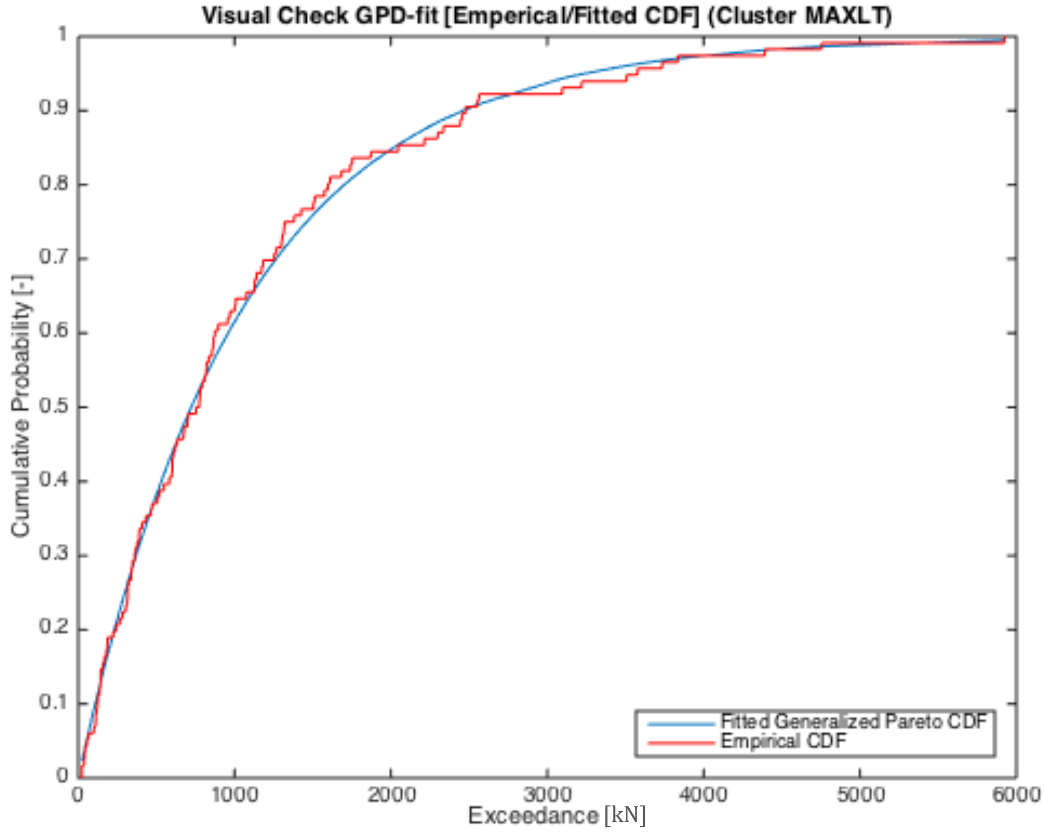
Visual Check GPD-fit [Emperical/Fitted CDF] (Cluster MAXLT)
Cumulative Probability [-]
Exceedance [kN]
Fitted Generalized Pareto CDF
Empirical CDF

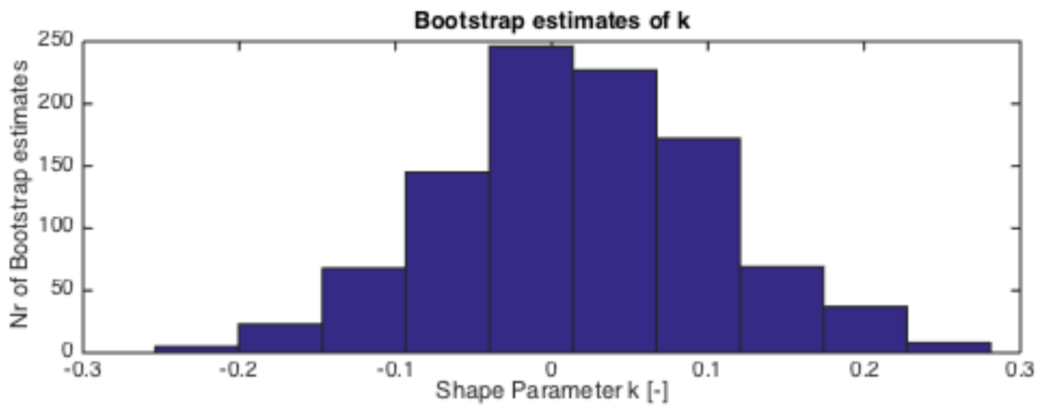
Bootstrap estimates of k
Nr of Bootstrap estimates
Shape Parameter k [-]

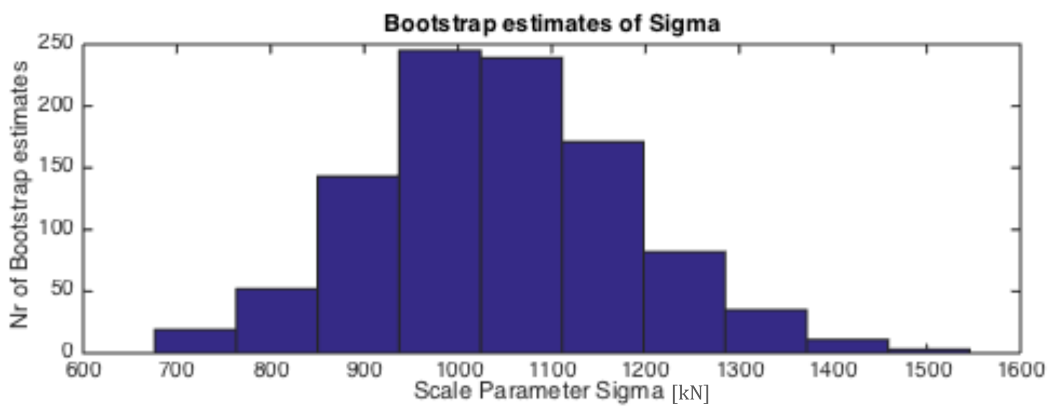
Bootstrap estimates of Sigma
Nr of Bootstrap estimates
Scale Parameter Sigma [kN]

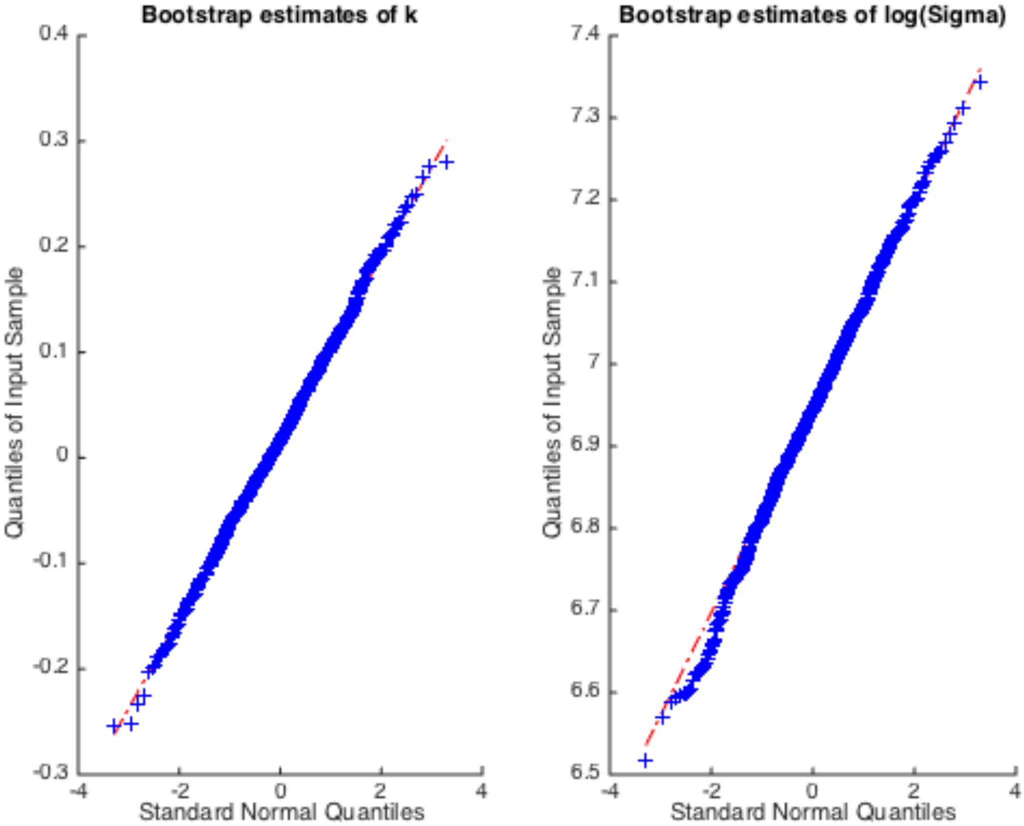
Bootstrap estimates of k
Quantiles of Input Sample
Standard Normal Quantiles
0.4
0.3
0.2
0.1
0
-0.1
-0.2
-0.3
-4
-2
0
2
4
Bootstrap estimates of log(Sigma)
Quantiles of Input Sample
Standard Normal Quantiles
7.4
7.3
7.2
7.1
7
6.9
6.8
6.7
6.6
6.5
-4
-2
0
2
4

III.II Results Quasi-dynamic analysis dataset II (10seeds)

It can be seen that the fit parameters are more or less stable between 2300 and 3300 kN. This can bee seen in the visual check of the cumulative distribution function. Between 0 and 1000 kN exceedance of the threshold there is a very good fit between the empirical data and the GPD. Above an exceedance of 1000 kN there is a misinterpretation. Both goodness-of-fit tests are accepted. The 100-year return level of 8955kN is about 10% lower then the BES value. The reason for this can be the misinterpretation in the 3300-5300 range.

The shape and scale parameters show standard normal behaviour as expected.

u [kN]	2300
σ [kN]	1350.4
ζ	-0.0808
N	100
n_y	2920
$ζ_u$	0.0018
100-year MAX LT	8955 kN
100-year MAX LT BES Dynamic	10094 kN

Test	*Significance level*	*Null-Hypothesis*	*Outcome*	*Simulation method*
Chi-Square	5%	DATASET II follows GPD	Accepted	Quasi-dynamic
Kolmogorov-Smirnov	5%	DATASET II follows GPD	Accepted	Quasi-dynamic

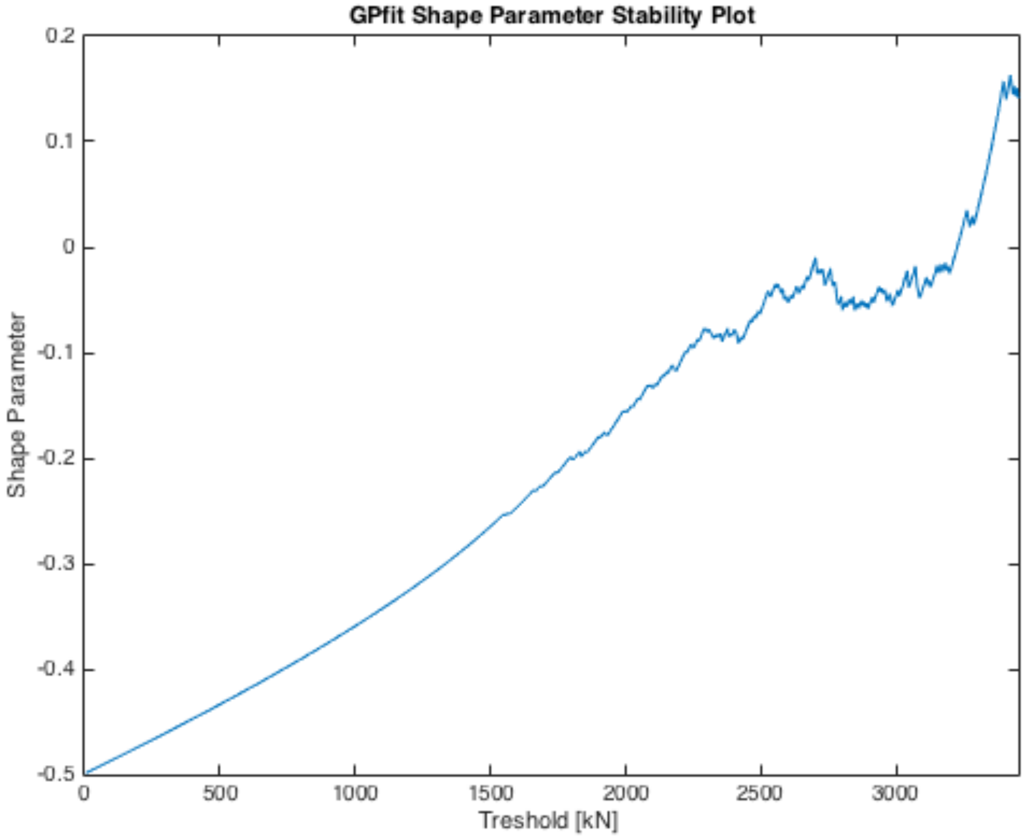
GPfit Shape Parameter Stability Plot
Shape Parameter
Treshold [kN]
0.2
0.1
0
-0.1
-0.2
-0.3
-0.4
-0.5
0
500
1000
1500
2000
2500
3000

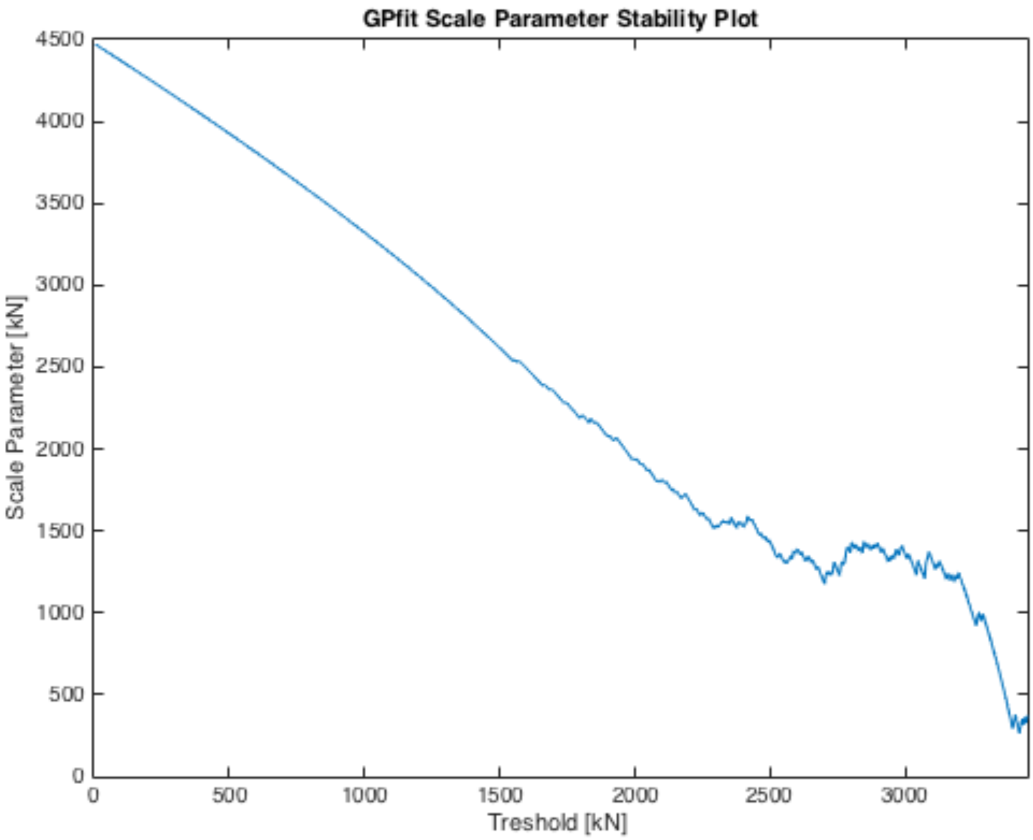
GPfit Scale Parameter Stability Plot
Scale Parameter [kN]
Treshold [kN]
4500
4000
3500
3000
2500
2000
1500
1000
500
0
0
500
1000
1500
2000
2500
3000

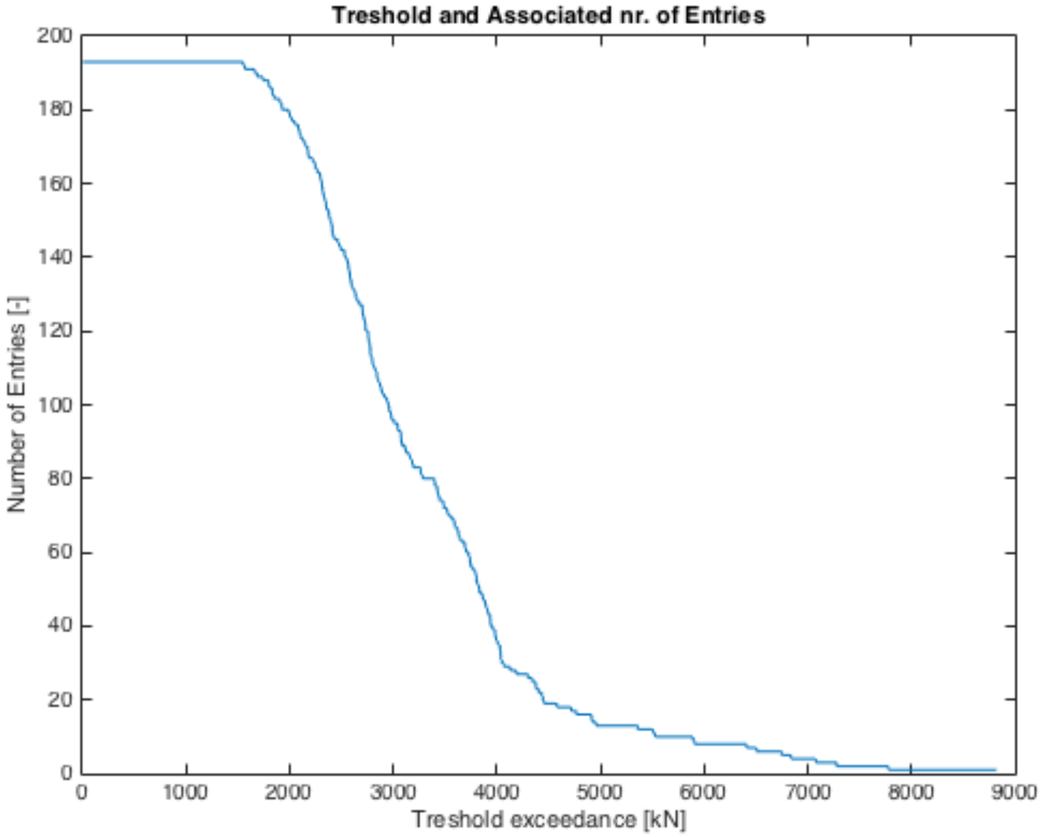
Treshold and Associated nr. of Entries
Number of Entries [-]
Treshold exceedance [kN]
0
20
40
60
80
100
120
140
160
180
200
0
1000
2000
3000
4000
5000
6000
7000
8000
9000

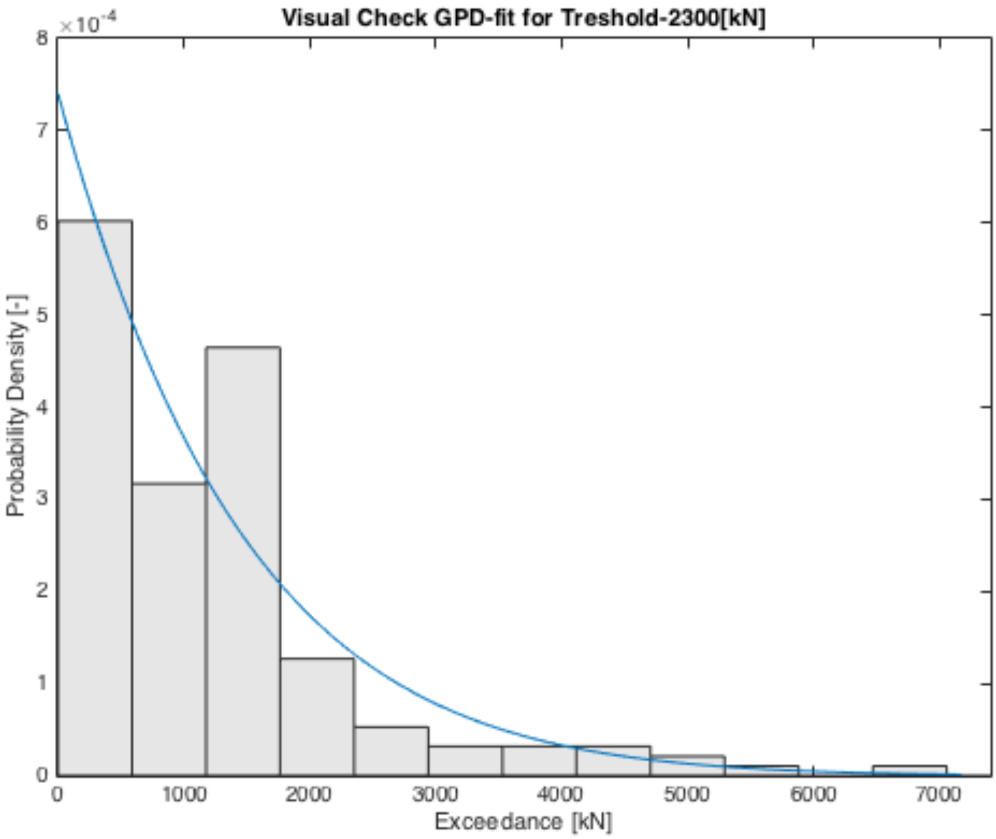
Visual Check GPD-fit for Treshold-2300[kN]
×10^-4
Probability Density [-]
Exceedance [kN]
0
1
2
3
4
5
6
7
8
0
1000
2000
3000
4000
5000
6000
7000

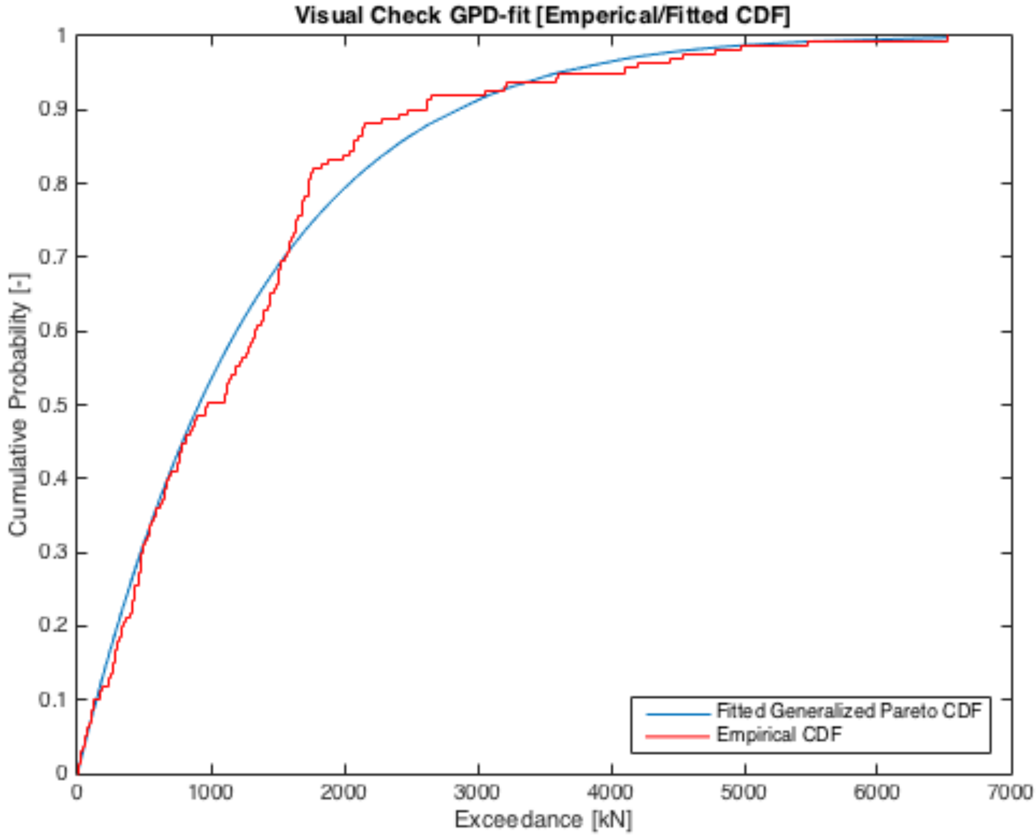

Visual Check GPD-fit [Emperical/Fitted CDF]
Cumulative Probability [-]
Exceedance [kN]
Fitted Generalized Pareto CDF
Empirical CDF
0
0.1
0.2
0.3
0.4
0.5
0.6
0.7
0.8
0.9
1
0
1000
2000
3000
4000
5000
6000
7000

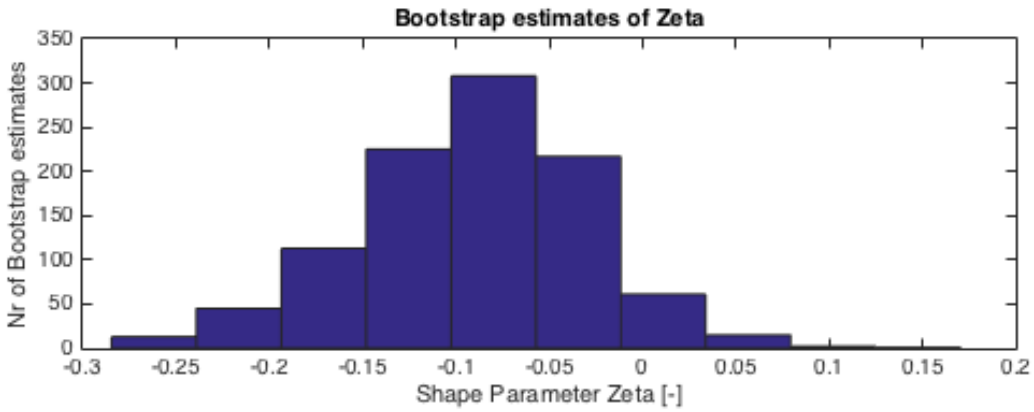

Bootstrap estimates of Zeta
Nr of Bootstrap estimates
Shape Parameter Zeta [-]
0
50
100
150
200
250
300
350
-0.3
-0.25
-0.2
-0.15
-0.1
-0.05
0
0.05
0.1
0.15
0.2

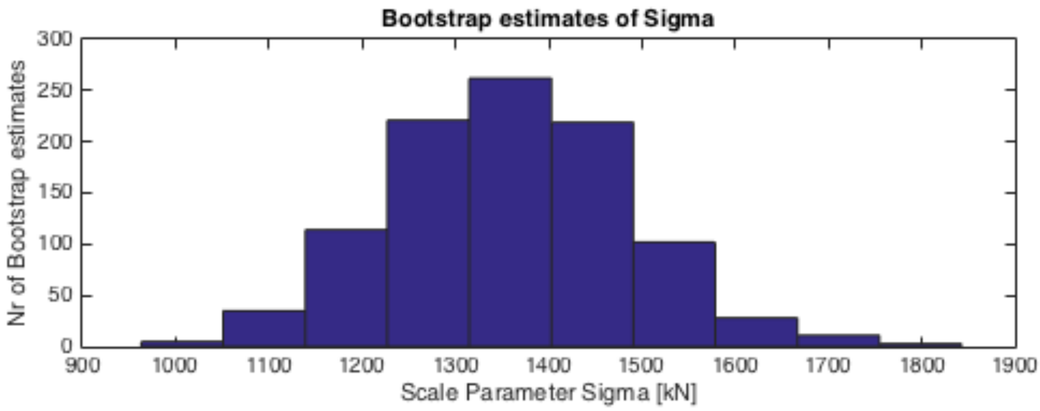

Bootstrap estimates of Sigma
Nr of Bootstrap estimates
Scale Parameter Sigma [kN]
0
50
100
150
200
250
300
900
1000
1100
1200
1300
1400
1500
1600
1700
1800
1900

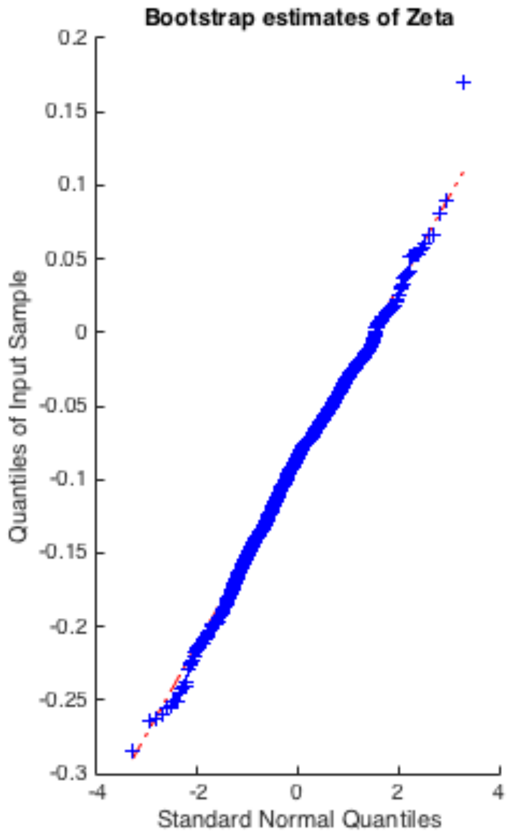
Bootstrap estimates of Zeta
Quantiles of Input Sample
Standard Normal Quantiles
0.2
0.15
0.1
0.05
0
-0.05
-0.1
-0.15
-0.2
-0.25
-0.3
-4
-2
0
2
4

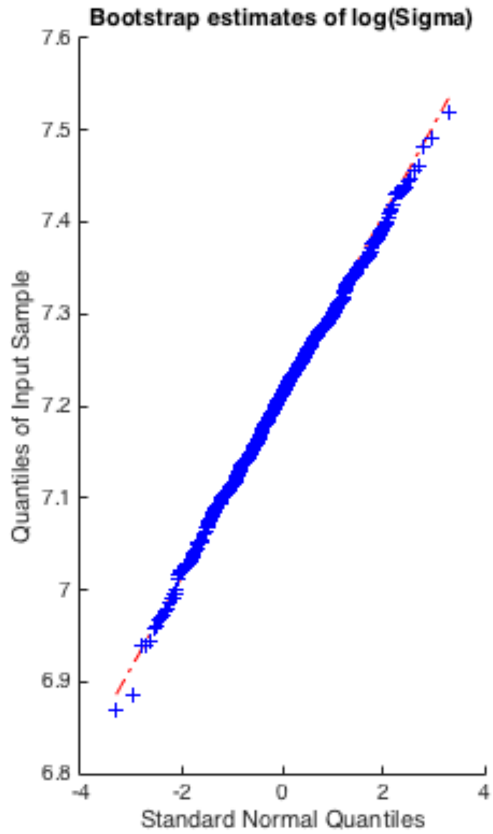
Bootstrap estimates of log(Sigma)
Quantiles of Input Sample
Standard Normal Quantiles
7.6
7.5
7.4
7.3
7.2
7.1
7
6.9
6.8
-4
-2
0
2
4

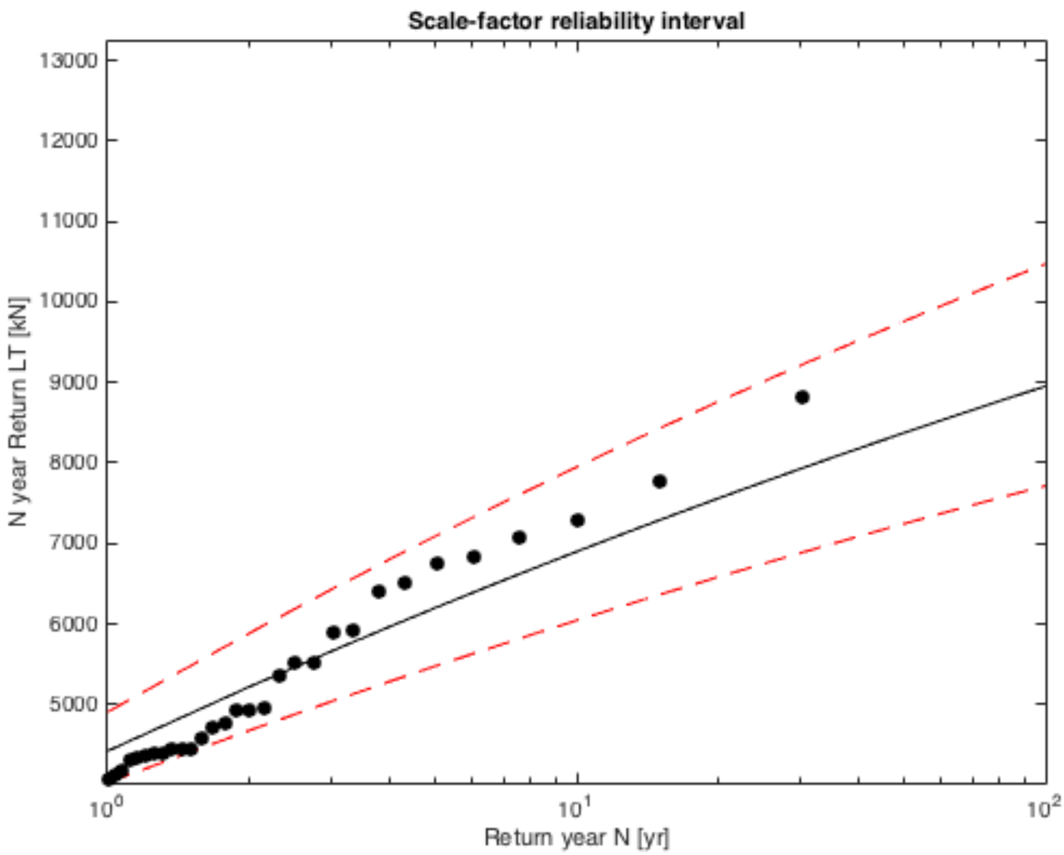
Scale-factor reliability interval
N year Return LT [kN]
Return year N [yr]
13000
12000
11000
10000
9000
8000
7000
6000
5000
10^0
10^1
10^2

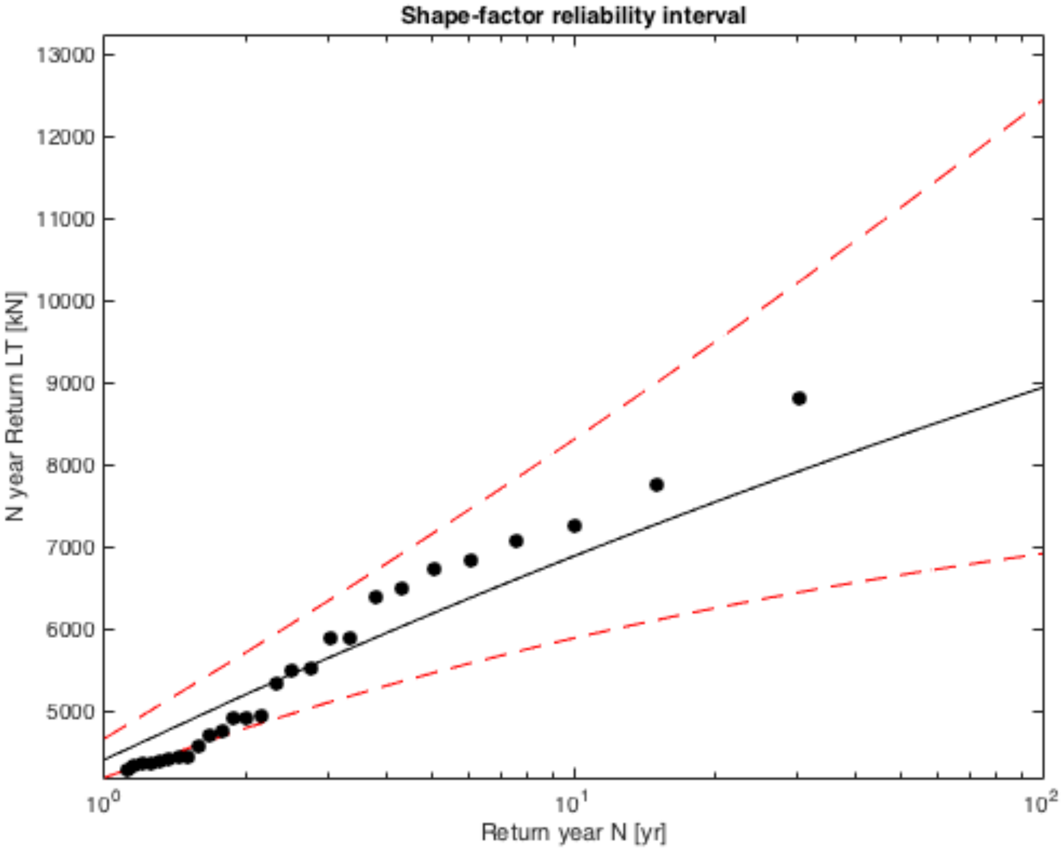
Shape-factor reliability interval
N year Return LT [kN]
Return year N [yr]
13000
12000
11000
10000
9000
8000
7000
6000
5000
10^0
10^1
10^2

III.III Results Quasi-dynamic analysis dataset II (25seeds)

It can be observed that the parameters become stable around 2100 kN. The parameters are stable, but have a larger fluctuation in comparison with the previous analysis around the mean stable value. There is an overall good fit above the set threshold of 2100 kN.

All goodness-of-fit tests are accepted for a 5% significant level. The bootstrap estimates of the shape and scale parameter show standard normal behaviour as expected.

It can be concluded that for the same dataset 25 seeds are produced instead of 10 this improves the fit of the empirical data on the distribution improves. This resulted in an extrapolation of 10143 kN which is close to the BES value.

u [kN]	2100
σ [kN]	1324.1
ζ	-0.0147
N	100
n_y	2920
ζ_u	0.002
100-year MAX LT	10143 kN
100-year MAX LT BES Dynamic	10094 kN

Test	*Significance level*	*Null-Hypothesis*	*Outcome*	*Simulation method*
Chi-Square	5%	DATASET II follows GPD	Accepted	Quasi-dynamic
Kolmogorov-Smirnov	5%	DATASET II follows GPD	Accepted	Quasi-dynamic

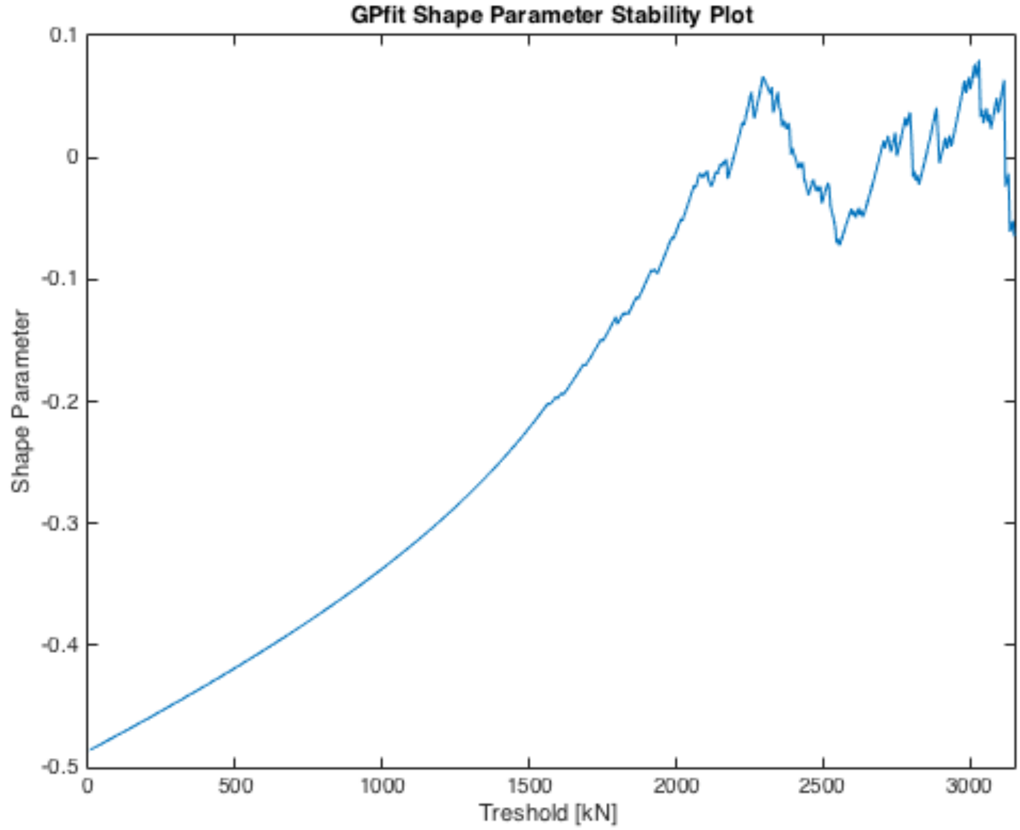
GPfit Shape Parameter Stability Plot
Shape Parameter
Treshold [kN]
0.1
0
-0.1
-0.2
-0.3
-0.4
-0.5
0
500
1000
1500
2000
2500
3000

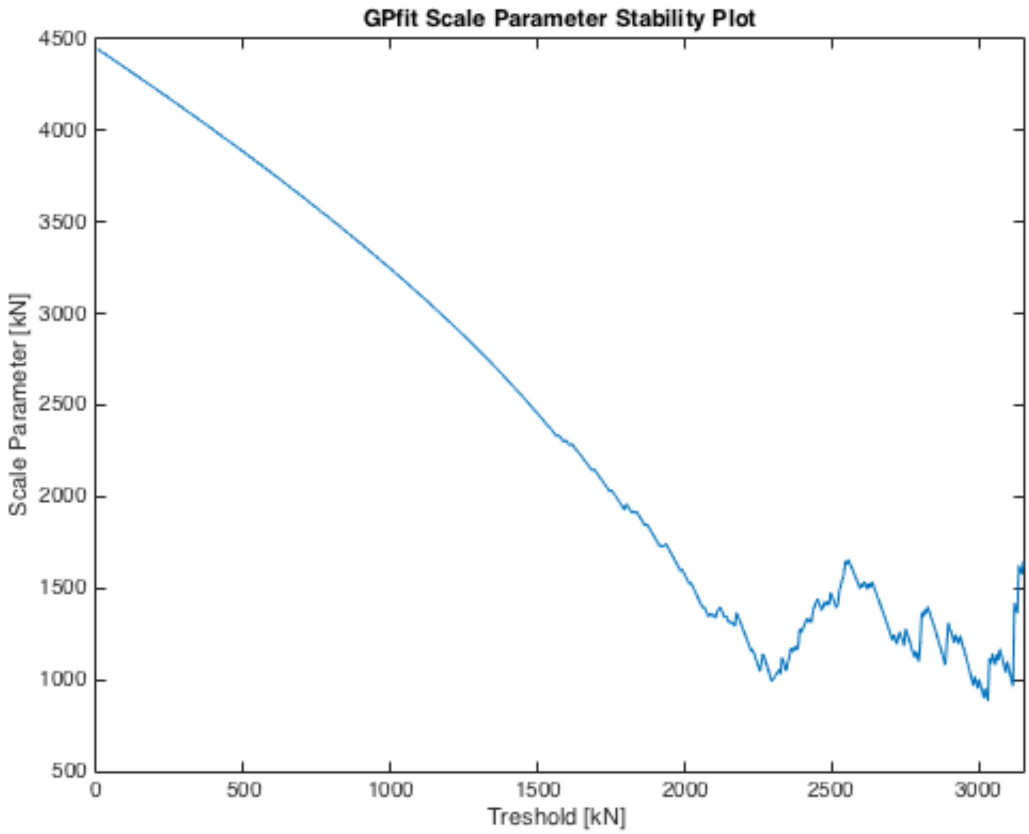
GPfit Scale Parameter Stability Plot
Scale Parameter [kN]
Treshold [kN]
4500
4000
3500
3000
2500
2000
1500
1000
500
0
500
1000
1500
2000
2500
3000

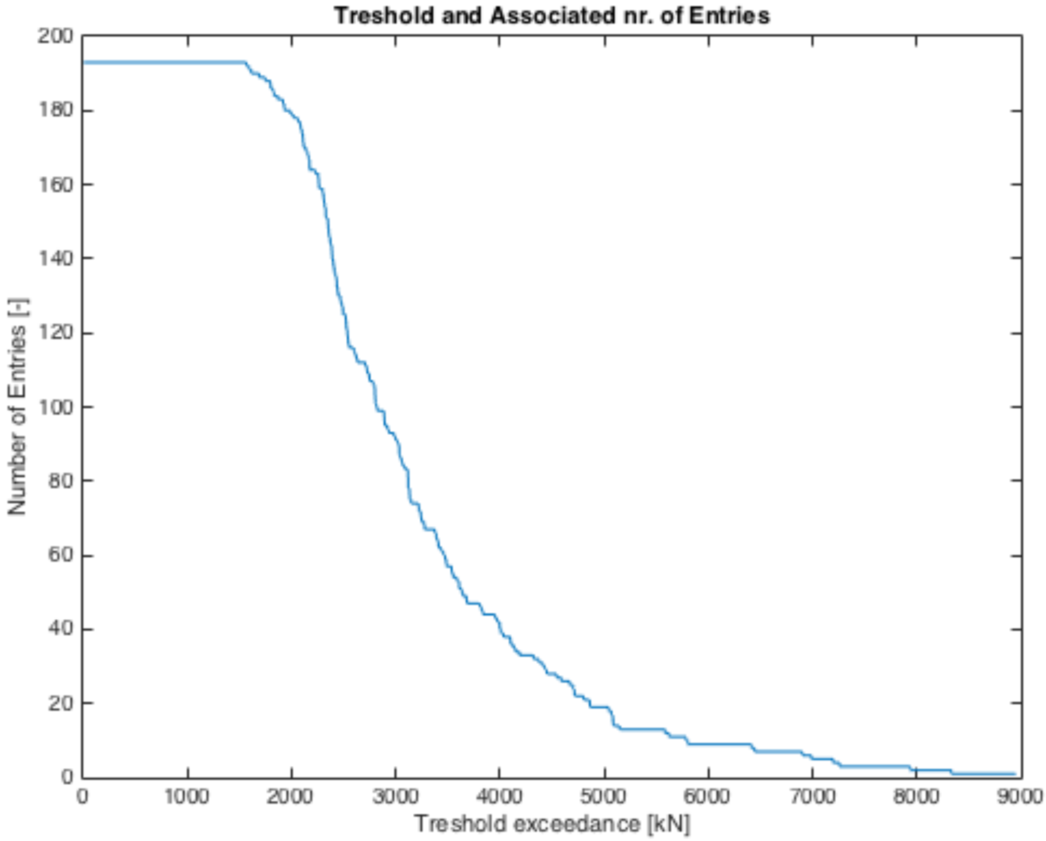

Treshold and Associated nr. of Entries
Number of Entries [-]
Treshold exceedance [kN]
200
180
160
140
120
100
80
60
40
20
0
0
1000
2000
3000
4000
5000
6000
7000
8000
9000

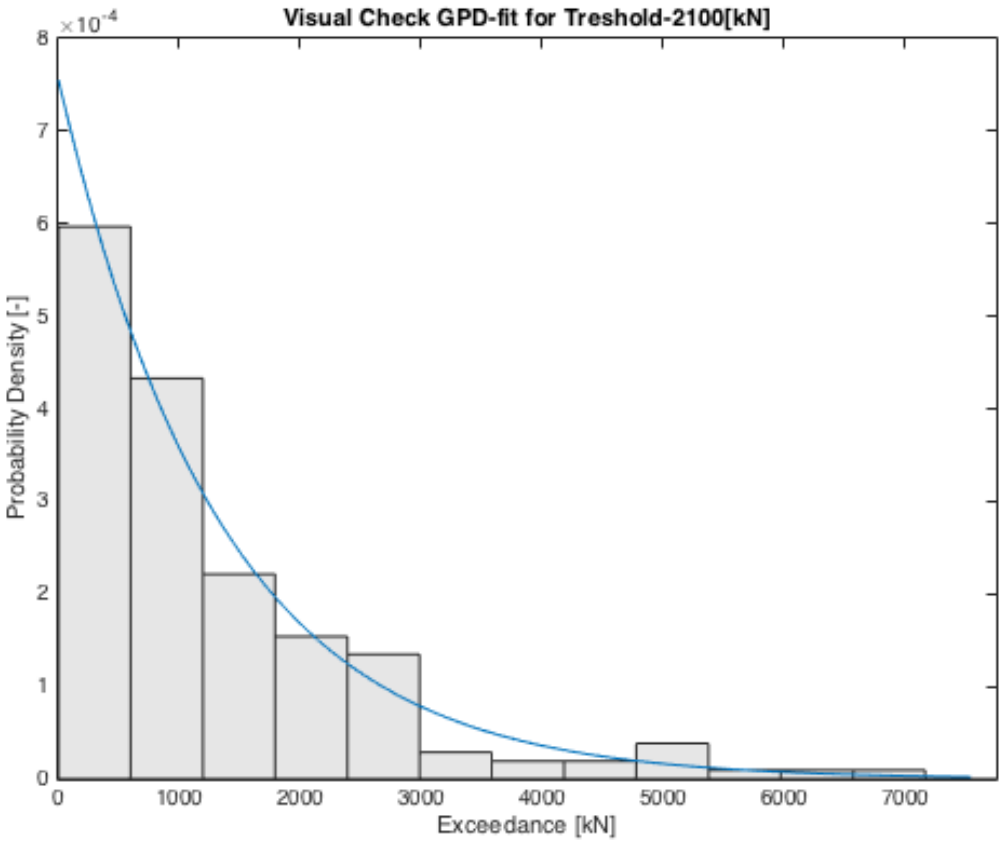

Visual Check GPD-fit for Treshold-2100[kN]
×10⁻⁴
Probability Density [-]
Exceedance [kN]
8
7
6
5
4
3
2
1
0
0
1000
2000
3000
4000
5000
6000
7000

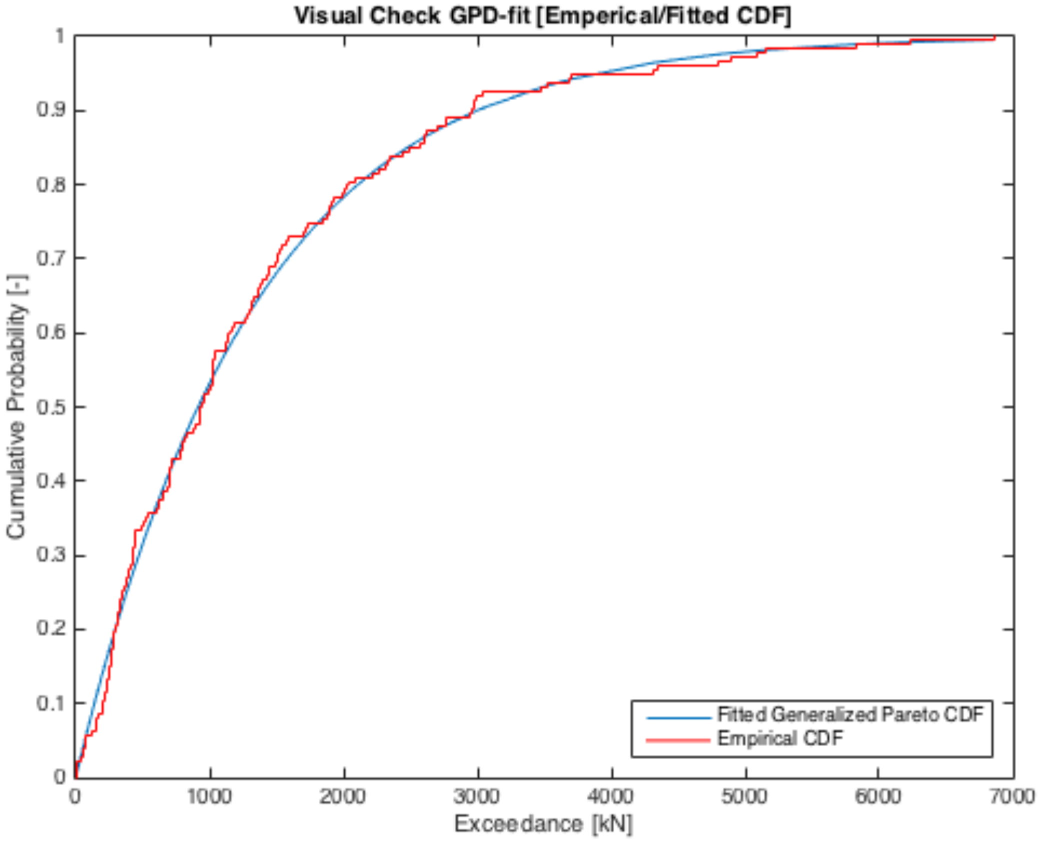
Visual Check GPD-fit [Emperical/Fitted CDF]
Cumulative Probability [-]
Exceedance [kN]
Fitted Generalized Pareto CDF
Empirical CDF
0
0.1
0.2
0.3
0.4
0.5
0.6
0.7
0.8
0.9
1
0
1000
2000
3000
4000
5000
6000
7000

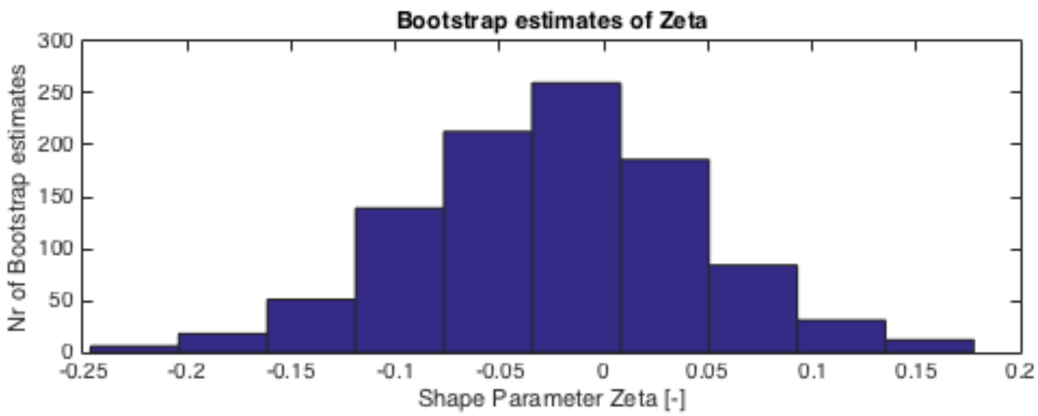
Bootstrap estimates of Zeta
Nr of Bootstrap estimates
Shape Parameter Zeta [-]
0
50
100
150
200
250
300
-0.25
-0.2
-0.15
-0.1
-0.05
0
0.05
0.1
0.15
0.2

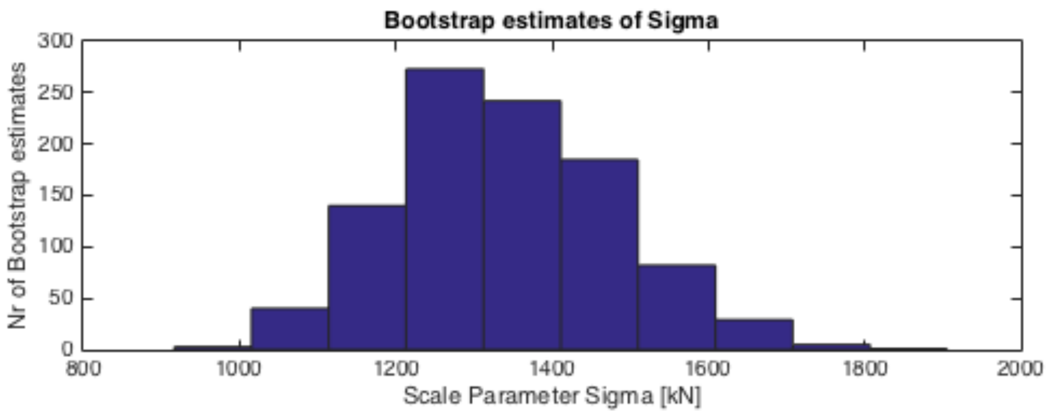
Bootstrap estimates of Sigma
Nr of Bootstrap estimates
Scale Parameter Sigma [kN]
0
50
100
150
200
250
300
800
1000
1200
1400
1600
1800
2000

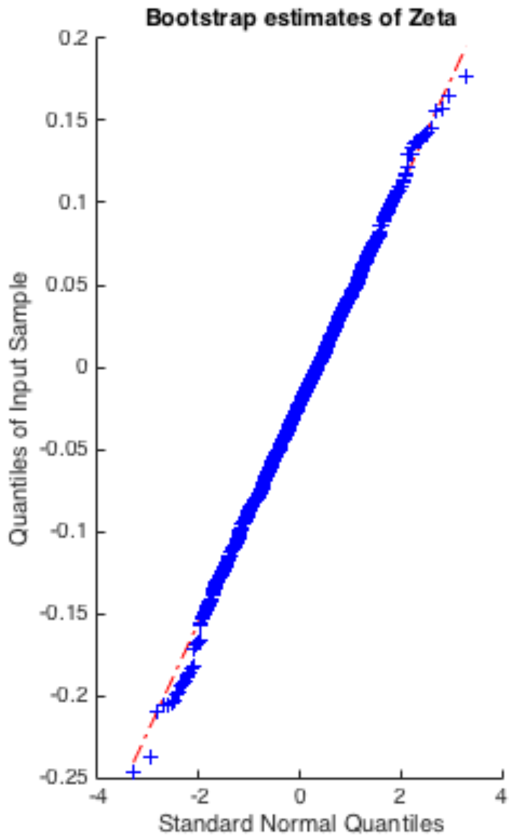

Bootstrap estimates of Zeta
Quantiles of Input Sample
Standard Normal Quantiles
0.2
0.15
0.1
0.05
0
-0.05
-0.1
-0.15
-0.2
-0.25
-4
-2
0
2
4

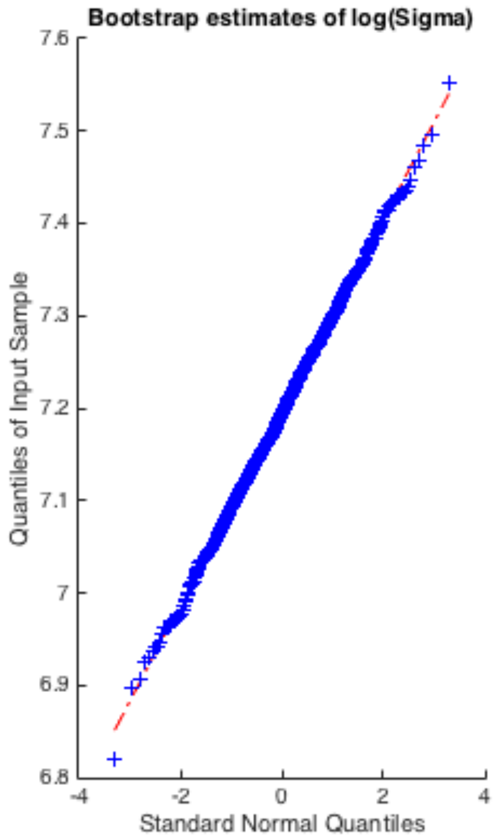

Bootstrap estimates of log(Sigma)
Quantiles of Input Sample
Standard Normal Quantiles
7.6
7.5
7.4
7.3
7.2
7.1
7
6.9
6.8
-4
-2
0
2
4

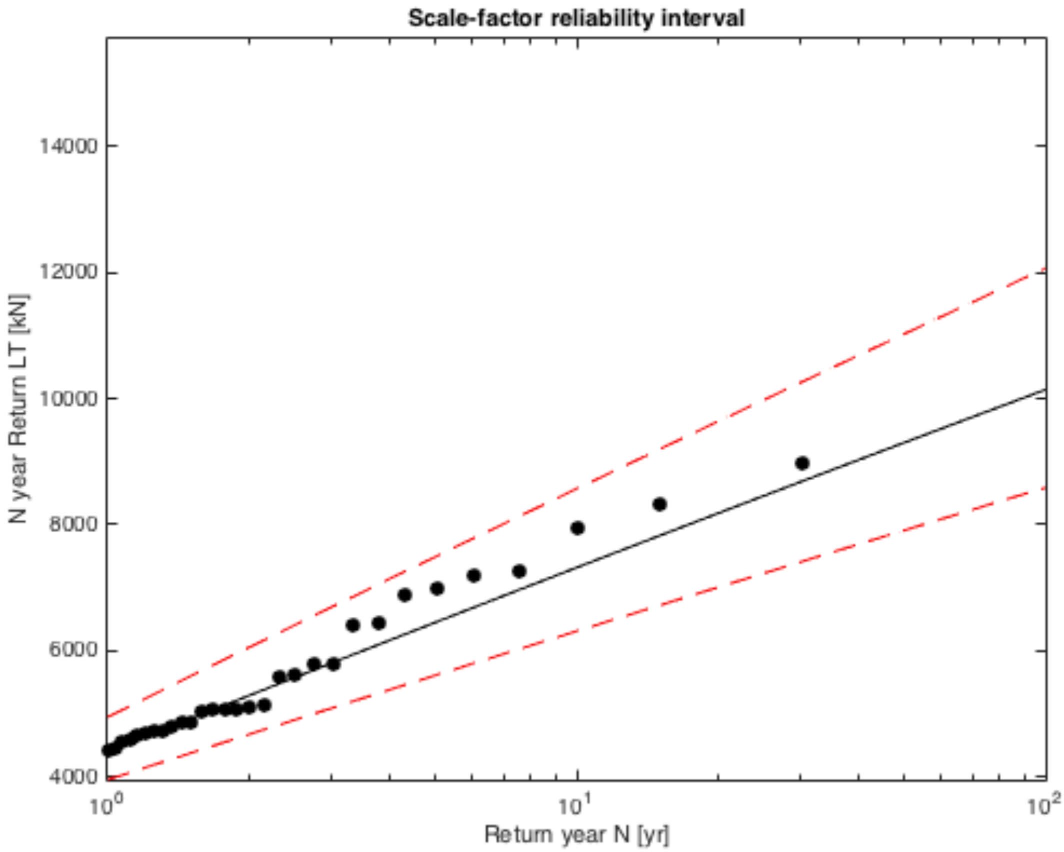

Scale-factor reliability interval
N year Return LT [kN]
Return year N [yr]
14000
12000
10000
8000
6000
4000
10^0
10^1
10^2

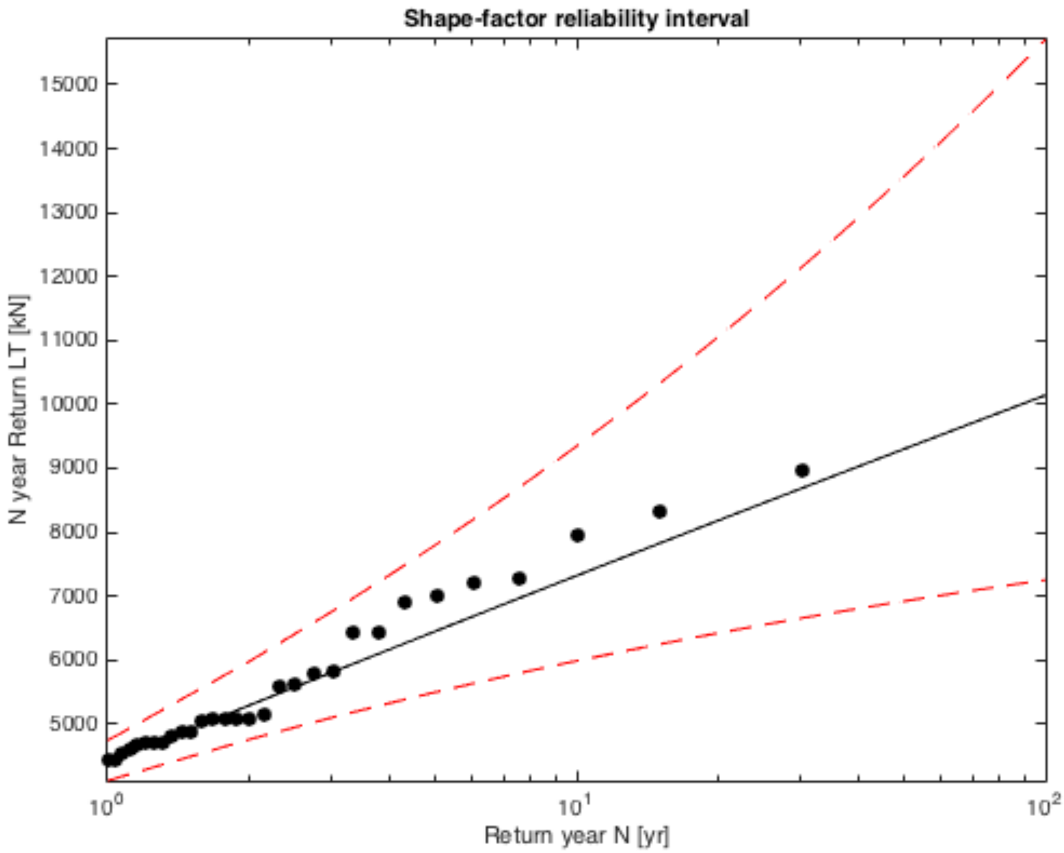
Shape-factor reliability interval
N year Return LT [kN]
15000
14000
13000
12000
11000
10000
9000
8000
7000
6000
5000
10^0
10^1
10^2
Return year N [yr]

III.IV Results Quasi-dynamic analysis dataset II for horizontal turret load (25seeds)

The fit parameters become stable around 3340 kN. After this point stable behaviour can be seen with some fluctuations (example around 4750 kN). This fluctuation can also be observed in the CDF at exceedance level of 1410 kN.

The bootstrap of the parameters show standard normal behaviour as expected. Some skewness can be seen for the shape parameter in the lower quantiles. These fluctuations are the result of the variations in the initial parameter stability.

All goodness-of-fit tests are accepted for a 5% significant level.

The 100-year return level for the horizontal turret load is 16845 kN. This a realistic value.

u [kN]	3340
σ [kN]	2289.5
ζ	-0.0254
N	100
n_y	2920
$ζ_u$	0.0020
100-year MAX HT	16845 kN

Test	*Significance level*	*Null-Hypothesis*	*Outcome*	*Simulation method*
Chi-Square	5%	DATASET II follows GPD	Accepted	Quasi-dynamic
Kolmogorov-Smirnov	5%	DATASET II follows GPD	Accepted	Quasi-dynamic

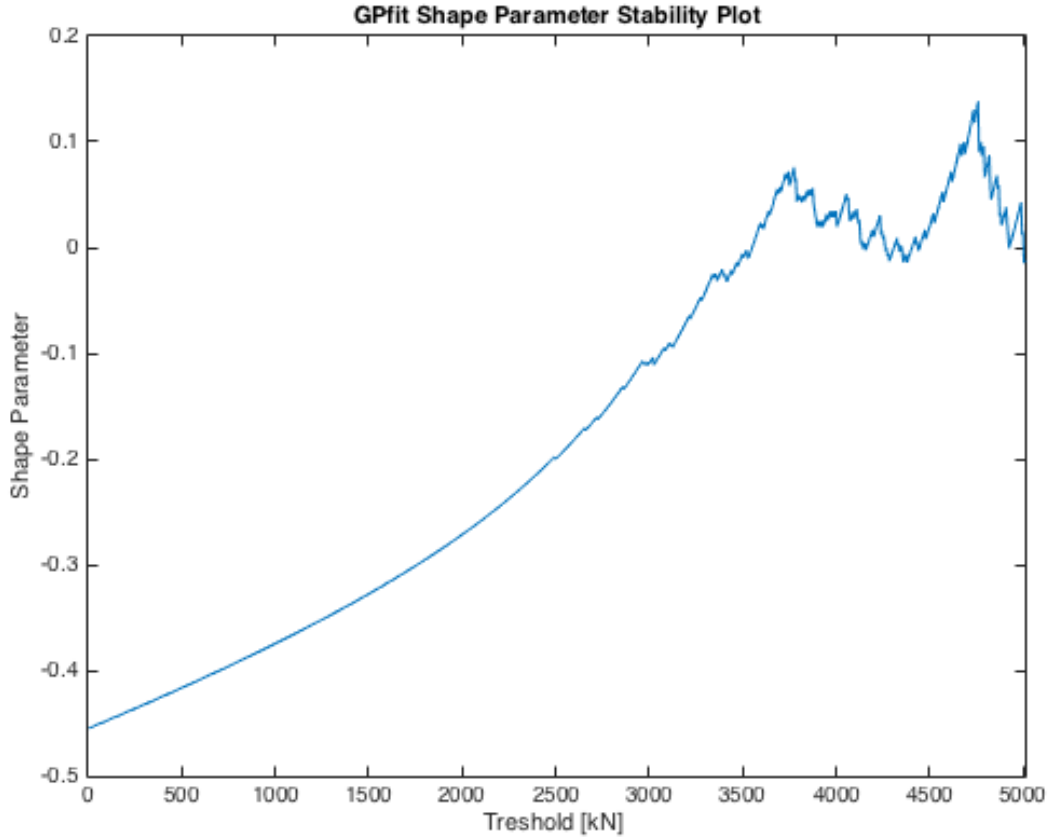
GPfit Shape Parameter Stability Plot
0.2
0.1
0
-0.1
-0.2
-0.3
-0.4
-0.5
Shape Parameter
0
500
1000
1500
2000
2500
3000
3500
4000
4500
5000
Treshold [kN]

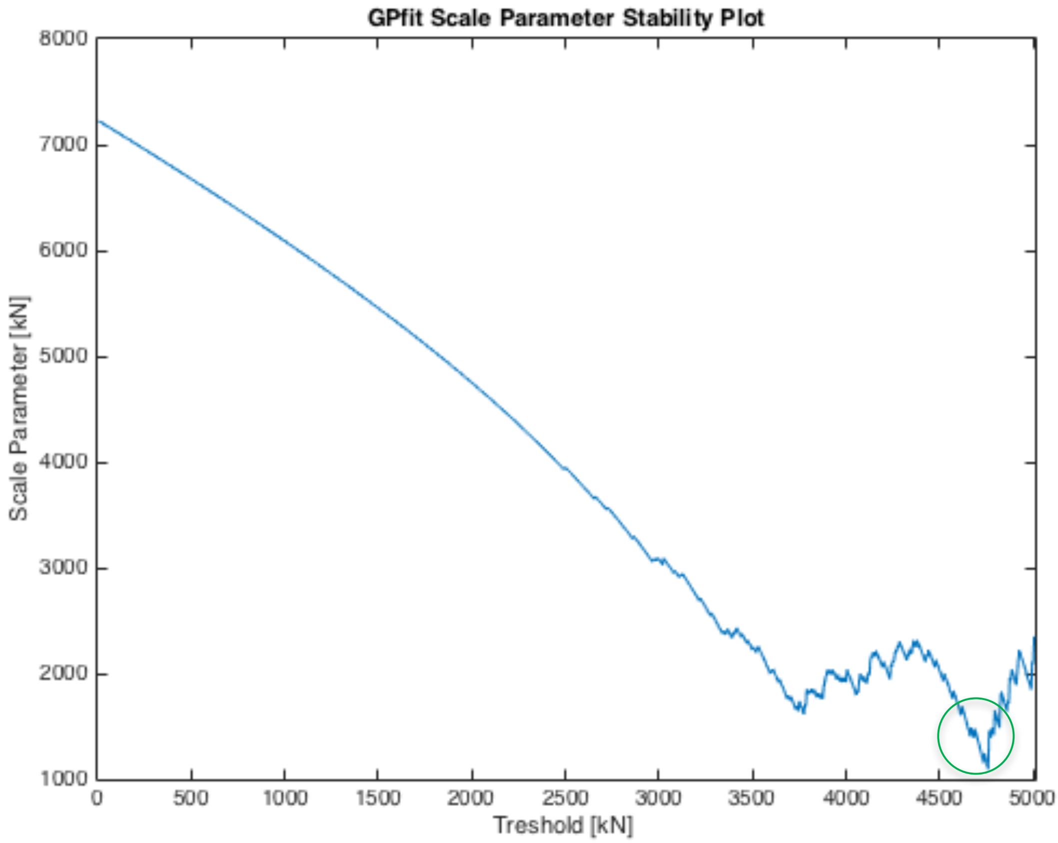
GPfit Scale Parameter Stability Plot
8000
7000
6000
5000
4000
3000
2000
1000
Scale Parameter [kN]
0
500
1000
1500
2000
2500
3000
3500
4000
4500
5000
Treshold [kN]

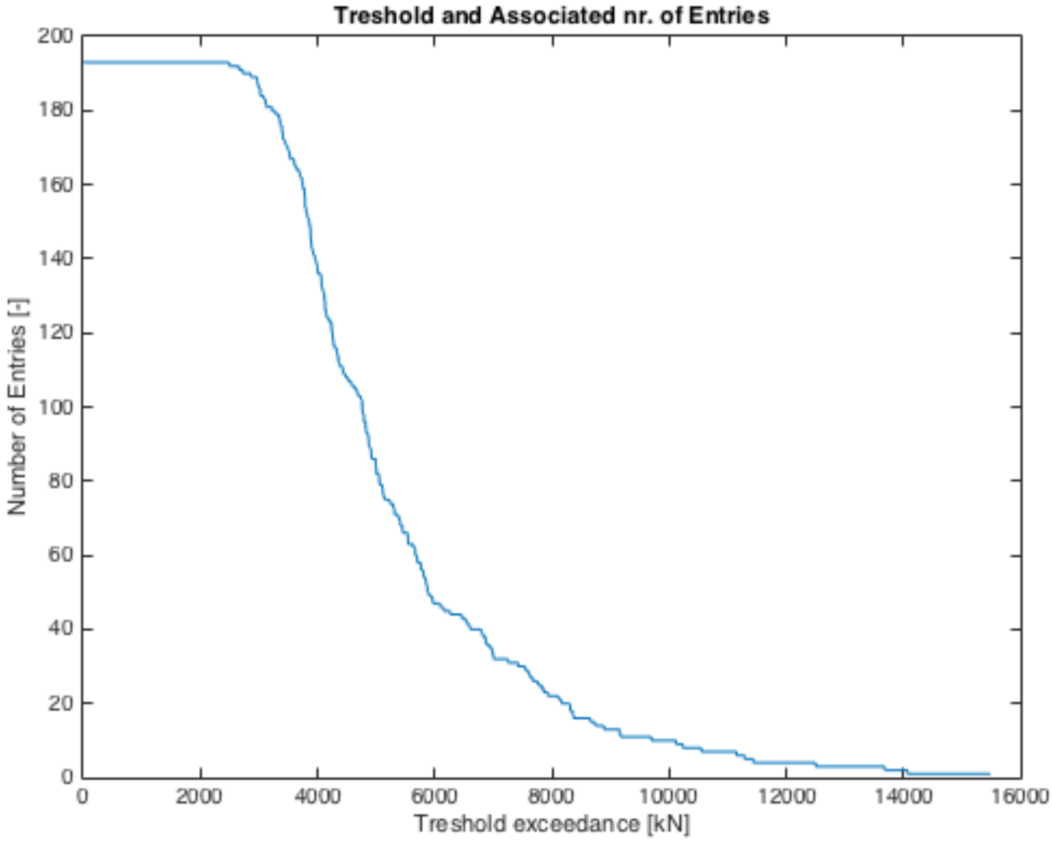
Treshold and Associated nr. of Entries
Number of Entries [-]
Treshold exceedance [kN]
0
20
40
60
80
100
120
140
160
180
200
0
2000
4000
6000
8000
10000
12000
14000
16000

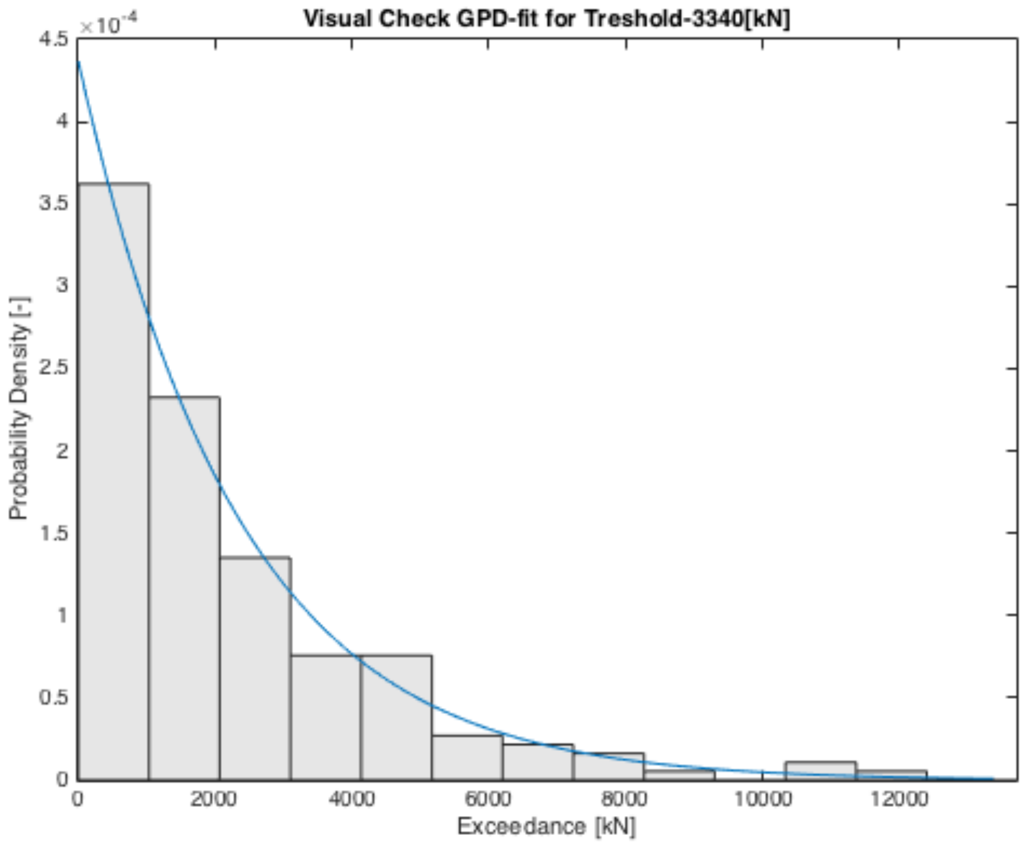
Visual Check GPD-fit for Treshold-3340[kN]
×10^-4
Probability Density [-]
Exceedance [kN]
0
0.5
1
1.5
2
2.5
3
3.5
4
4.5
0
2000
4000
6000
8000
10000
12000

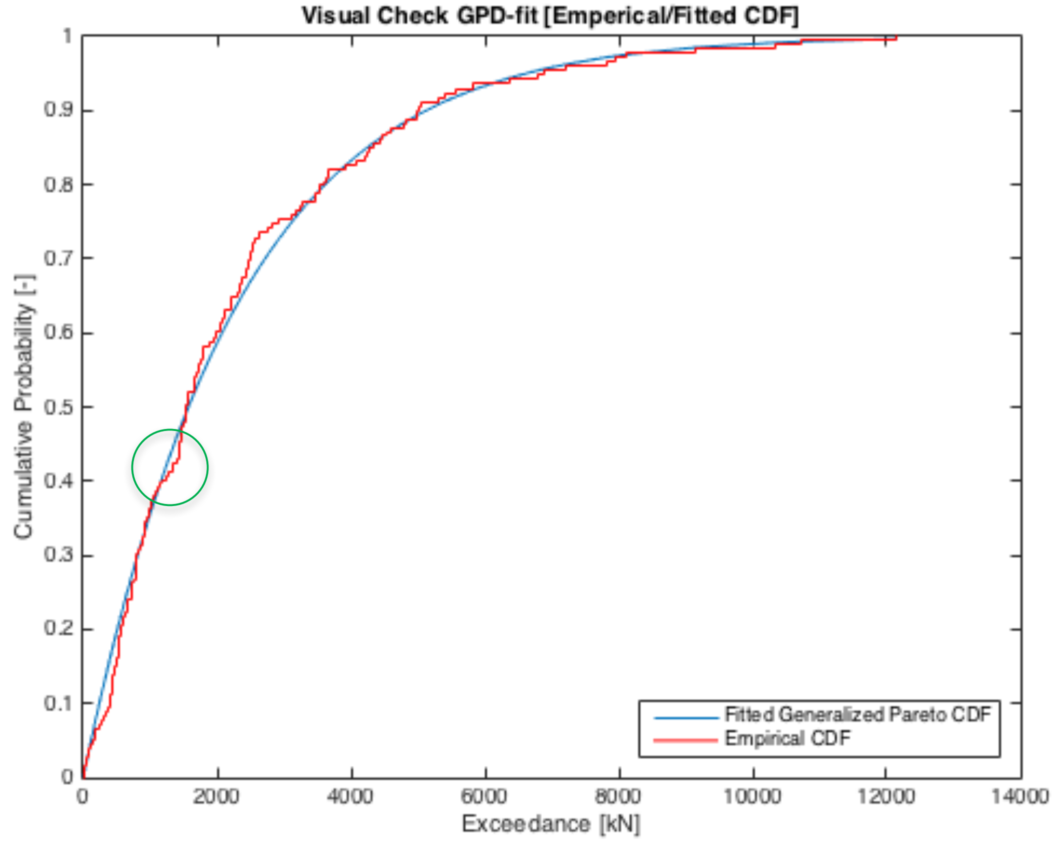
Visual Check GPD-fit [Emperical/Fitted CDF]
Cumulative Probability [-]
Exceedance [kN]
Fitted Generalized Pareto CDF
Empirical CDF
0
0.1
0.2
0.3
0.4
0.5
0.6
0.7
0.8
0.9
1
0
2000
4000
6000
8000
10000
12000
14000

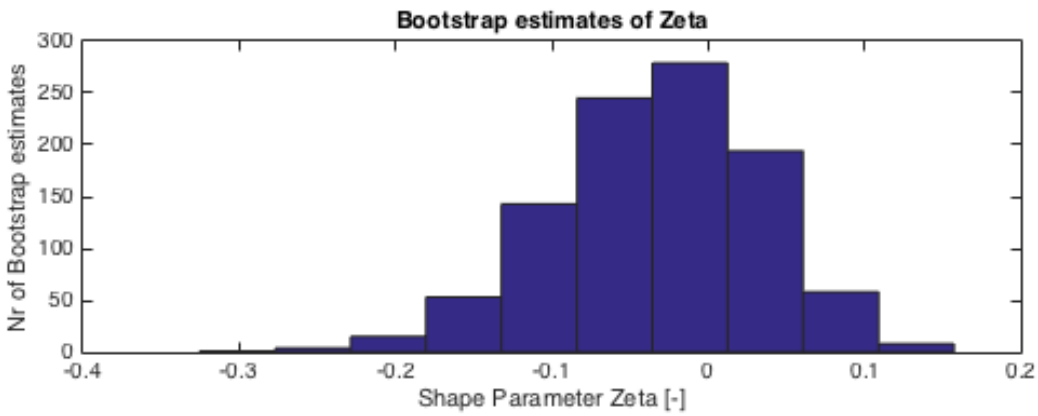
Bootstrap estimates of Zeta
Nr of Bootstrap estimates
Shape Parameter Zeta [-]
0
50
100
150
200
250
300
-0.4
-0.3
-0.2
-0.1
0
0.1
0.2

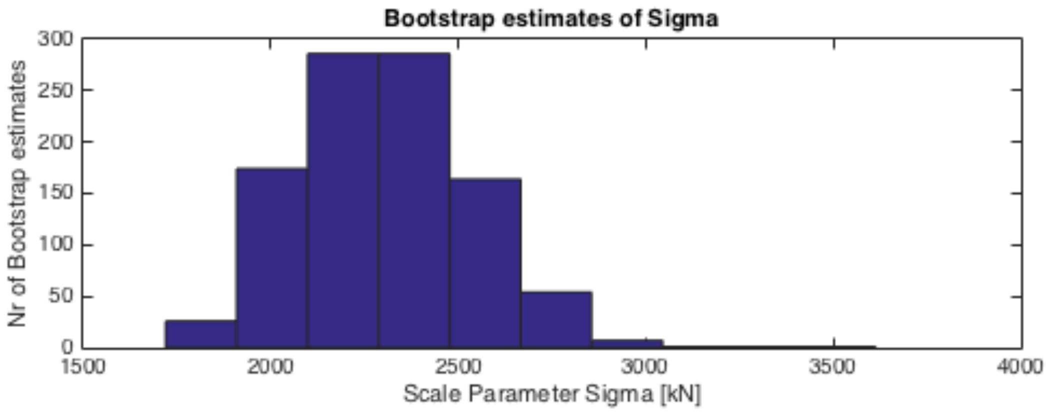
Bootstrap estimates of Sigma
Nr of Bootstrap estimates
Scale Parameter Sigma [kN]
0
50
100
150
200
250
300
1500
2000
2500
3000
3500
4000

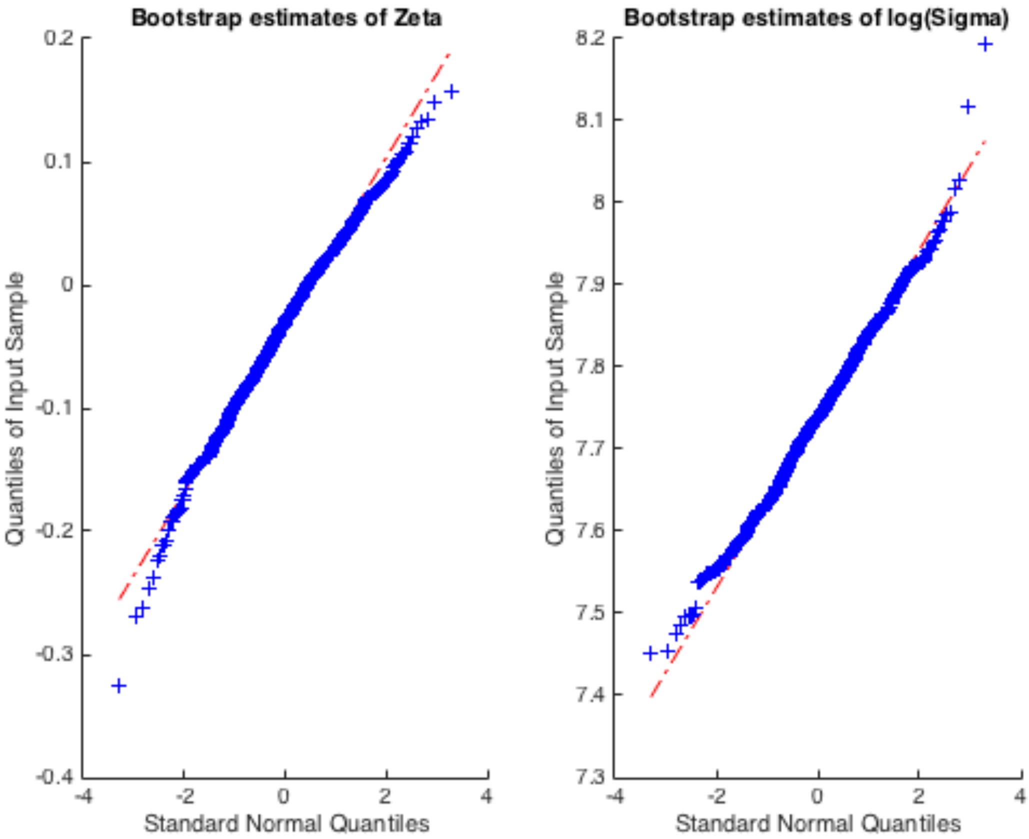
Bootstrap estimates of Zeta
Quantiles of Input Sample
Standard Normal Quantiles
0.2
0.1
0
-0.1
-0.2
-0.3
-0.4
-4
-2
0
2
4
Bootstrap estimates of log(Sigma)
Quantiles of Input Sample
Standard Normal Quantiles
8.2
8.1
8
7.9
7.8
7.7
7.6
7.5
7.4
7.3

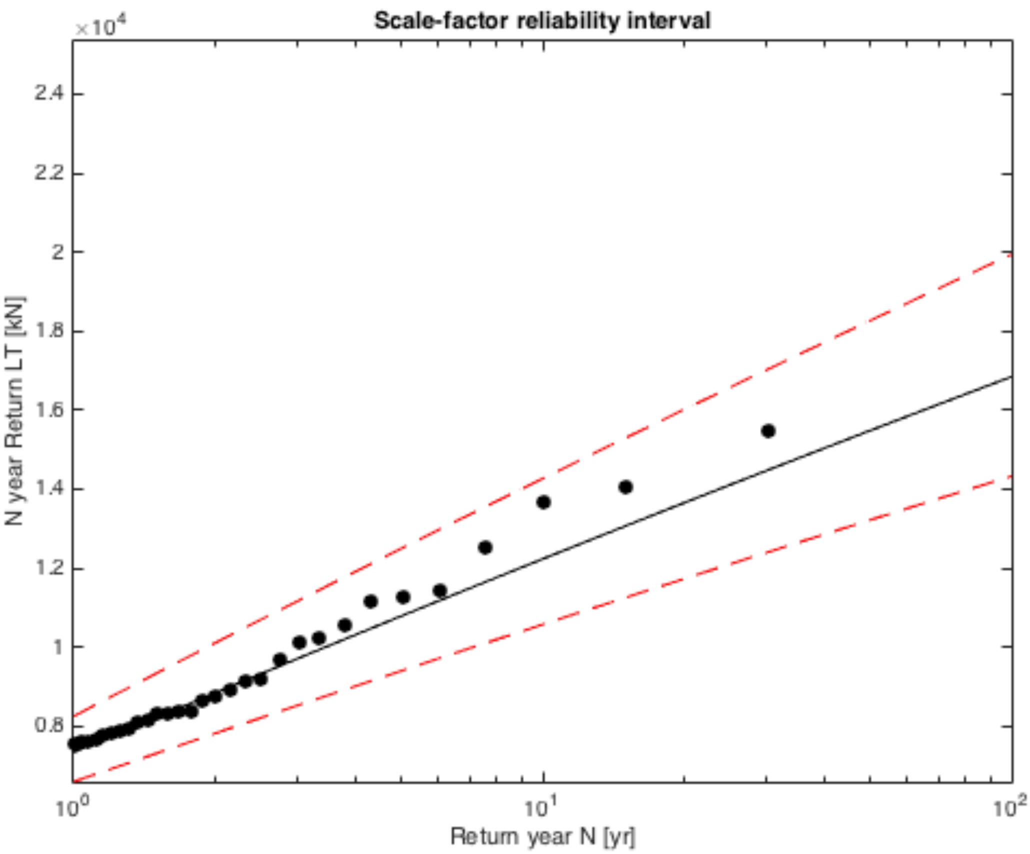
Scale-factor reliability interval
×10^4
2.4
2.2
2
1.8
1.6
1.4
1.2
1
0.8
N year Return LT [kN]
10^0
10^1
10^2
Return year N [yr]

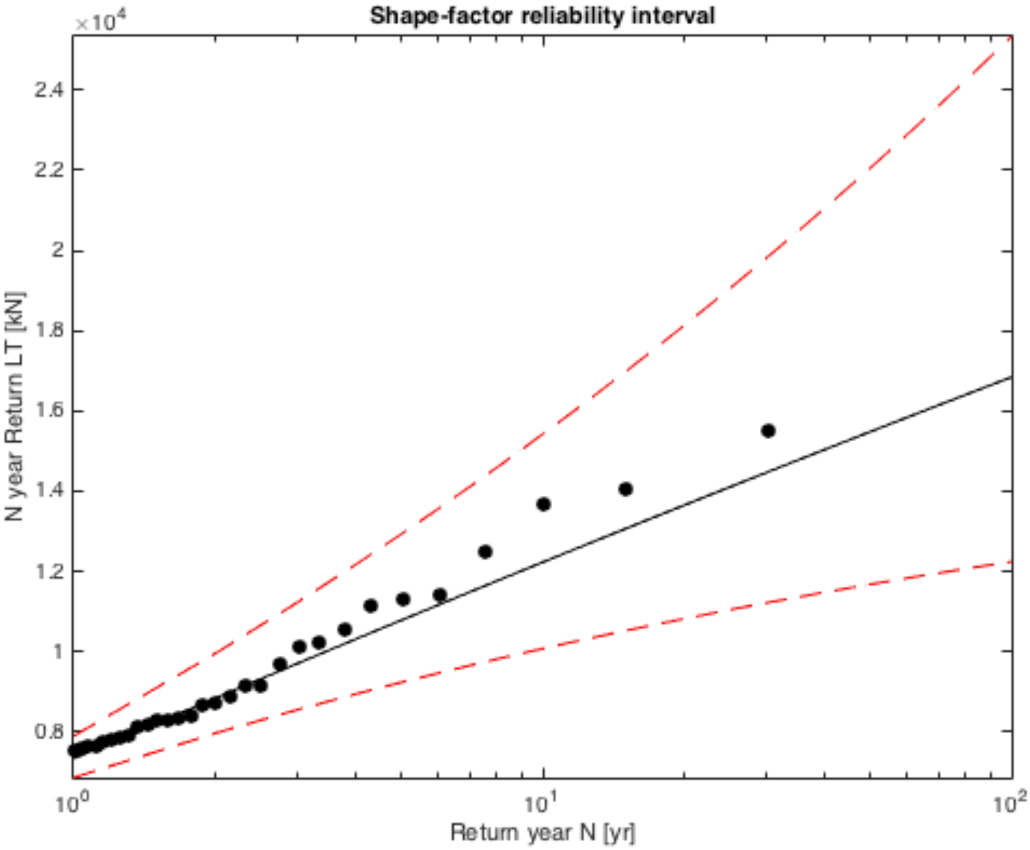
Shape-factor reliability interval
×10^4
2.4
2.2
2
1.8
1.6
1.4
1.2
1
0.8
N year Return LT [kN]
10^0
10^1
10^2
Return year N [yr]

III.V Results Quasi-dynamic analysis dataset II 3X3 Mooring system (25seeds)

For the 3X3 mooring system it can be observed that the fit parameters show some weird behaviour. The parameters become stable around a threshold of 2450 kN. This results in only ± 40 entries to fit on a GPD. This resulted in a fit that passed all goodness-of-fit test for a 5% significance level however, if the plots are studied visually it can be seen that the amount of data points are to limited to produce reliable fits.

The boostrap estimates of the fit parameters show skewness, so the bootstraps are not standard normally distributed as would have been expected.

The distribution leads to a 100-year return level of 6029.6 kN. As expected the maximum line tension is lower in comparison with the 8X1 mooring system. Despite that the distribution passed the goodness-of-fit test, it can be said the extrapolation is not reliable.

u [kN]	2450
σ [kN]	1282.3
ζ	-0.2570
N	100
n_y	2920
ζ_u	0.000468
100-year MAX LT	6029.6 kN

Test	*Significance level*	*Null-Hypothesis*	*Outcome*	*Simulation method*
Chi-Square	5%	DATASET II follows GPD	Accepted	Quasi-dynamic
Kolmogorov-Smirnov	5%	DATASET II follows GPD	Accepted	Quasi-dynamic

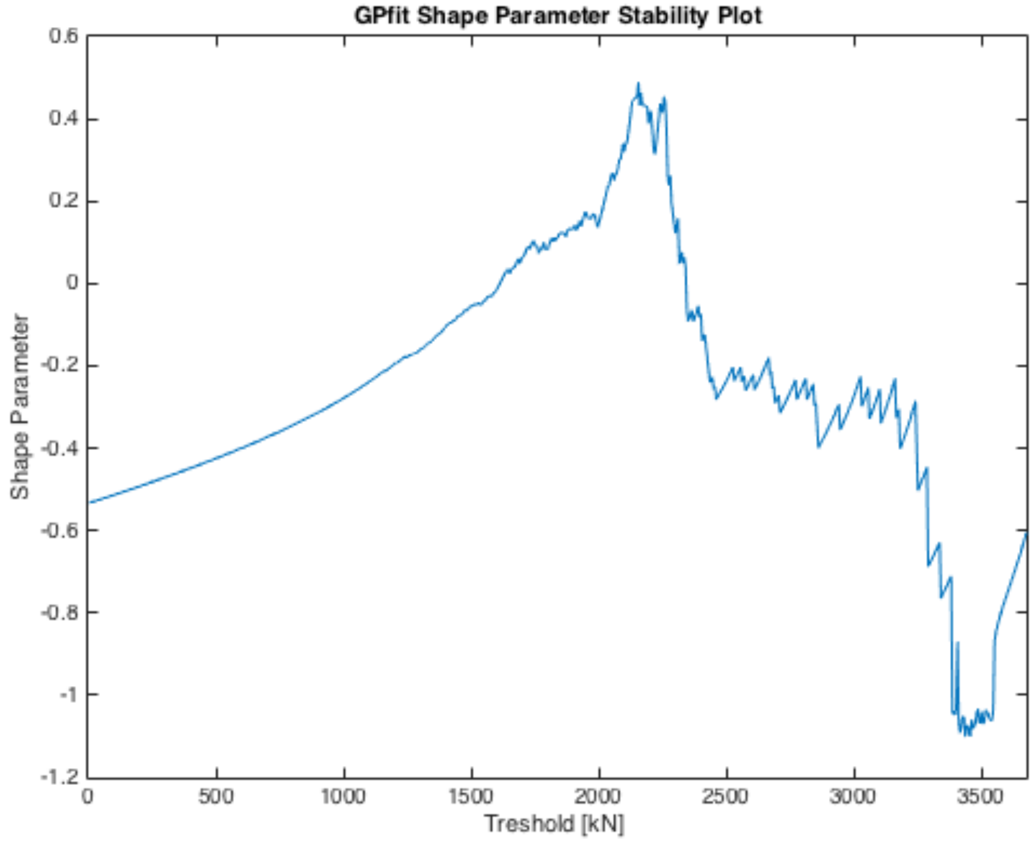
GPfit Shape Parameter Stability Plot
Shape Parameter
0.6
0.4
0.2
0
-0.2
-0.4
-0.6
-0.8
-1
-1.2
0
500
1000
1500
2000
2500
3000
3500
Treshold [kN]

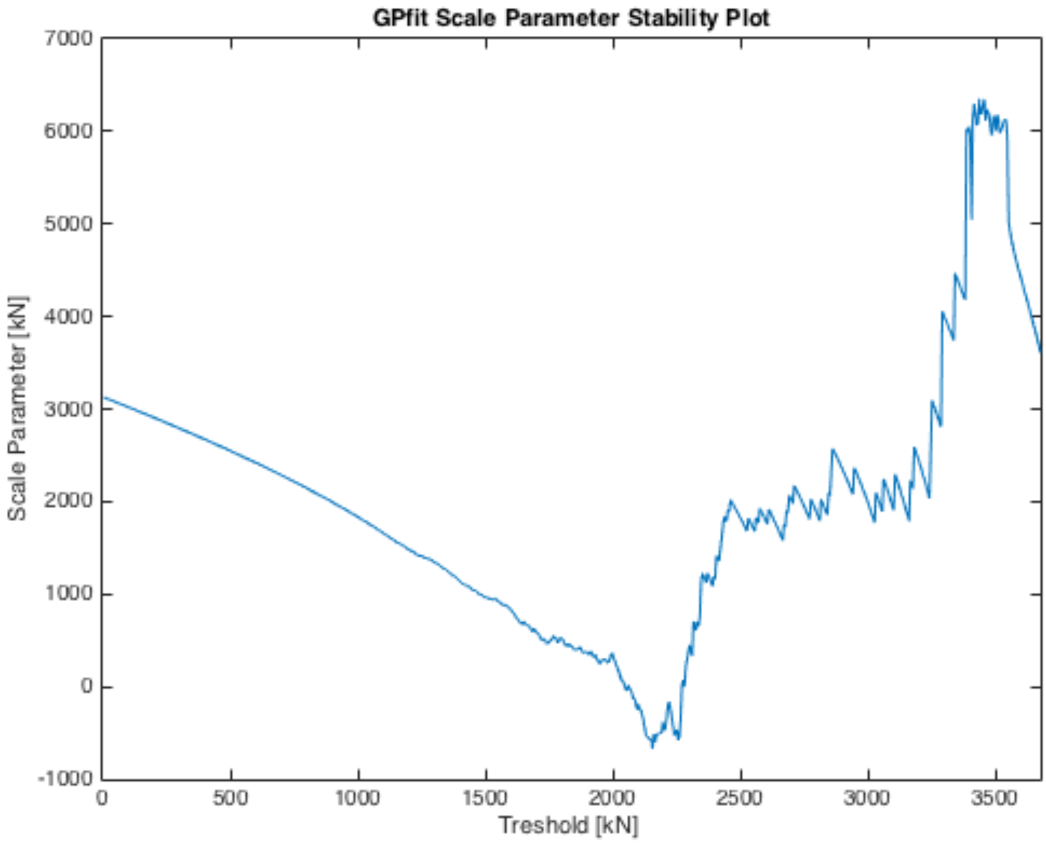
GPfit Scale Parameter Stability Plot
Scale Parameter [kN]
7000
6000
5000
4000
3000
2000
1000
0
-1000
0
500
1000
1500
2000
2500
3000
3500
Treshold [kN]

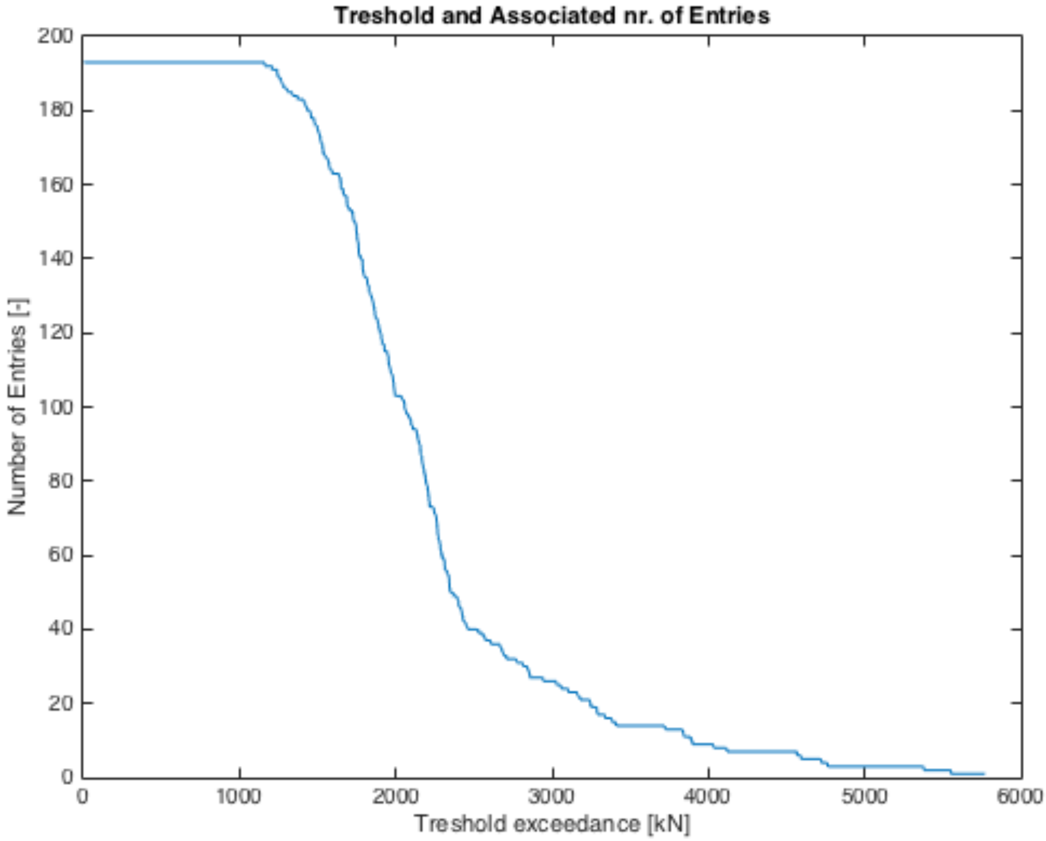
Treshold and Associated nr. of Entries
Number of Entries [-]
200
180
160
140
120
100
80
60
40
20
0
0
1000
2000
3000
4000
5000
6000
Treshold exceedance [kN]

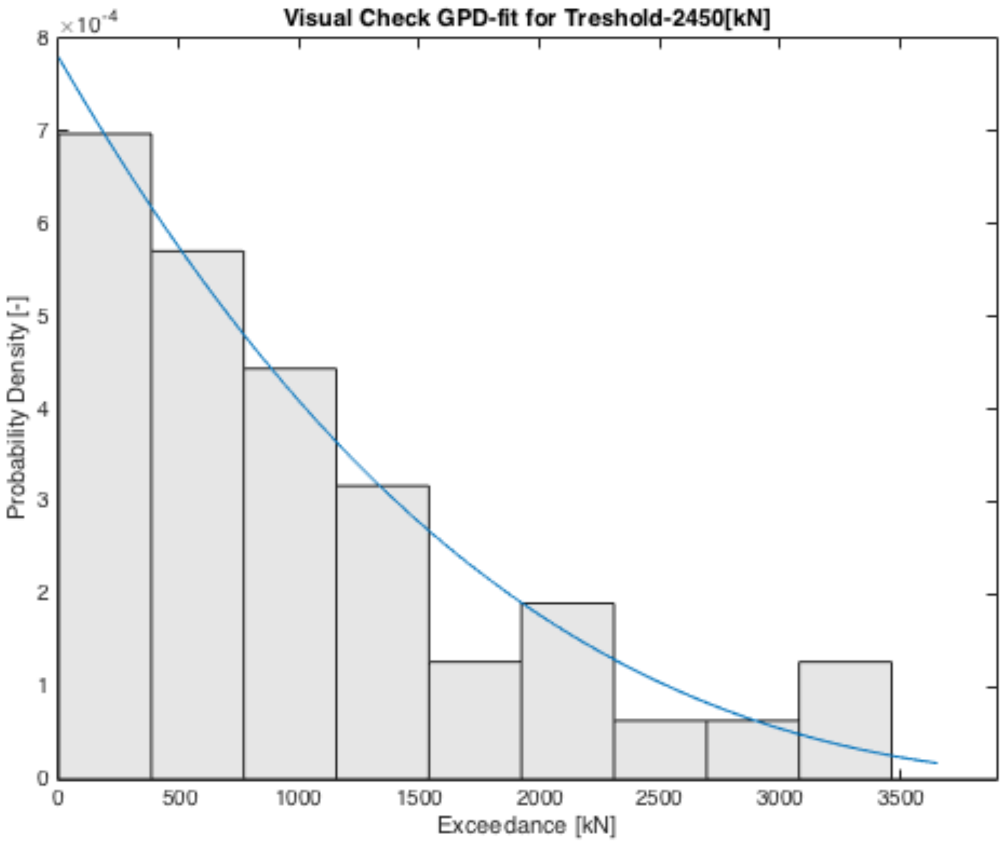
Visual Check GPD-fit for Treshold-2450[kN]
×10^-4
Probability Density [-]
8
7
6
5
4
3
2
1
0
0
500
1000
1500
2000
2500
3000
3500
Exceedance [kN]

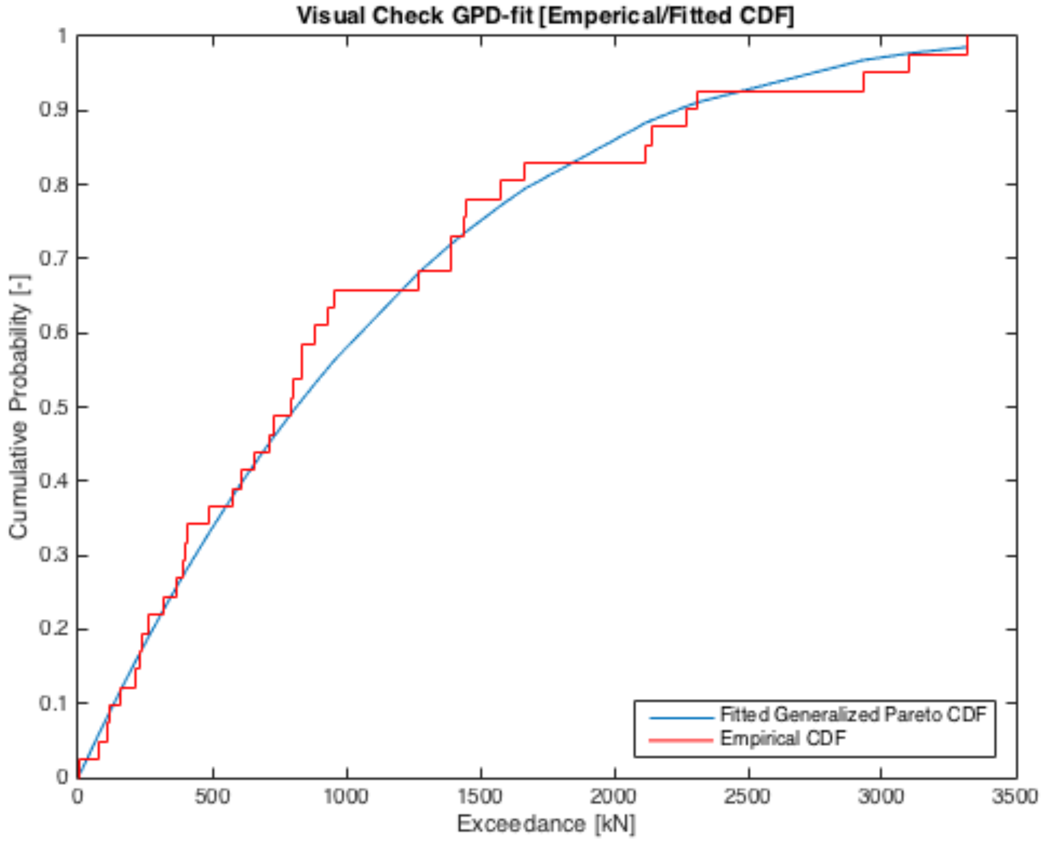
Visual Check GPD-fit [Emperical/Fitted CDF]
Cumulative Probability [-]
Exceedance [kN]
Fitted Generalized Pareto CDF
Empirical CDF
0
0.1
0.2
0.3
0.4
0.5
0.6
0.7
0.8
0.9
1
0
500
1000
1500
2000
2500
3000
3500

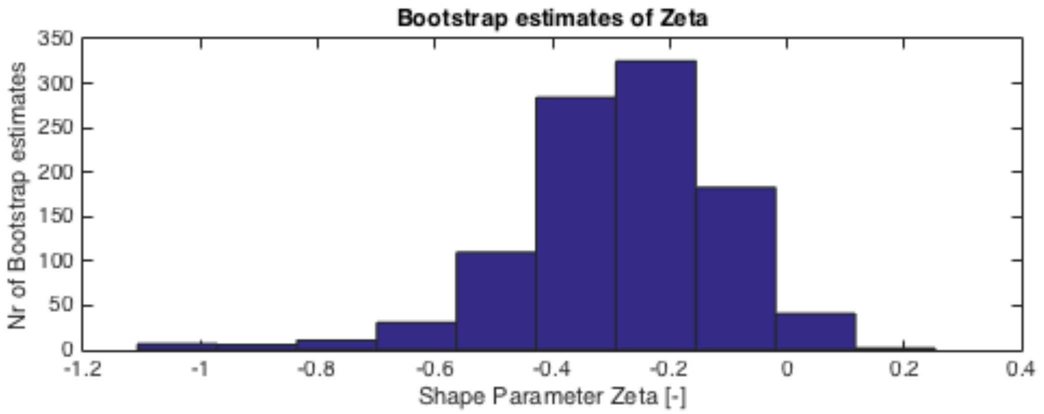
Bootstrap estimates of Zeta
Nr of Bootstrap estimates
Shape Parameter Zeta [-]
0
50
100
150
200
250
300
350
-1.2
-1
-0.8
-0.6
-0.4
-0.2
0
0.2
0.4

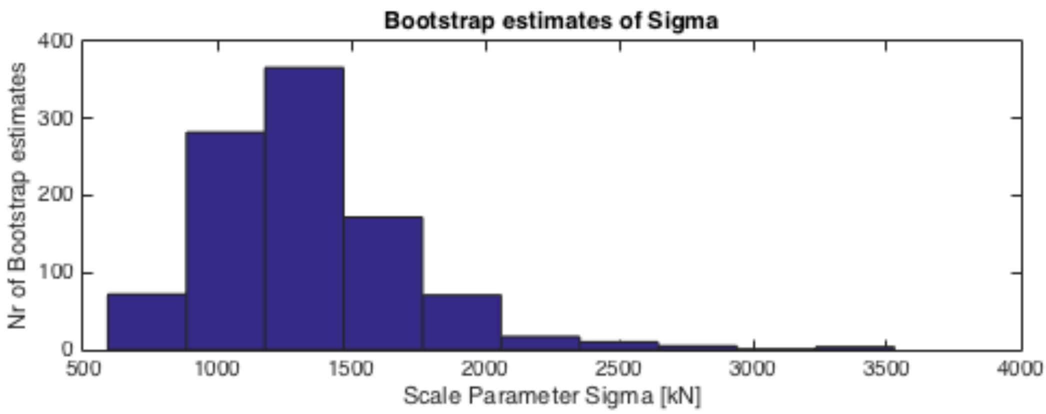
Bootstrap estimates of Sigma
Nr of Bootstrap estimates
Scale Parameter Sigma [kN]
0
100
200
300
400
500
1000
1500
2000
2500
3000
3500
4000

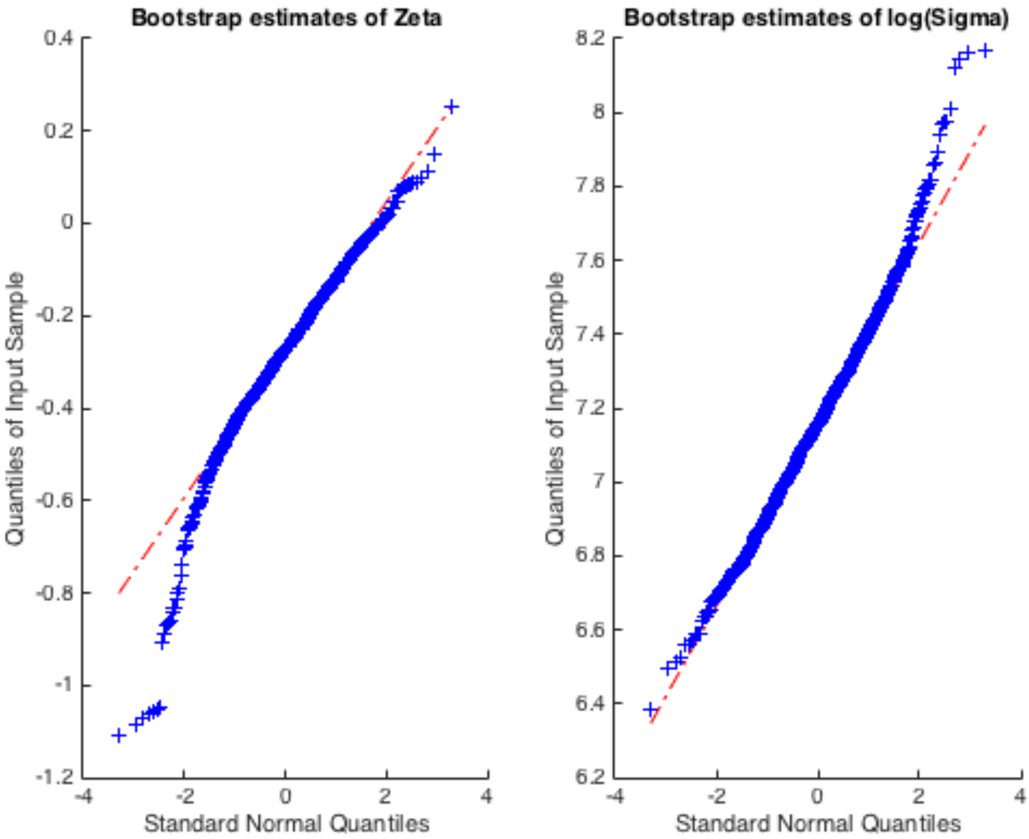
Bootstrap estimates of Zeta
Quantiles of Input Sample
Standard Normal Quantiles
0.4
0.2
0
-0.2
-0.4
-0.6
-0.8
-1
-1.2
-4
-2
0
2
4
Bootstrap estimates of log(Sigma)
Quantiles of Input Sample
Standard Normal Quantiles
8.2
8
7.8
7.6
7.4
7.2
7
6.8
6.6
6.4
6.2

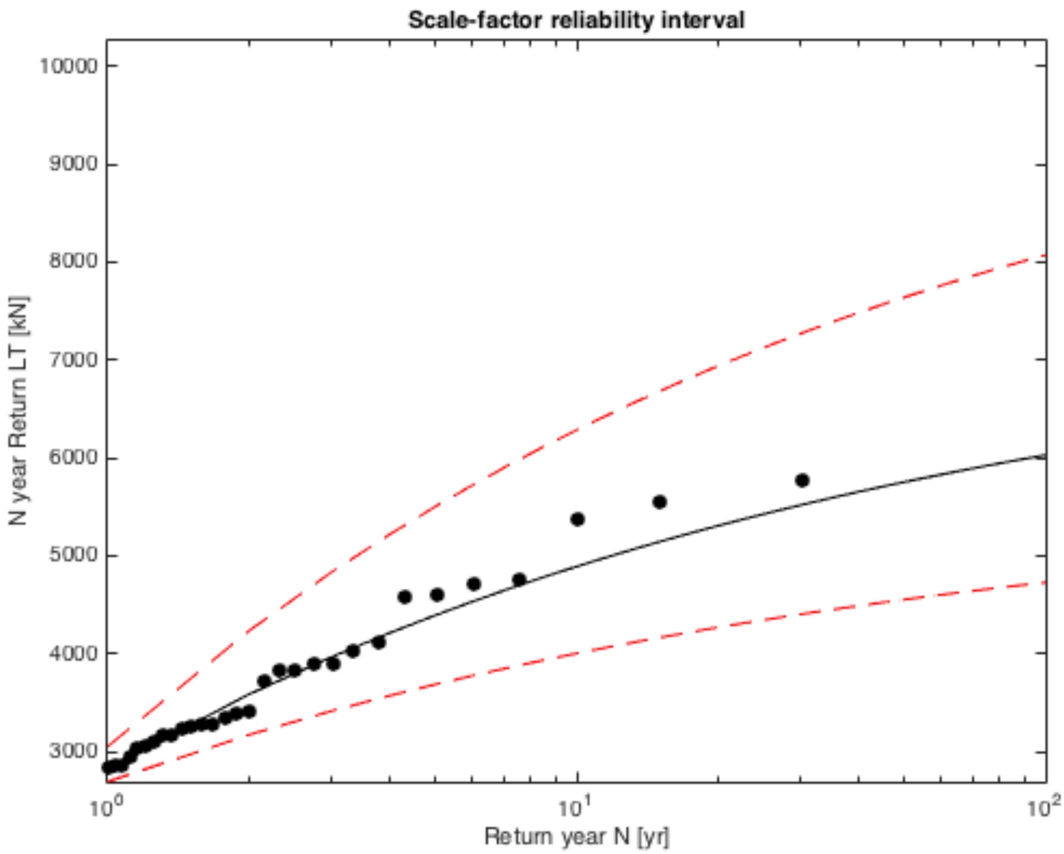
Scale-factor reliability interval
N year Return LT [kN]
Return year N [yr]
10000
9000
8000
7000
6000
5000
4000
3000
10^0
10^1
10^2

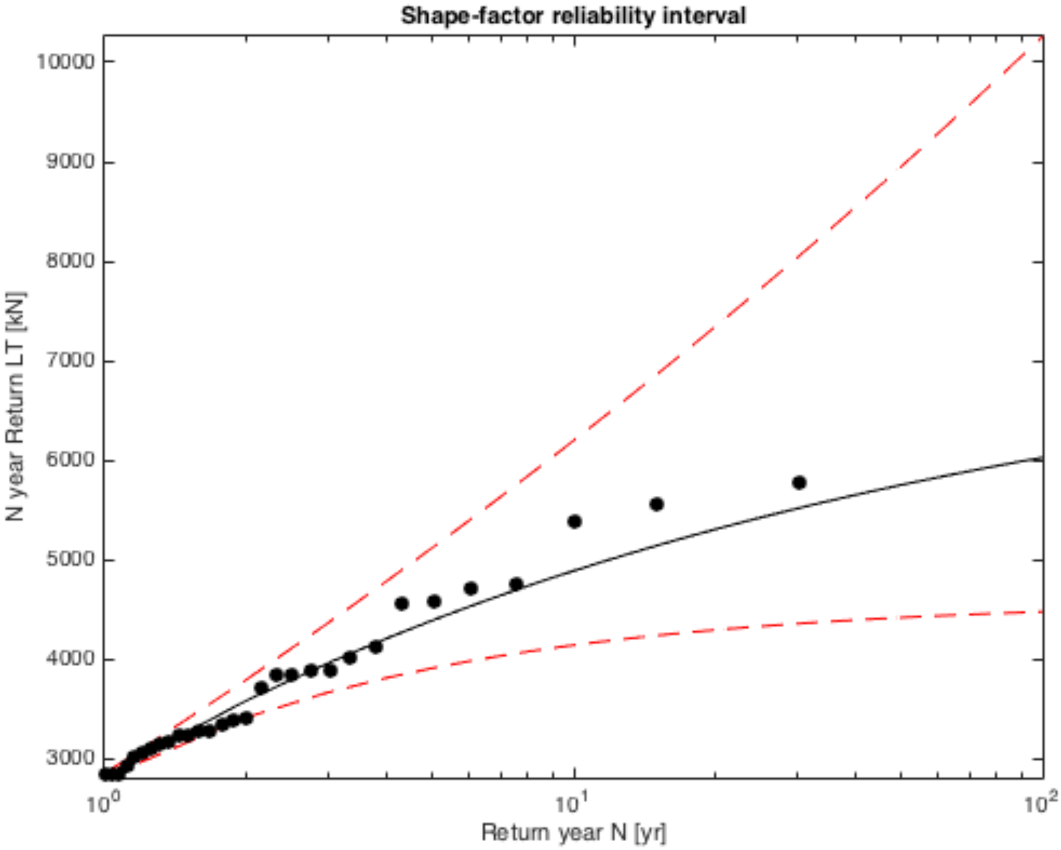

Shape-factor reliability interval
N year Return LT [kN]
10000
9000
8000
7000
6000
5000
4000
3000
10^0
10^1
10^2
Return year N [yr]

III.VI Results Quasi-dynamic analysis West of Shetland dataset (25seeds)

The environment at the West of Shetland is more severe then at the Pierce field. We would expect a larger 100-year return level for the line tension. The parameters become stable around 4500 kN with some fluctuations around the mean. These fluctuations can also been observed in the CDF starting around an exceedance level of 2000kN.

The boostrap estimates for the scale parameter showed standard normal behaviour. For the shape parameter some skewness could be observed for the lower quantiles. The distribution passed all goodness-of-fit tests for a 5% significance level.

The final extrapolation is 14326 kN for the 100-year line load. If the extrapolations of the Pierce field (Hs:6.5m, 100-year LT:10143) and the West of Shetland (Hs:8.5m, 100-year LT:14326), we can conclude that extrapolation for the more severe environment of the West of Shetland is realistic.

u [kN]	4500
σ [kN]	1868.3
ζ	-0.0432
N	100
n_y	2920
ζ_u	0.0013
100-year MAX LT	14326 kN

Test	*Significance level*	*Null-Hypothesis*	*Outcome*	*Simulation method*
Chi-Square	5%	DATASET II follows GPD	Accepted	Quasi-dynamic
Kolmogorov-Smirnov	5%	DATASET II follows GPD	Accepted	Quasi-dynamic

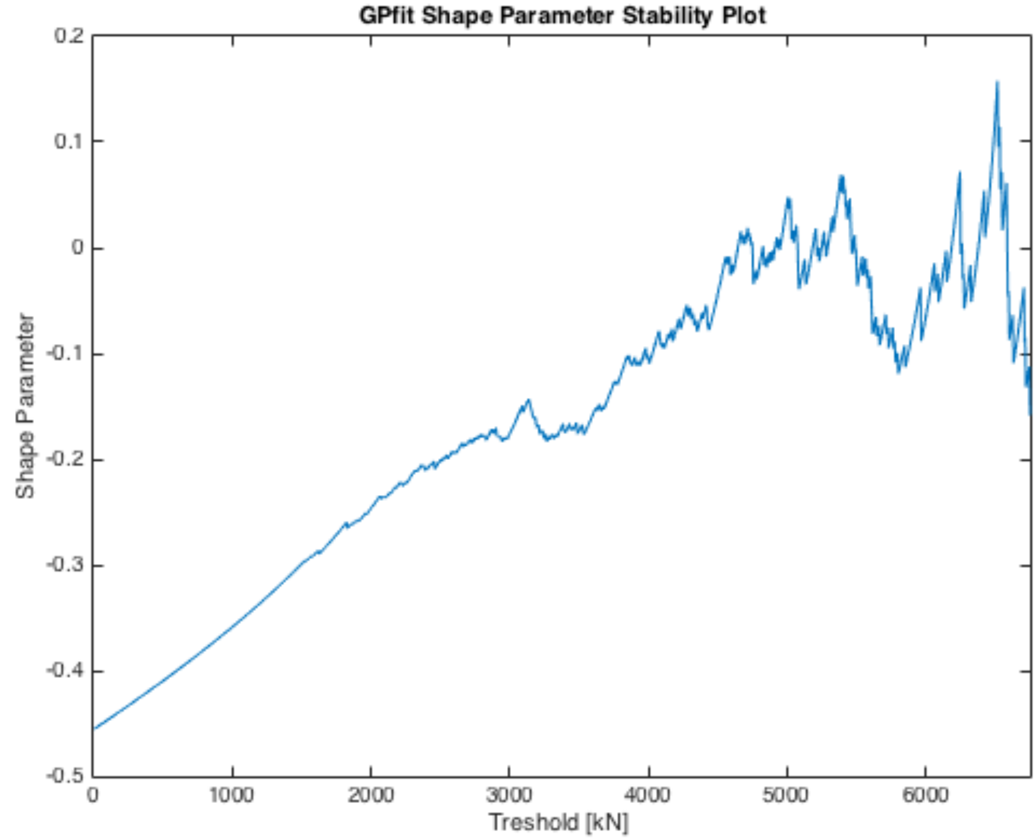
GPfit Shape Parameter Stability Plot
Shape Parameter
Treshold [kN]
0.2
0.1
0
-0.1
-0.2
-0.3
-0.4
-0.5
0
1000
2000
3000
4000
5000
6000

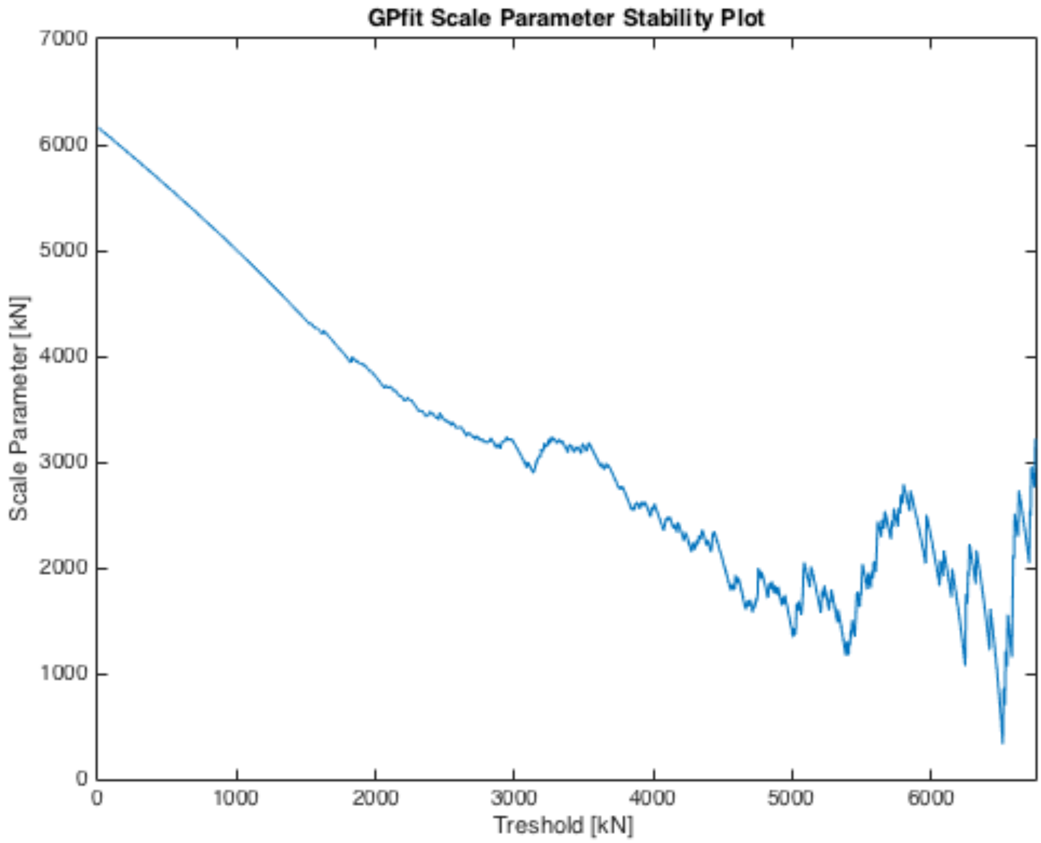
GPfit Scale Parameter Stability Plot
Scale Parameter [kN]
Treshold [kN]
7000
6000
5000
4000
3000
2000
1000
0
0
1000
2000
3000
4000
5000
6000

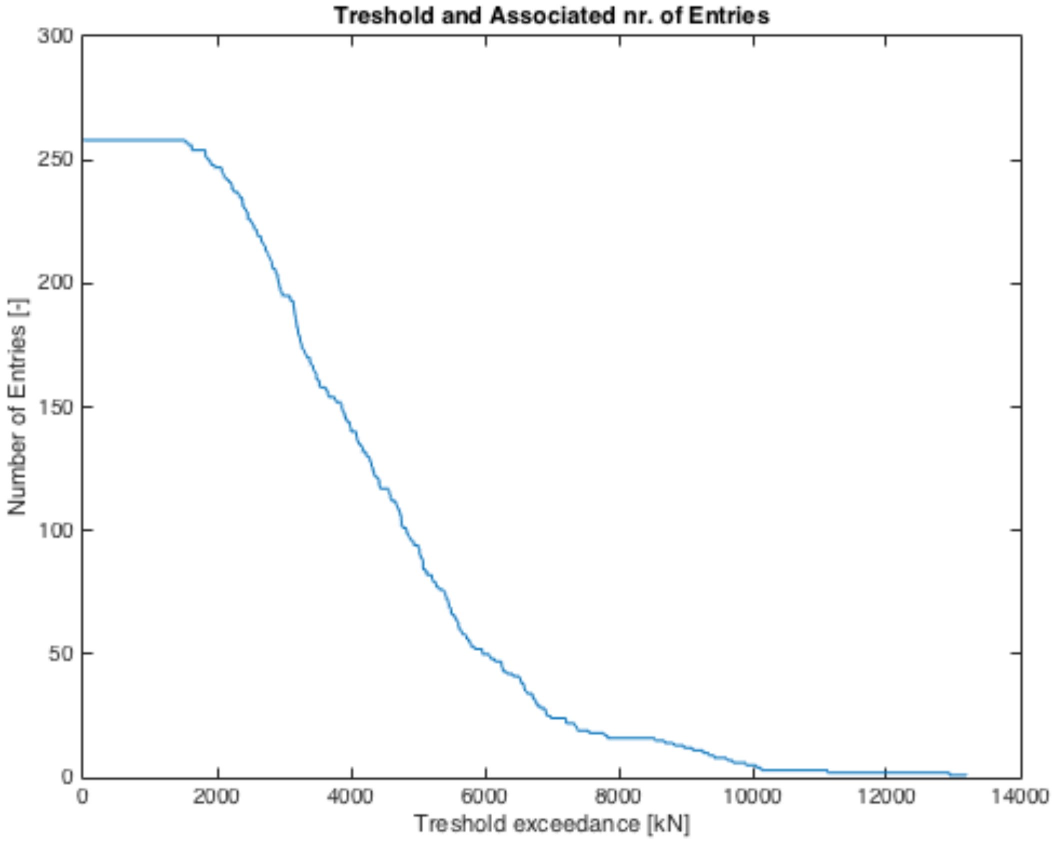

Treshold and Associated nr. of Entries
Number of Entries [-]
Treshold exceedance [kN]

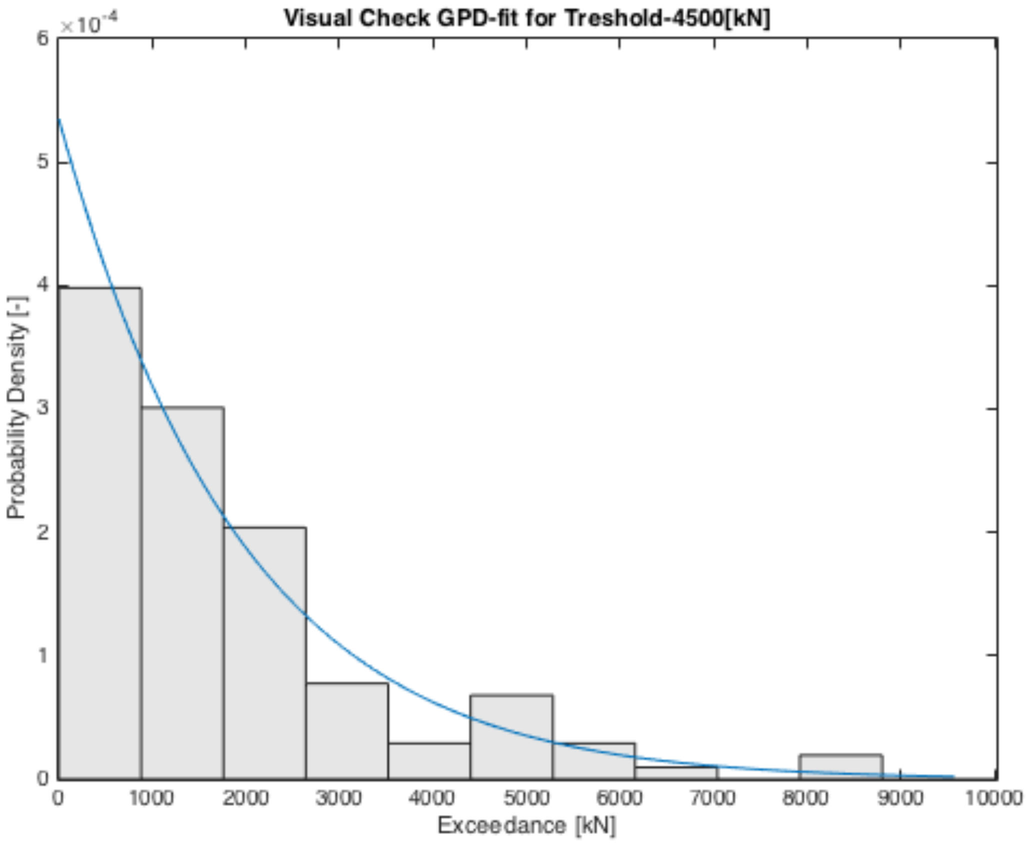

Visual Check GPD-fit for Treshold-4500[kN]
×10^-4
Probability Density [-]
Exceedance [kN]

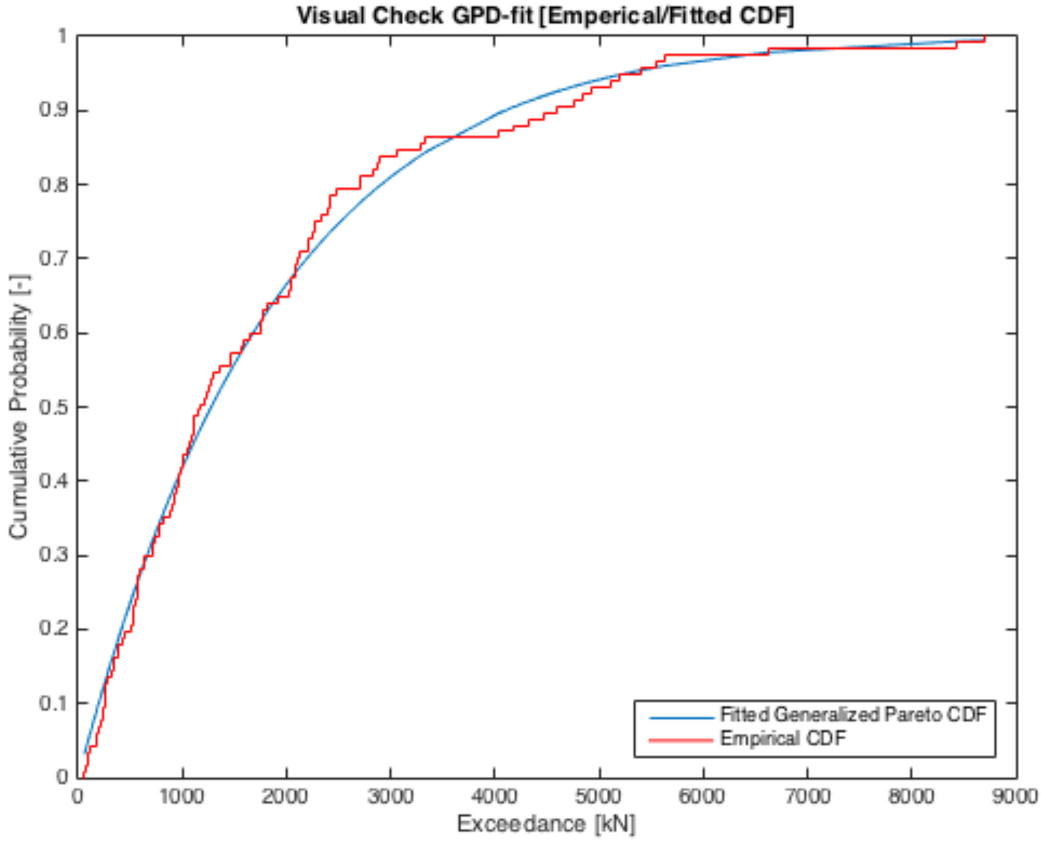
Visual Check GPD-fit [Emperical/Fitted CDF]
Cumulative Probability [-]
Exceedance [kN]
Fitted Generalized Pareto CDF
Empirical CDF
0
0.1
0.2
0.3
0.4
0.5
0.6
0.7
0.8
0.9
1
0
1000
2000
3000
4000
5000
6000
7000
8000
9000

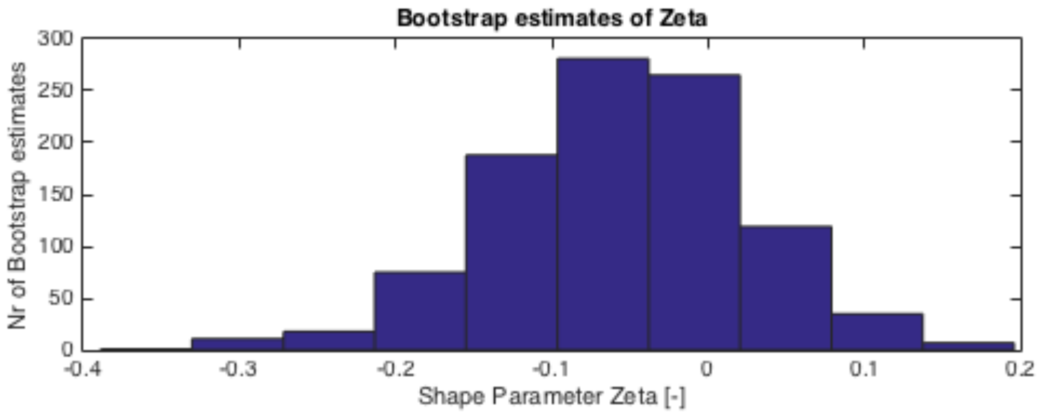
Bootstrap estimates of Zeta
Nr of Bootstrap estimates
Shape Parameter Zeta [-]
0
50
100
150
200
250
300
-0.4
-0.3
-0.2
-0.1
0
0.1
0.2

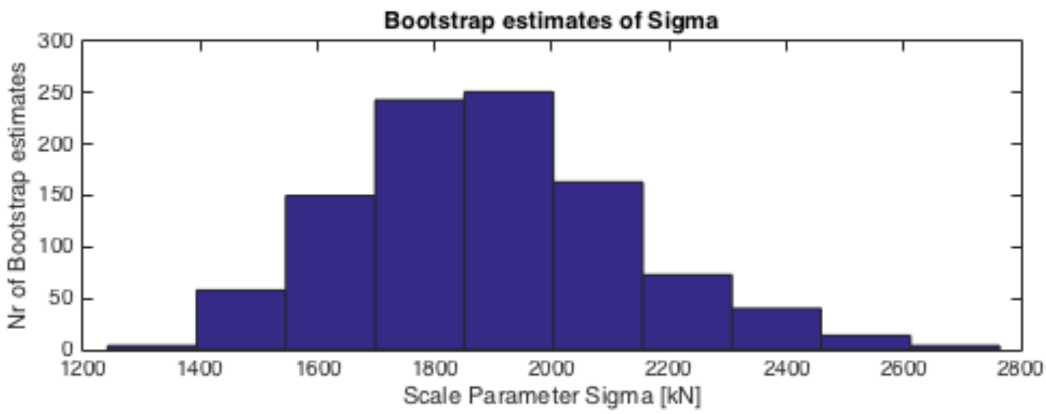
Bootstrap estimates of Sigma
Nr of Bootstrap estimates
Scale Parameter Sigma [kN]
0
50
100
150
200
250
300
1200
1400
1600
1800
2000
2200
2400
2600
2800

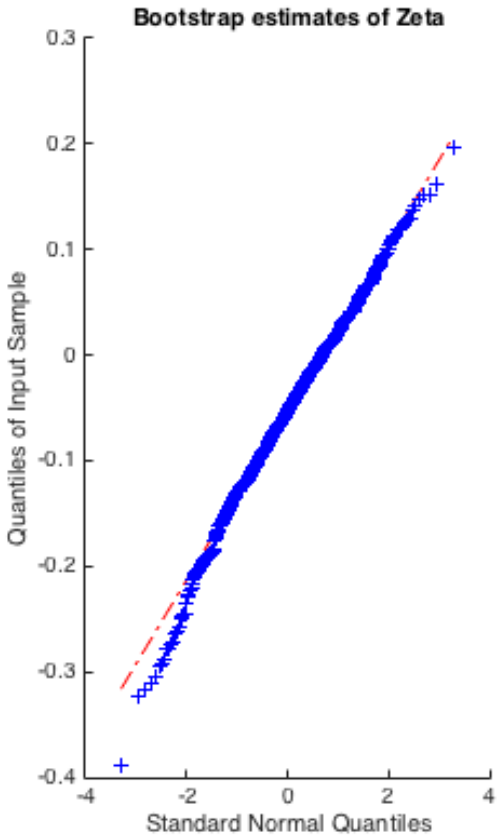
Bootstrap estimates of Zeta
Quantiles of Input Sample
Standard Normal Quantiles

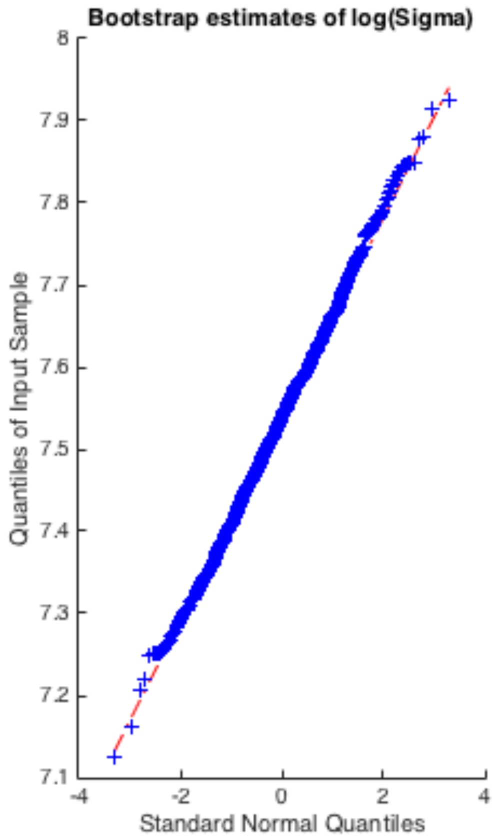
Bootstrap estimates of log(Sigma)
Quantiles of Input Sample
Standard Normal Quantiles

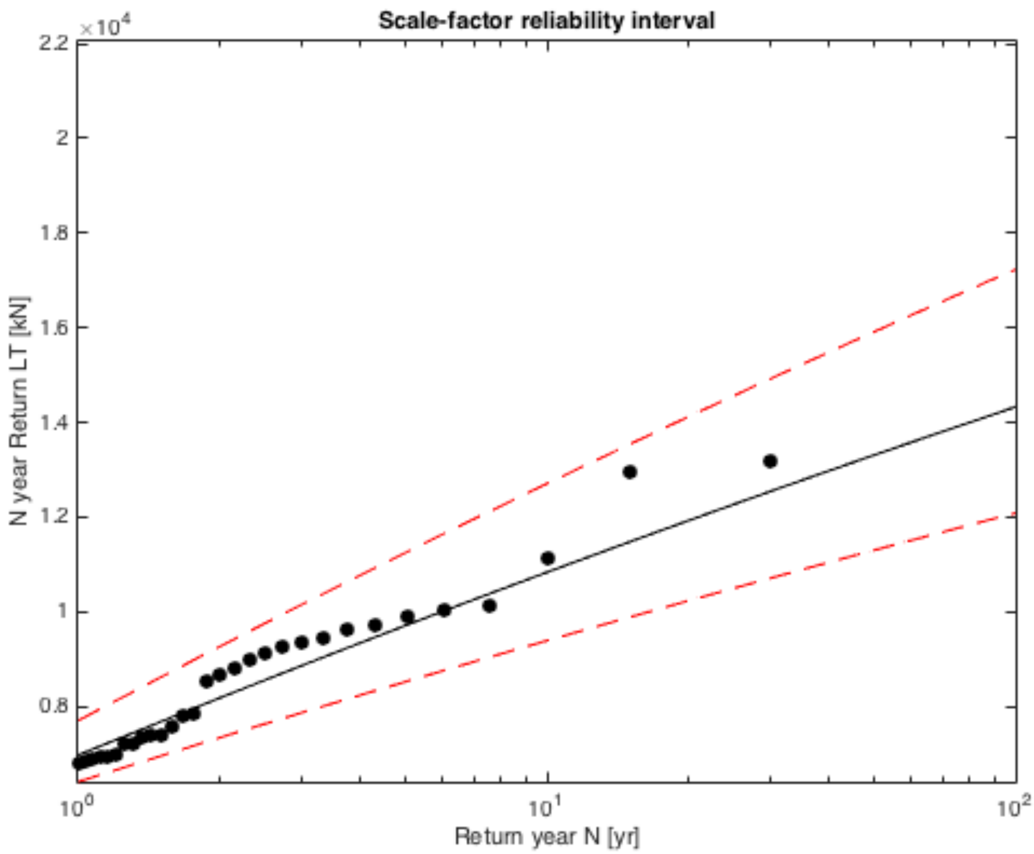
Scale-factor reliability interval
N year Return LT [kN]
Return year N [yr]

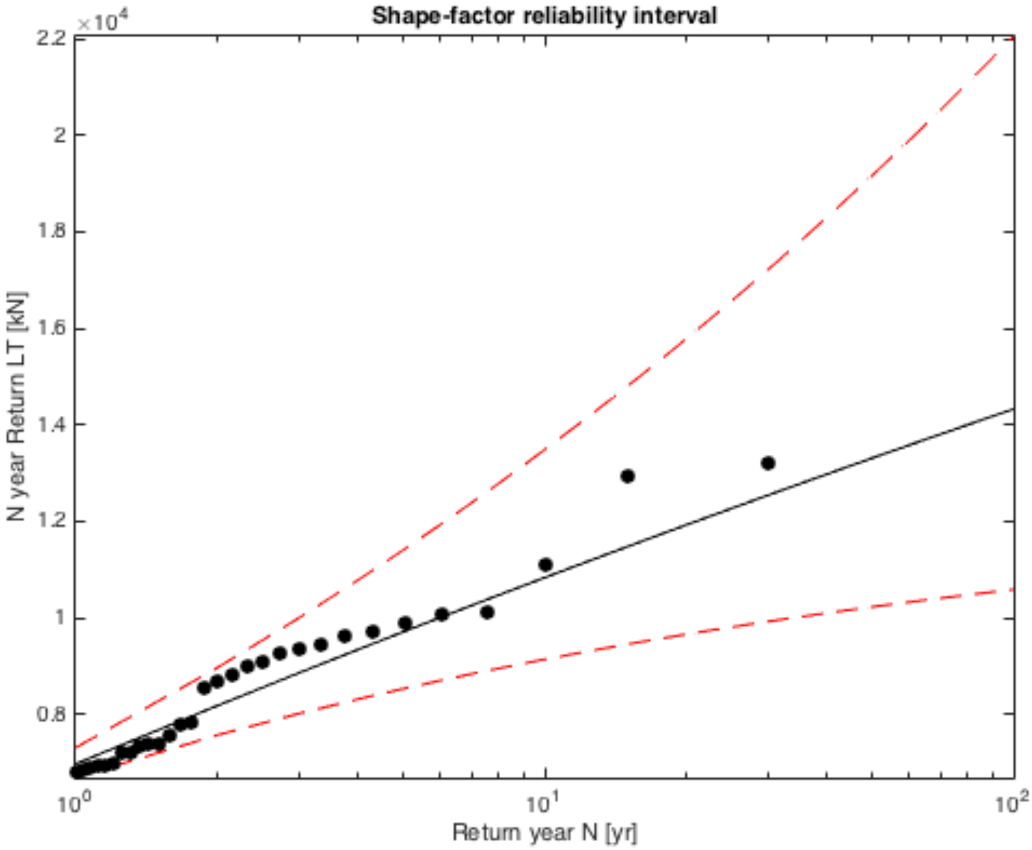

Shape-factor reliability interval
×10^4
2.2
2
1.8
1.6
1.4
1.2
1
0.8
N year Return LT [kN]
10^0
10^1
10^2
Return year N [yr]

III.VII Results Quasi-dynamic analysis dataset II for offset (25seeds)

It can be seen that the fit parameters are more or less stable around 12m. The distribution passed all goodness-of-fit tests and the bootstrap estimates of parameters show standard normal behaviour as expected. The 100-year return level for the offset is 22.21m. On the observations it can be concluded that the distribution and the extrapolation is reliable.

u [m]	12
σ [m]	2.9476
ζ	-0.2136
N	100
n_y	2920
ζ_u	0.0019
100-year MAX LT	22.2098 m

Test	*Significance level*	*Null-Hypothesis*	*Outcome*	*Simulation method*
Chi-Square	5%	DATASET II follows GPD	Accepted	Quasi-dynamic
Kolmogorov-Smirnov	5%	DATASET II follows GPD	Accepted	Quasi-dynamic

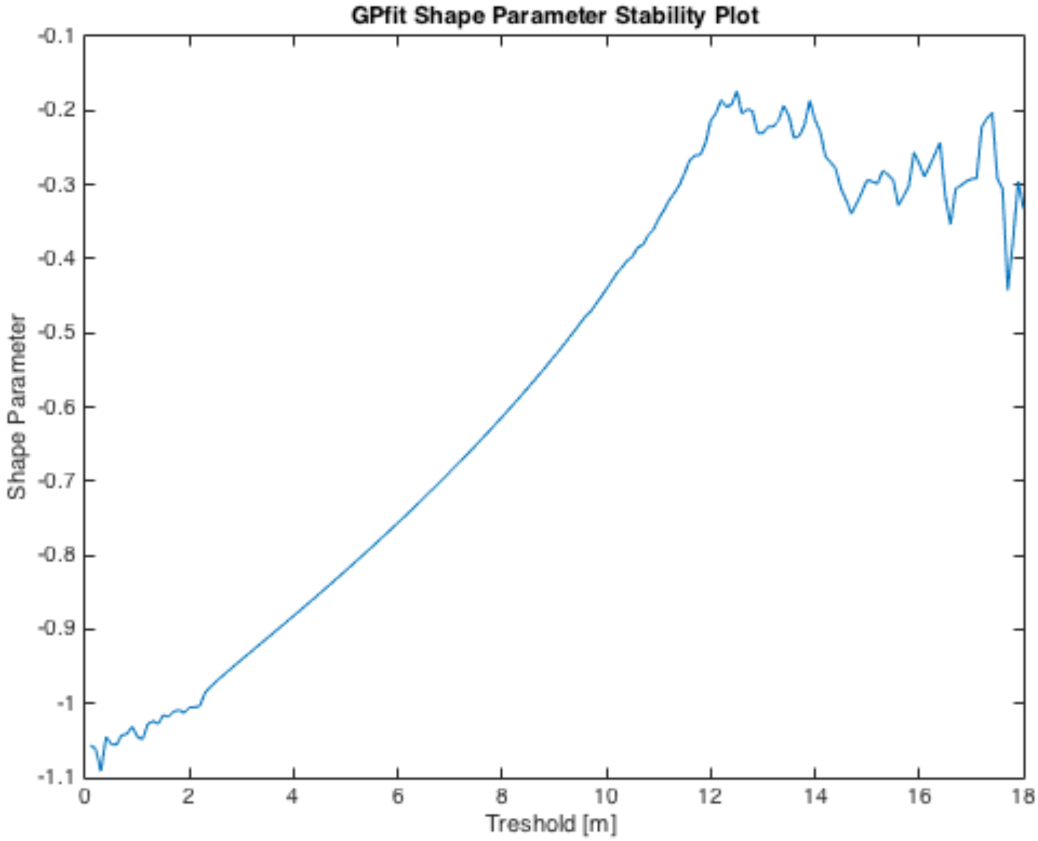
GPfit Shape Parameter Stability Plot
Shape Parameter
Treshold [m]

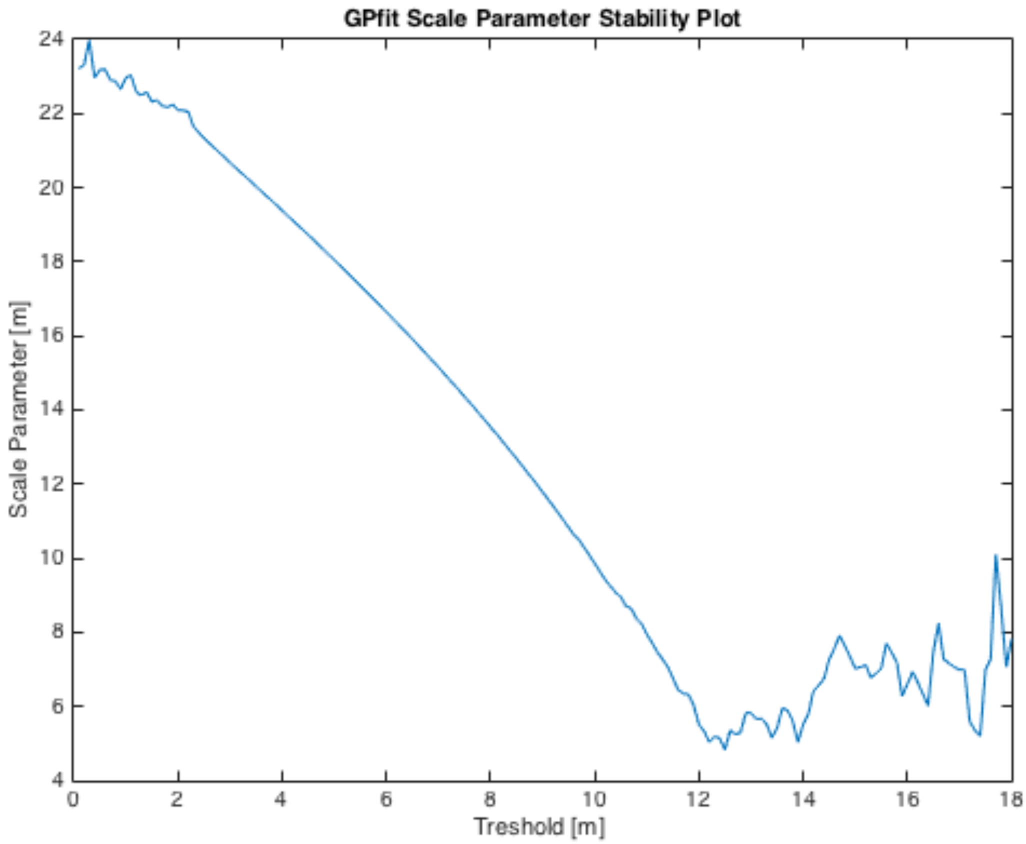
GPfit Scale Parameter Stability Plot
Scale Parameter [m]
Treshold [m]

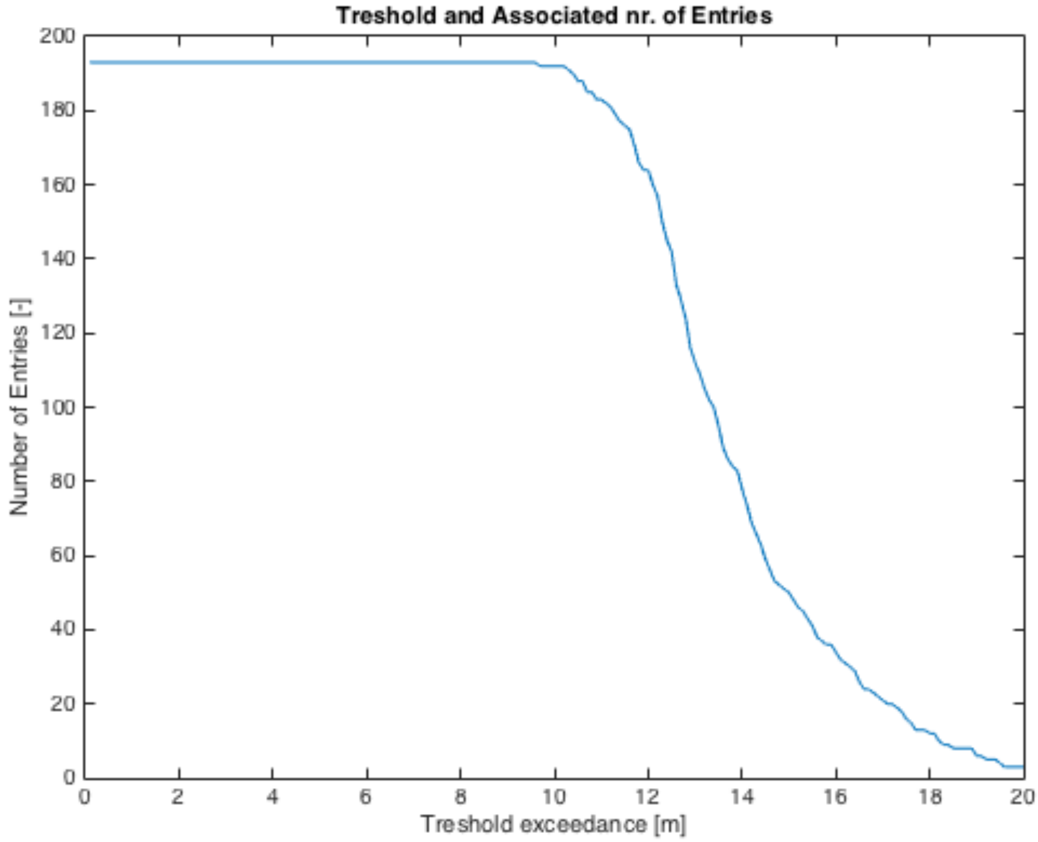
Treshold and Associated nr. of Entries
Number of Entries [-]
Treshold exceedance [m]
0
2
4
6
8
10
12
14
16
18
20
0
20
40
60
80
100
120
140
160
180
200

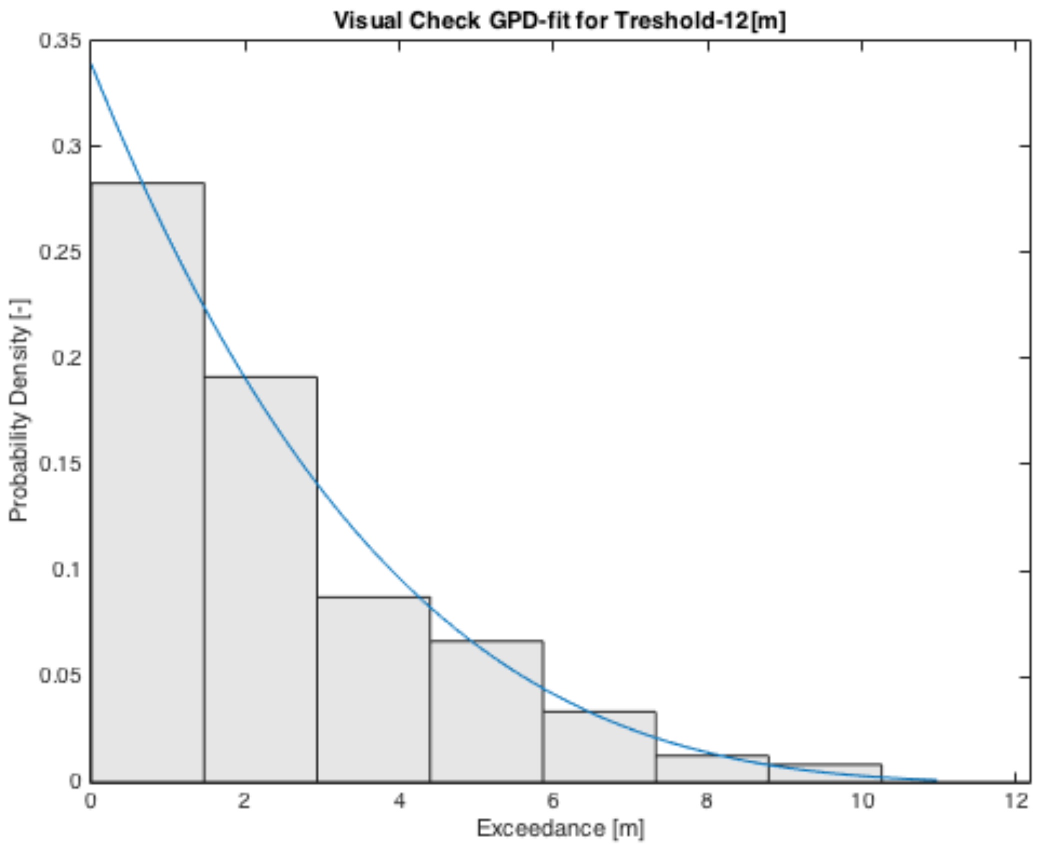
Visual Check GPD-fit for Treshold-12[m]
Probability Density [-]
Exceedance [m]
0
2
4
6
8
10
12
0
0.05
0.1
0.15
0.2
0.25
0.3
0.35

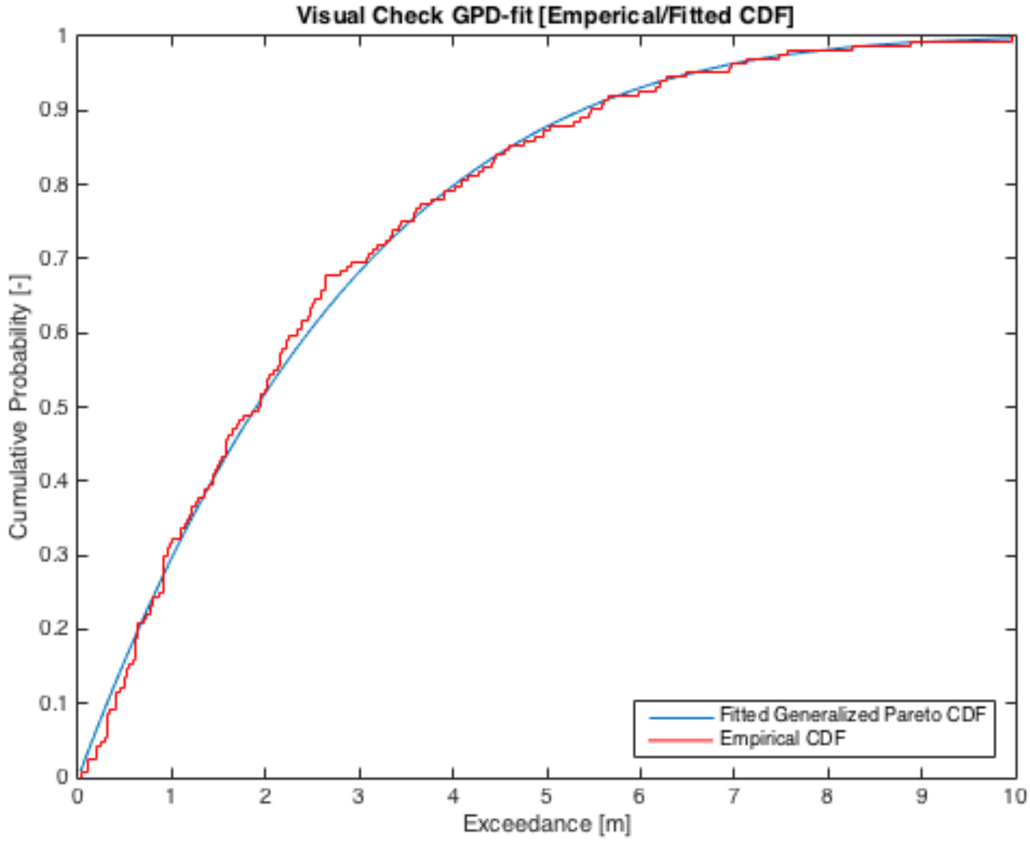
Visual Check GPD-fit [Emperical/Fitted CDF]
Cumulative Probability [-]
Exceedance [m]
0 0.1 0.2 0.3 0.4 0.5 0.6 0.7 0.8 0.9 1
0 1 2 3 4 5 6 7 8 9 10
Fitted Generalized Pareto CDF
Empirical CDF

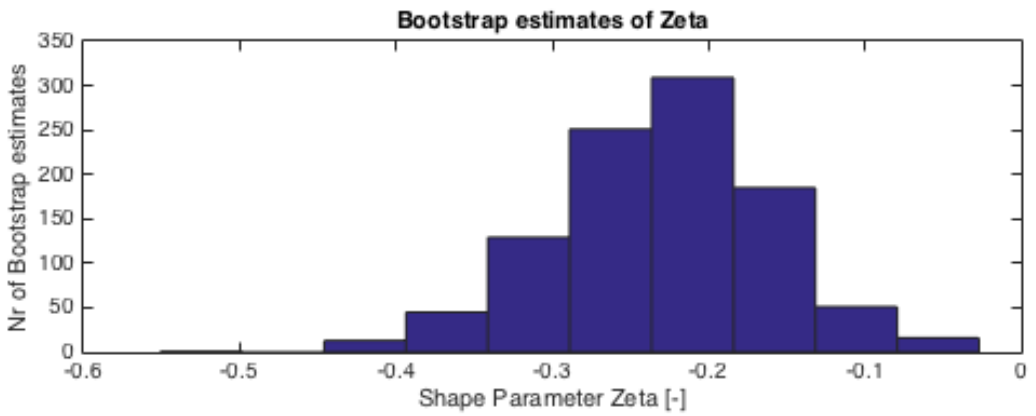
Bootstrap estimates of Zeta
Nr of Bootstrap estimates
Shape Parameter Zeta [-]
0 50 100 150 200 250 300 350
-0.6 -0.5 -0.4 -0.3 -0.2 -0.1 0

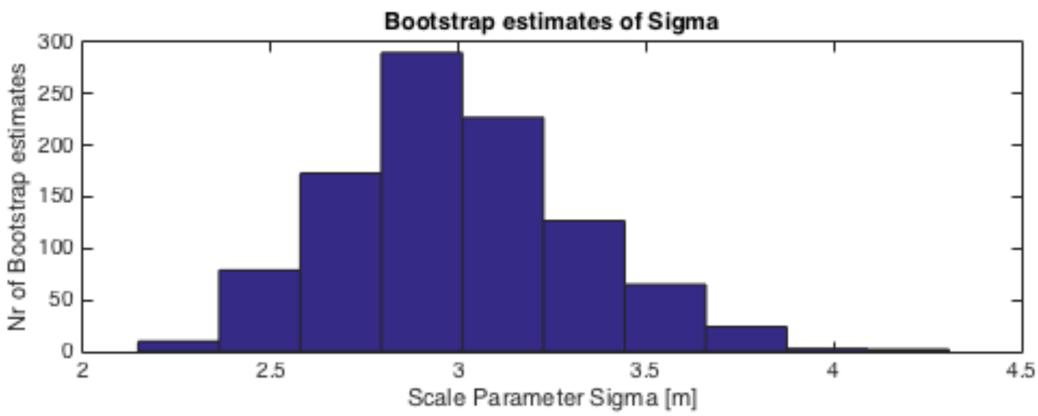
Bootstrap estimates of Sigma
Nr of Bootstrap estimates
Scale Parameter Sigma [m]
0 50 100 150 200 250 300
2 2.5 3 3.5 4 4.5

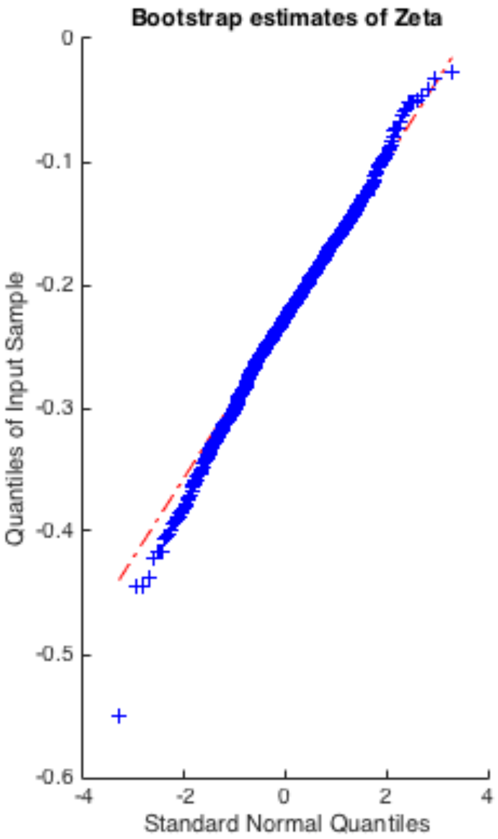

Bootstrap estimates of Zeta
Quantiles of Input Sample
Standard Normal Quantiles

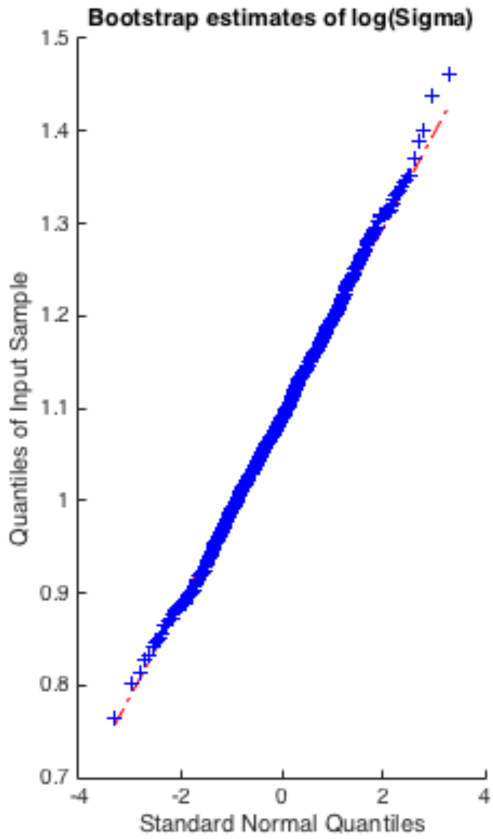

Bootstrap estimates of log(Sigma)
Quantiles of Input Sample
Standard Normal Quantiles

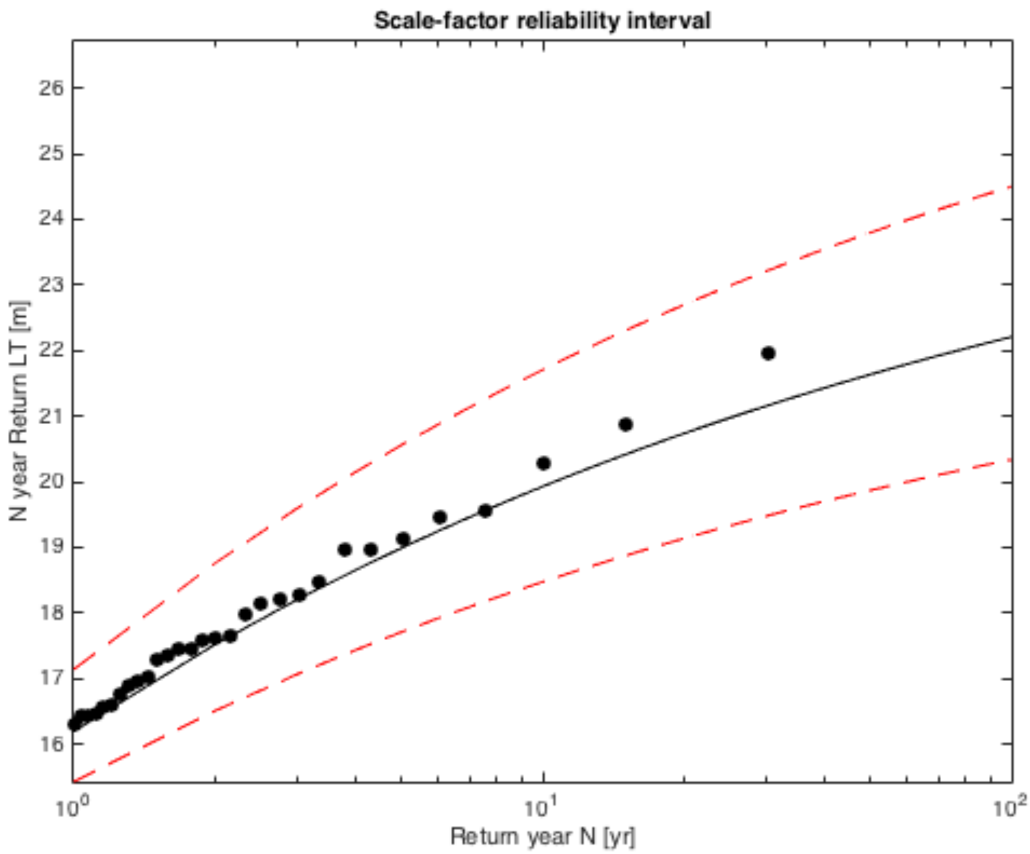

Scale-factor reliability interval
N year Return LT [m]
Return year N [yr]

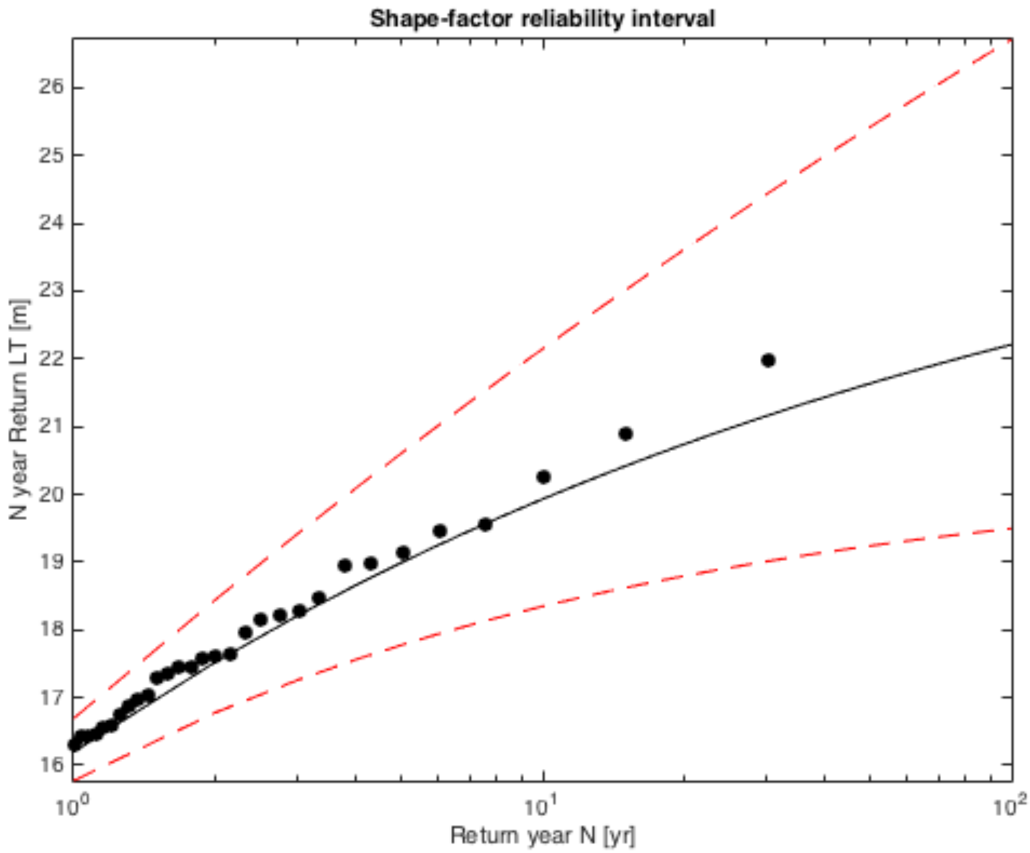
Shape-factor reliability interval
N year Return LT [m]
26
25
24
23
22
21
20
19
18
17
16
10^0
10^1
10^2
Return year N [yr]

III.VIII Results Quasi-dynamic analysis dataset II for turret bending moment (25seeds)

The fit of the empirical data of the turret bending moment has the best fit to the distribution of all variations used in the parameter study. The distribution passed all goodness-of-fit tests and the bootstrap estimates showed standard normal behaviour. The 100-year return level for the turret bending moment is 22211 kNm which is a realistic value.

u [kNm]	8600
σ [kNm]	3403.2
ζ	-0.1570
N	100
n_y	2920
ζ_u	0.0019
100-year MAX LT	22211 kNm

Test	*Significance level*	*Null-Hypothesis*	*Outcome*	*Simulation method*
Chi-Square	5%	DATASET II follows GPD	Accepted	Quasi-dynamic
Kolmogorov-Smirnov	5%	DATASET II follows GPD	Accepted	Quasi-dynamic

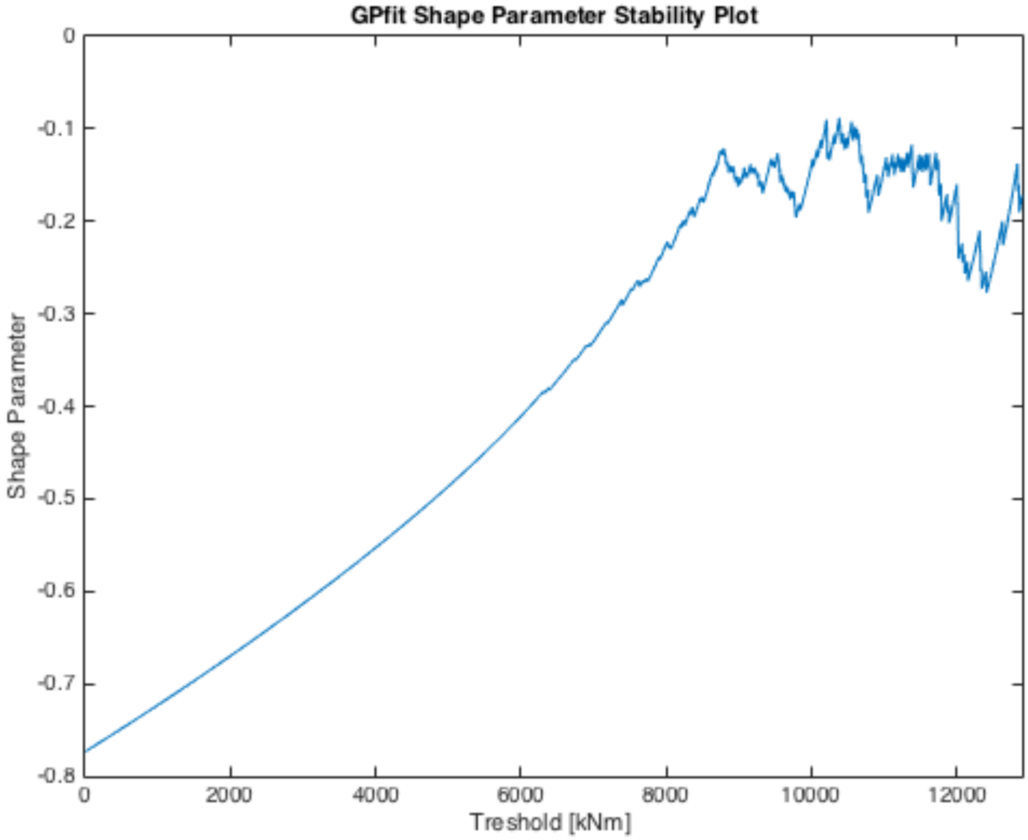
GPfit Shape Parameter Stability Plot
Shape Parameter
Treshold [kNm]
0
-0.1
-0.2
-0.3
-0.4
-0.5
-0.6
-0.7
-0.8
0
2000
4000
6000
8000
10000
12000

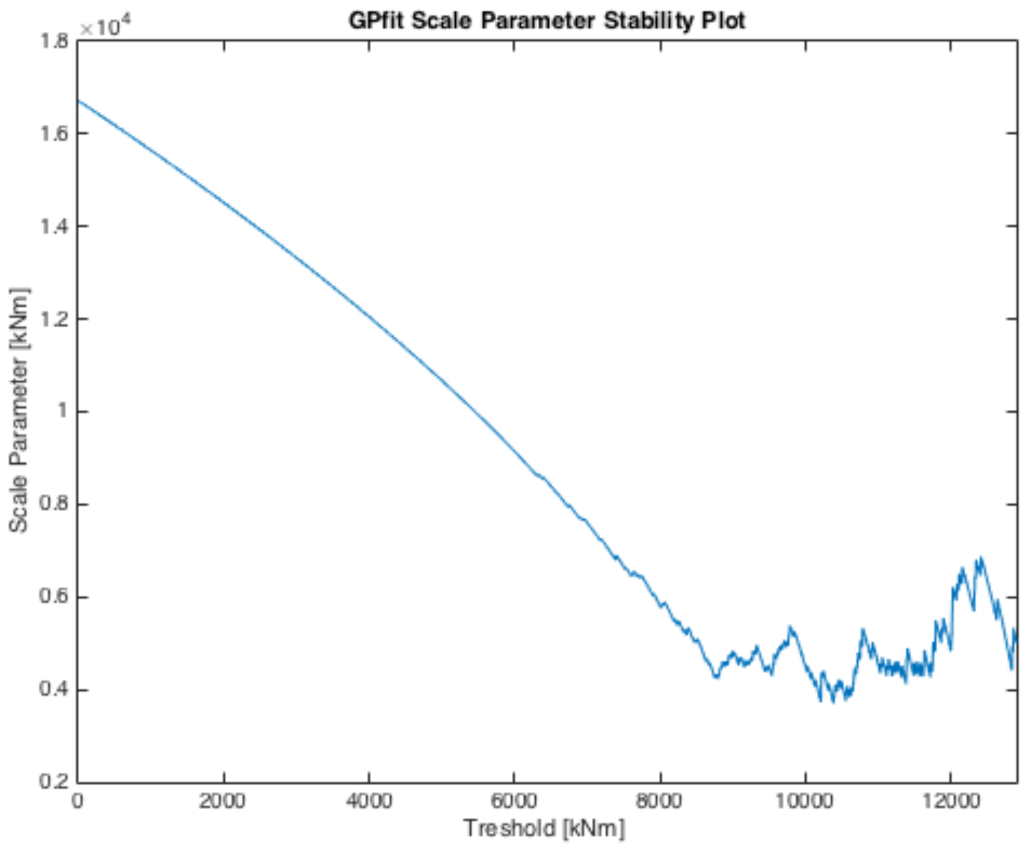
GPfit Scale Parameter Stability Plot
×10^4
Scale Parameter [kNm]
Treshold [kNm]
1.8
1.6
1.4
1.2
1
0.8
0.6
0.4
0.2
0
2000
4000
6000
8000
10000
12000

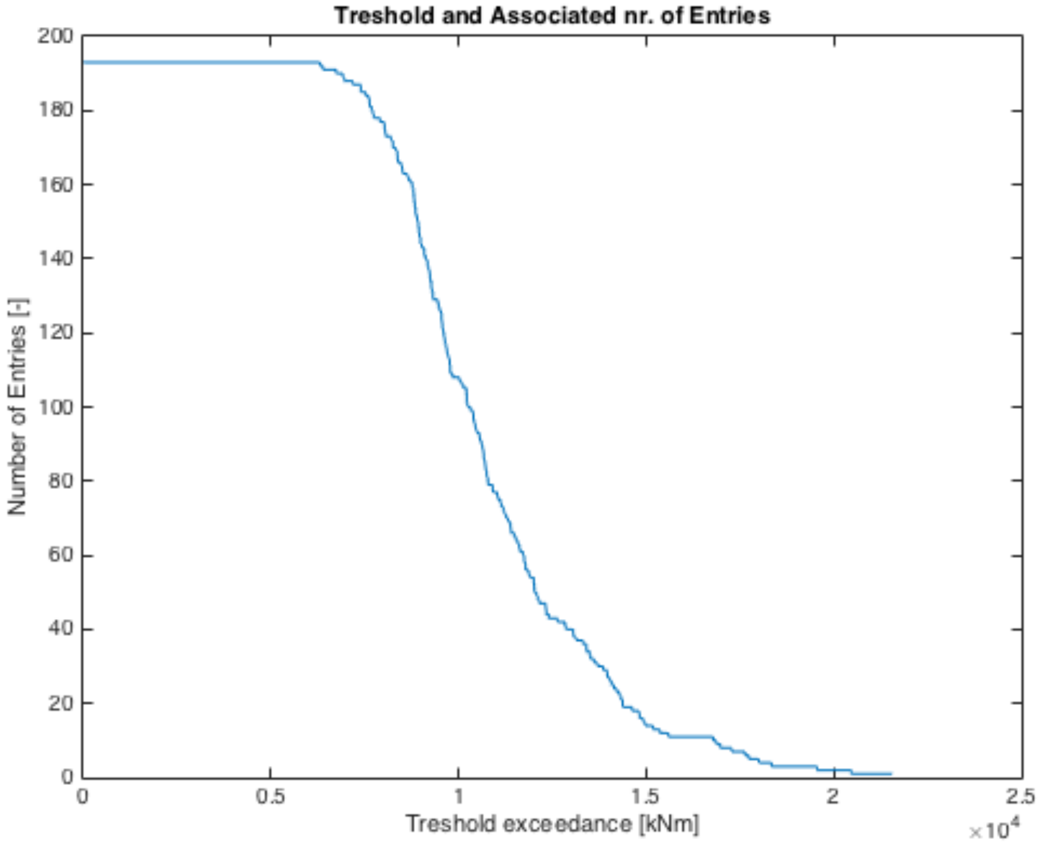
Treshold and Associated nr. of Entries
200
180
160
140
120
100
80
60
40
20
0
Number of Entries [-]
0
0.5
1
1.5
2
2.5
Treshold exceedance [kNm]
×10^4

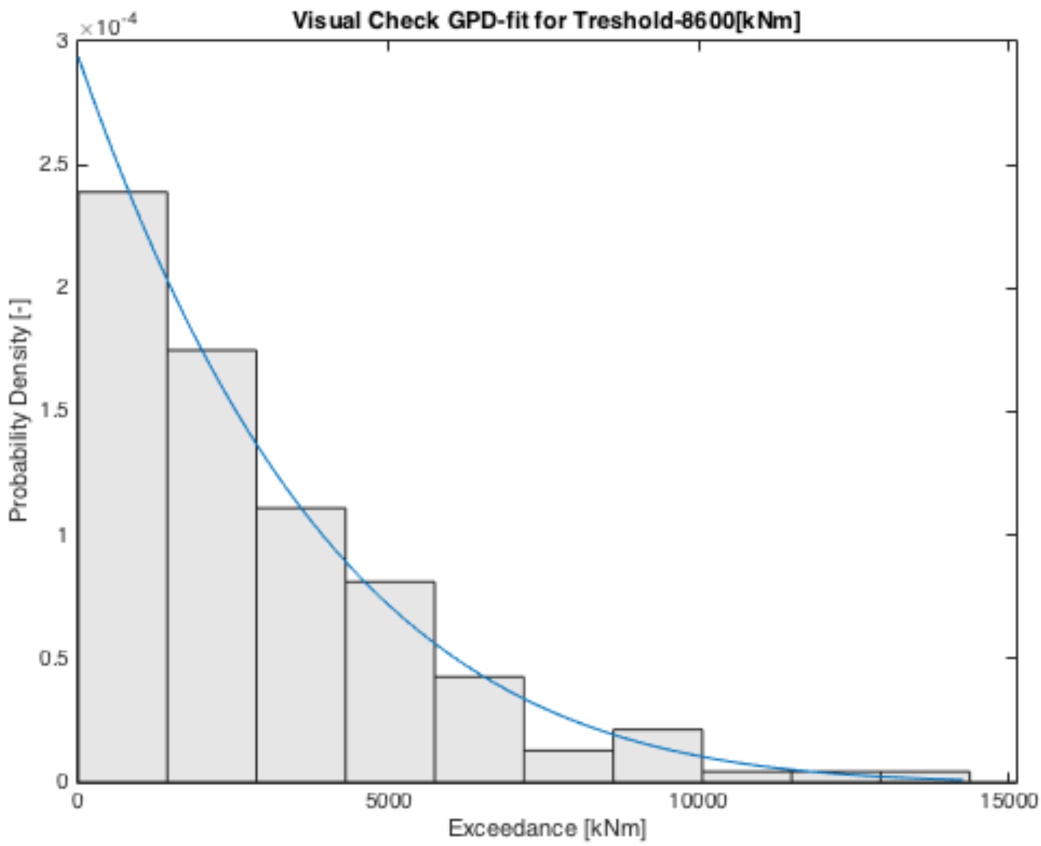
Visual Check GPD-fit for Treshold-8600[kNm]
×10^-4
3
2.5
2
1.5
1
0.5
0
Probability Density [-]
0
5000
10000
15000
Exceedance [kNm]

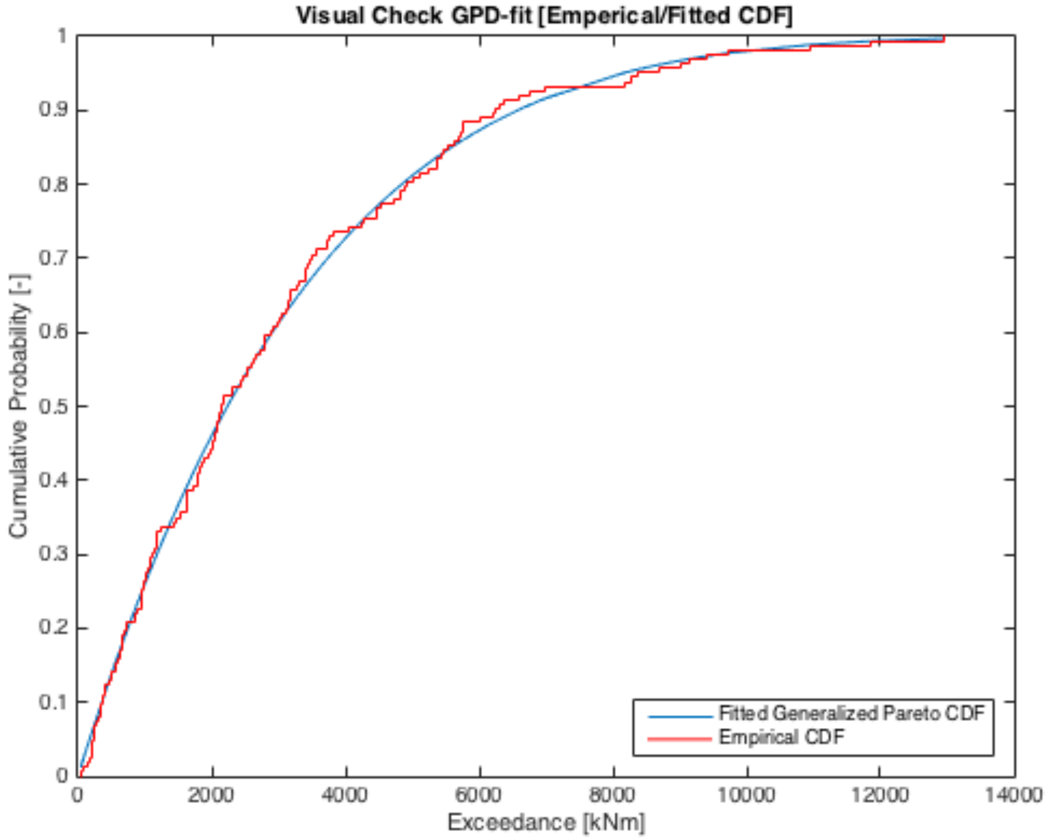
Visual Check GPD-fit [Emperical/Fitted CDF]
Cumulative Probability [-]
Exceedance [kNm]
Fitted Generalized Pareto CDF
Empirical CDF
0
0.1
0.2
0.3
0.4
0.5
0.6
0.7
0.8
0.9
1
0
2000
4000
6000
8000
10000
12000
14000

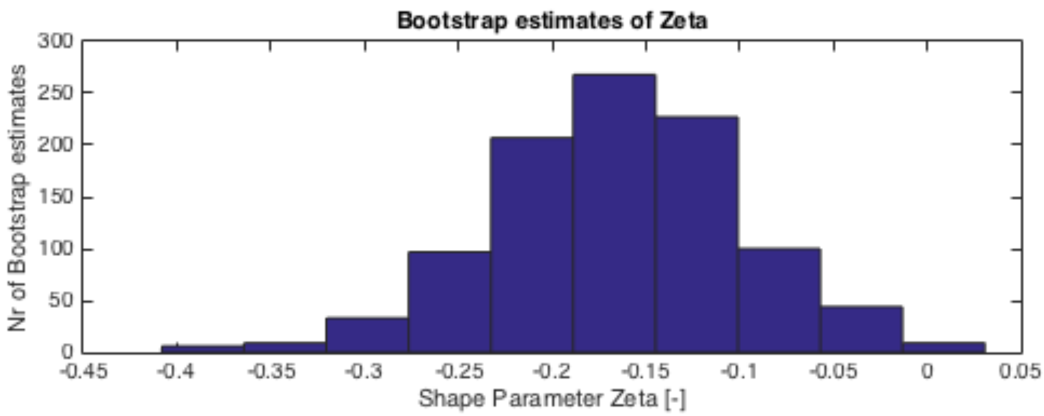
Bootstrap estimates of Zeta
Nr of Bootstrap estimates
Shape Parameter Zeta [-]
0
50
100
150
200
250
300
-0.45
-0.4
-0.35
-0.3
-0.25
-0.2
-0.15
-0.1
-0.05
0
0.05

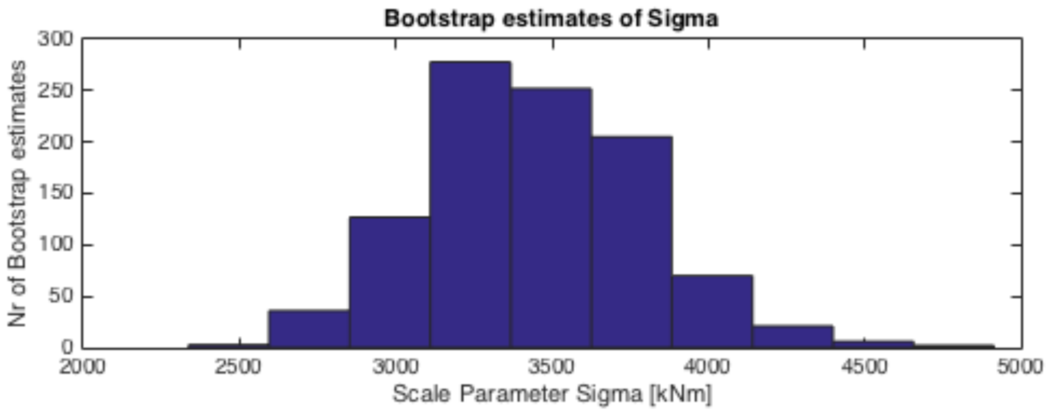
Bootstrap estimates of Sigma
Nr of Bootstrap estimates
Scale Parameter Sigma [kNm]
0
50
100
150
200
250
300
2000
2500
3000
3500
4000
4500
5000

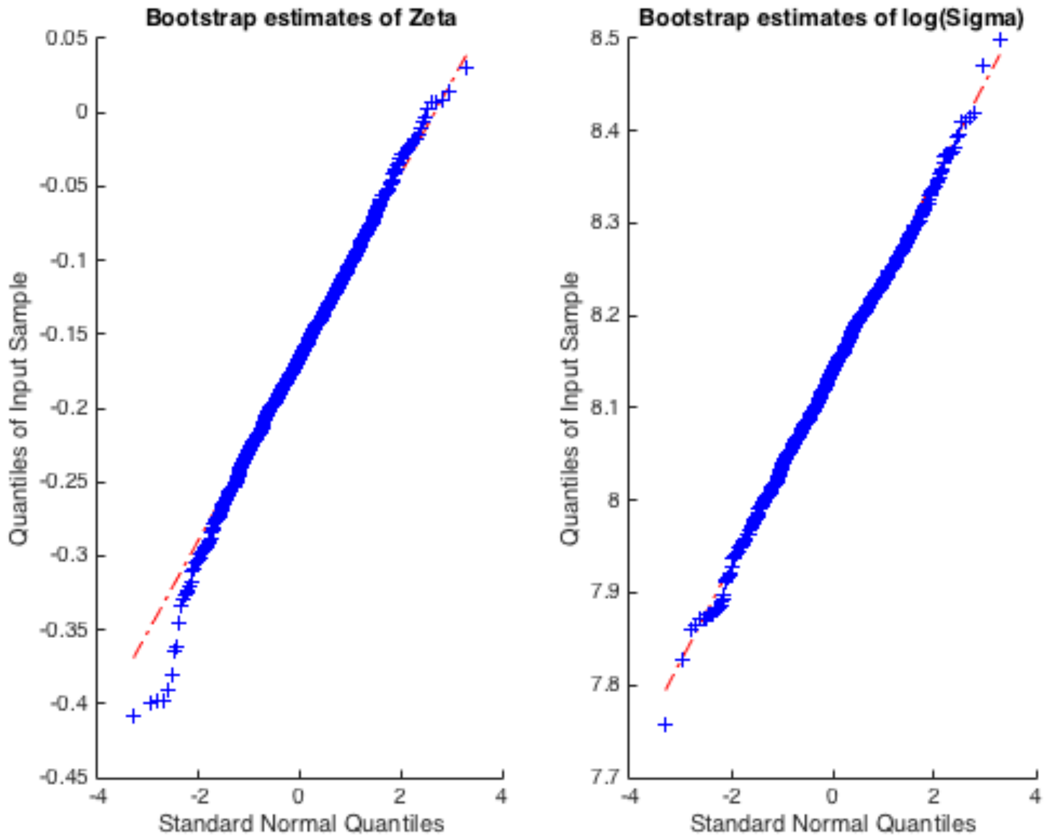

Bootstrap estimates of Zeta
Quantiles of Input Sample
Standard Normal Quantiles
0.05
0
-0.05
-0.1
-0.15
-0.2
-0.25
-0.3
-0.35
-0.4
-0.45
-4
-2
0
2
4
Bootstrap estimates of log(Sigma)
Quantiles of Input Sample
Standard Normal Quantiles
8.5
8.4
8.3
8.2
8.1
8
7.9
7.8
7.7

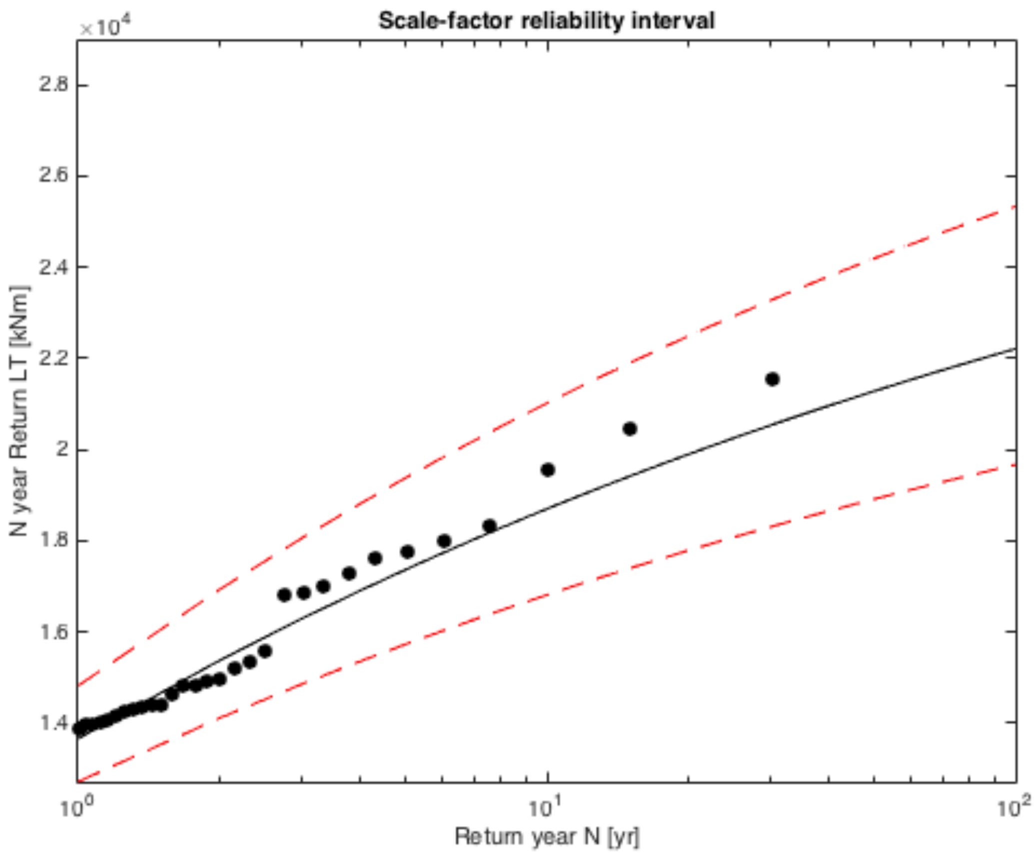

Scale-factor reliability interval
$\times 10^4$
N year Return LT [kNm]
2.8
2.6
2.4
2.2
2
1.8
1.6
1.4
10^0
10^1
10^2
Return year N [yr]

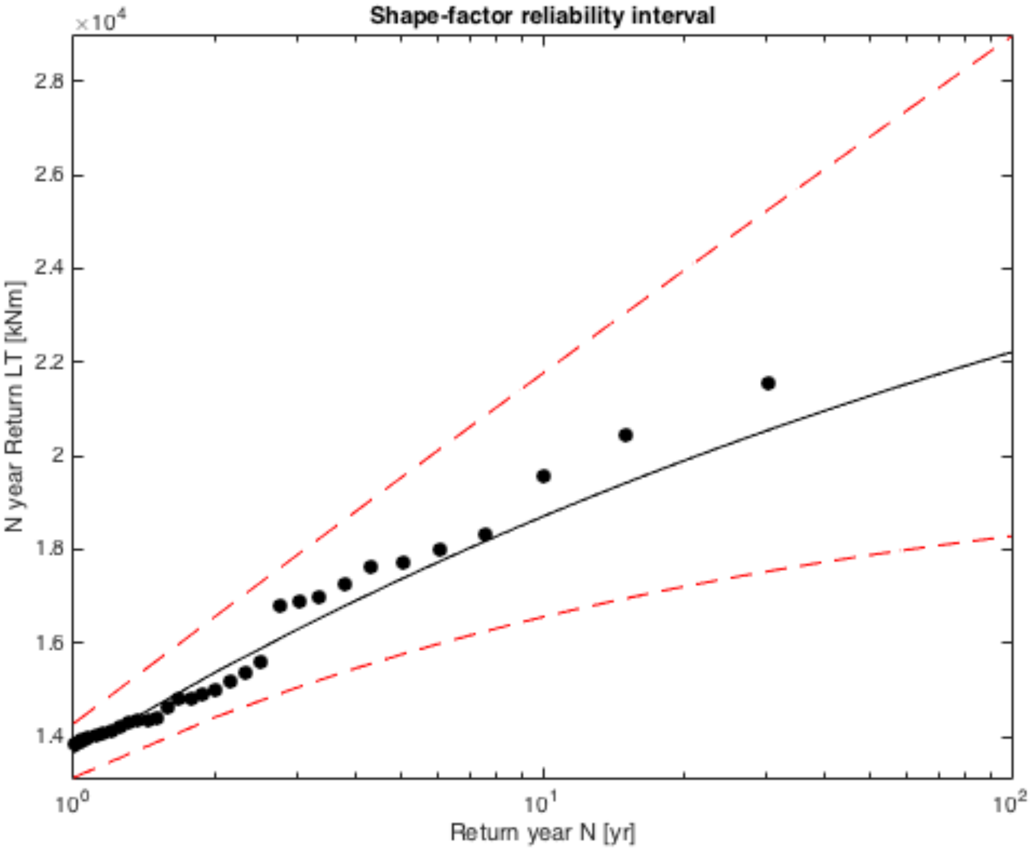

Shape-factor reliability interval
×10^4
2.8
2.6
2.4
2.2
2
1.8
1.6
1.4
N year Return LT [kNm]
10^0
10^1
10^2
Return year N [yr]

III.IX Results Quasi-dynamic analysis dataset II for vertical turret load (25seeds)

If the parameter stability plots of the analysis of the vertical turret load are observed, it can be seen that there only occurs some stability in the range between 1980 kN and 2100 kN. The reason for this behaviour is the small variation of the vertical turret load over the total wave spectrum... . These small variations make it difficult to fit a distribution on the data, but it is possible.

A threshold of 1980 kN is chosen to fit the empirical data to the distribution. This resulted in a 100-year vertical turret load of 2191.4 kN which is a realistic value.

The distribution passed all goodness-of-fit tests and showed approximately standard normal behaviour for the bootstrap estimates for the parameters. Some bi-modal behaviour can be seen in the bootstrap estimates. From this bi-modal behaviour it could be concluded that there is a second stable parameter estimate besides the initial stable point.

u [kN]	1980
σ [kN]	162.8101
ζ	-0.7616
N	100
n_y	2920
ζ_u	0.0012
100-year MAX LT	2191.4kN

Test	*Significance level*	*Null-Hypothesis*	*Outcome*	*Simulation method*
Chi-Square	5%	DATASET II follows GPD	Accepted	Quasi-dynamic
Kolmogorov-Smirnov	5%	DATASET II follows GPD	Accepted	Quasi-dynamic

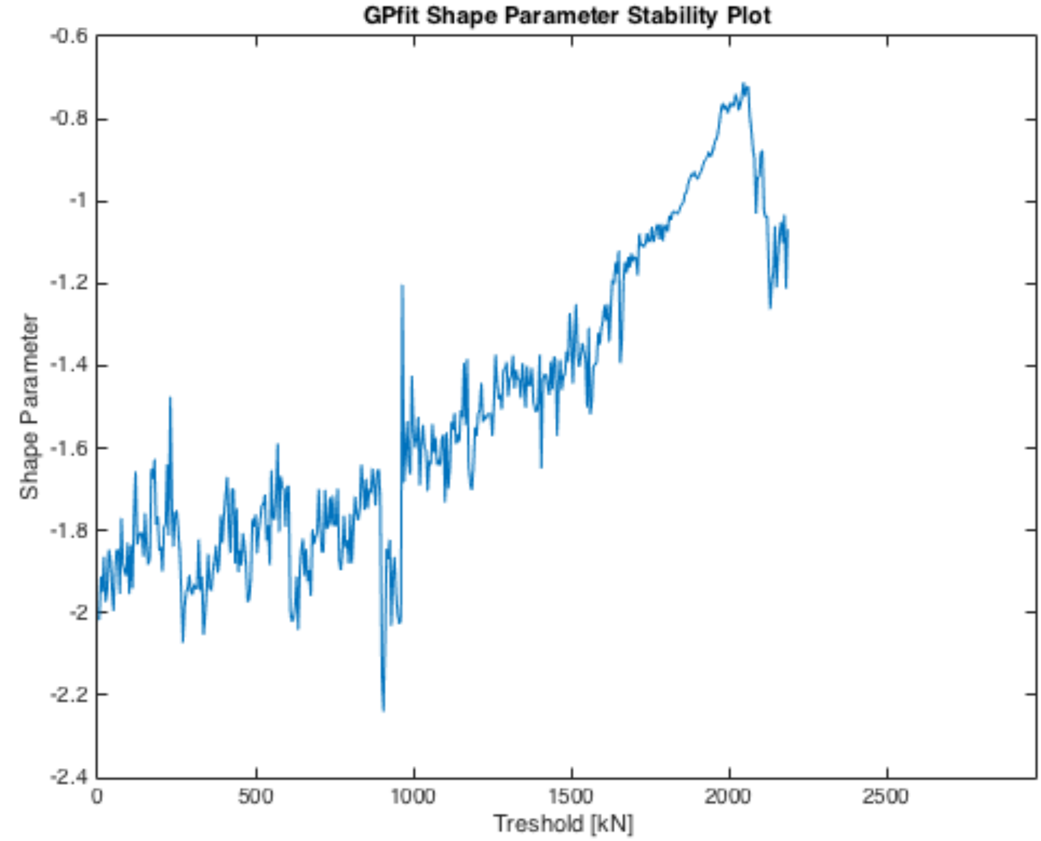
GPfit Shape Parameter Stability Plot
Shape Parameter
Treshold [kN]
-0.6
-0.8
-1
-1.2
-1.4
-1.6
-1.8
-2
-2.2
-2.4
0
500
1000
1500
2000
2500

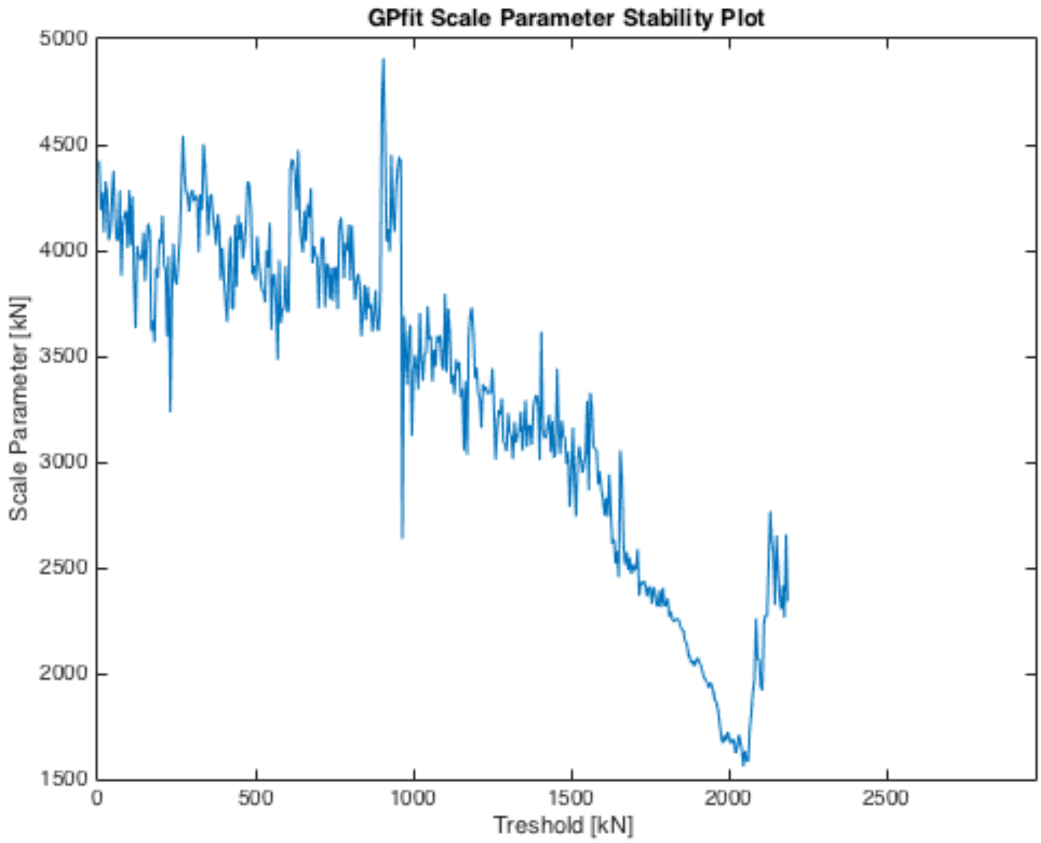
GPfit Scale Parameter Stability Plot
Scale Parameter [kN]
Treshold [kN]
5000
4500
4000
3500
3000
2500
2000
1500
0
500
1000
1500
2000
2500

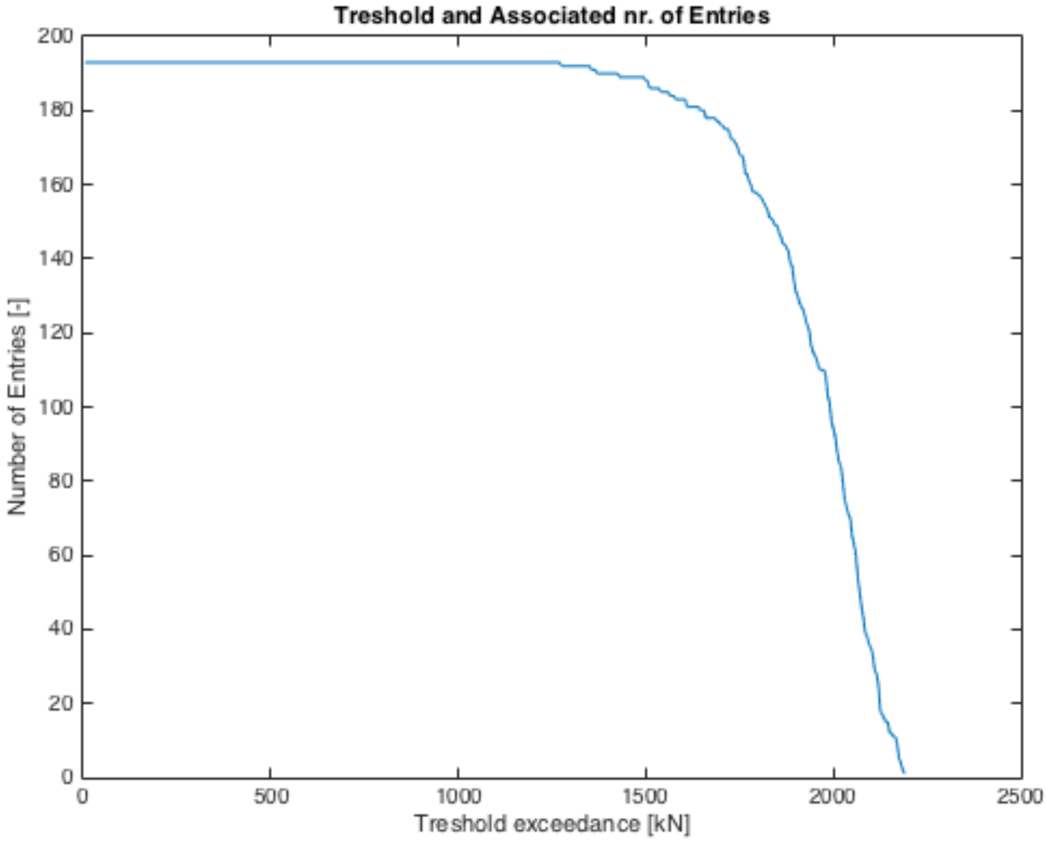
Treshold and Associated nr. of Entries
Number of Entries [-]
200
180
160
140
120
100
80
60
40
20
0
0
500
1000
1500
2000
2500
Treshold exceedance [kN]

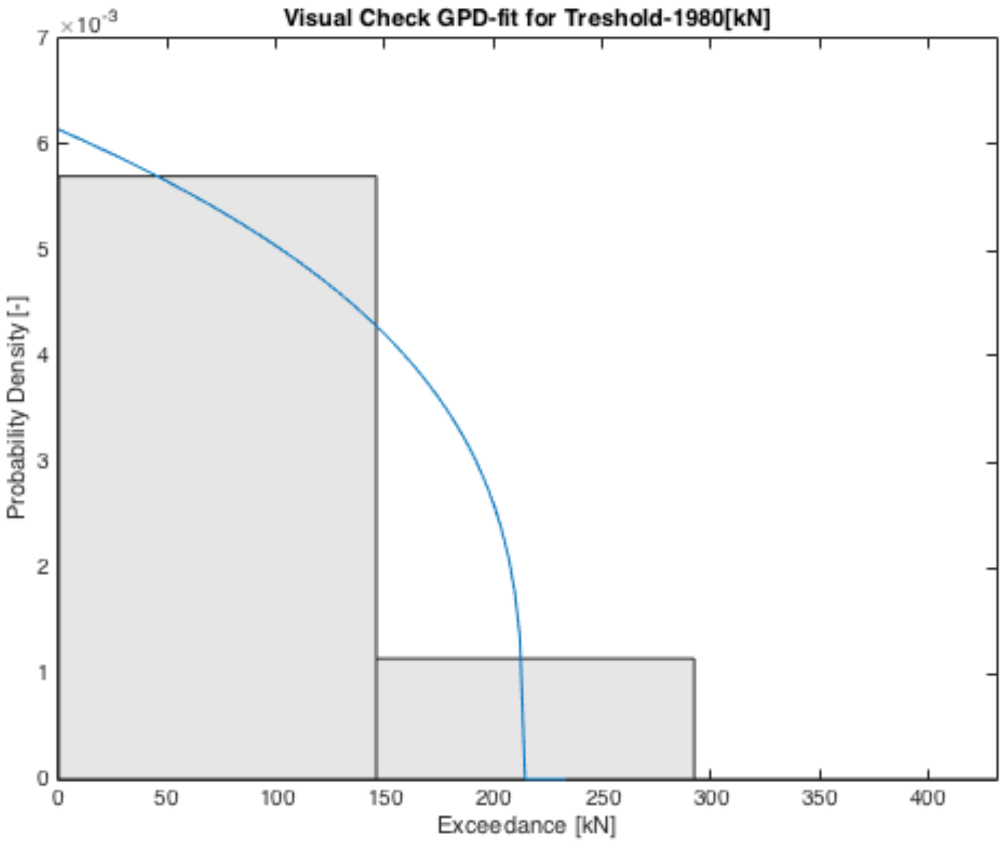
Visual Check GPD-fit for Treshold-1980[kN]
×10^-3
Probability Density [-]
7
6
5
4
3
2
1
0
0
50
100
150
200
250
300
350
400
Exceedance [kN]

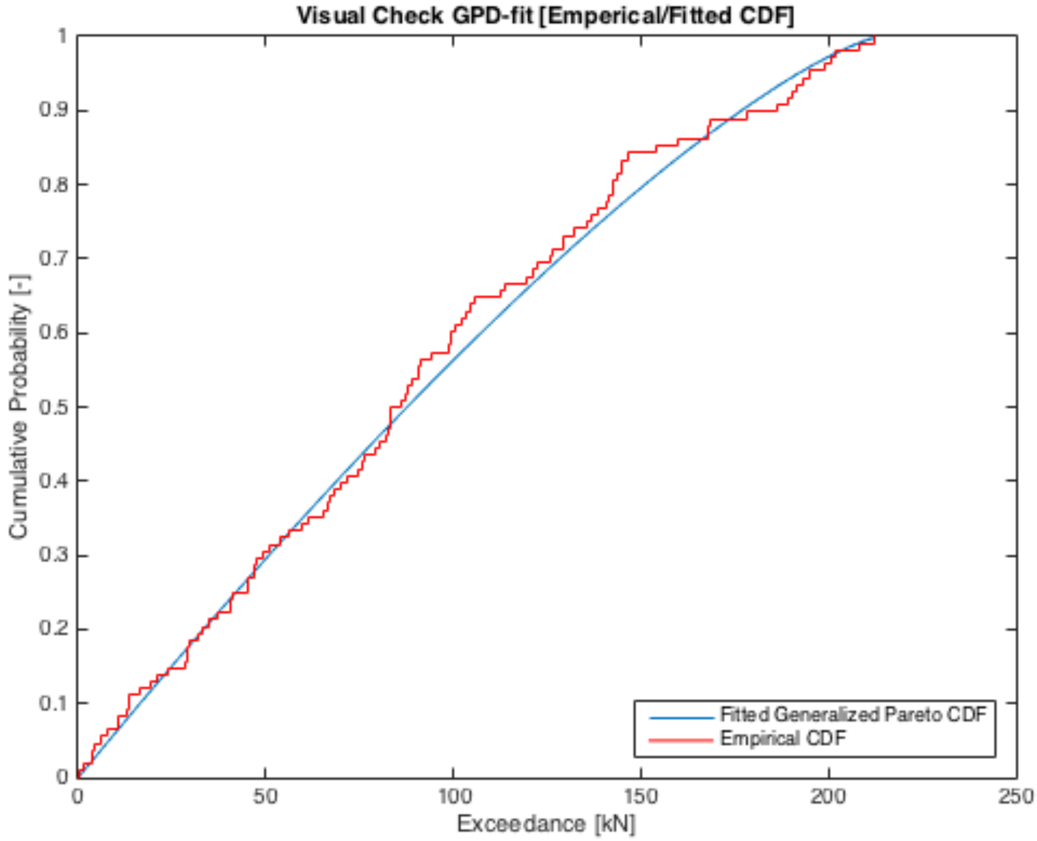
Visual Check GPD-fit [Emperical/Fitted CDF]
Cumulative Probability [-]
Exceedance [kN]
Fitted Generalized Pareto CDF
Empirical CDF
0
0.1
0.2
0.3
0.4
0.5
0.6
0.7
0.8
0.9
1
0
50
100
150
200
250

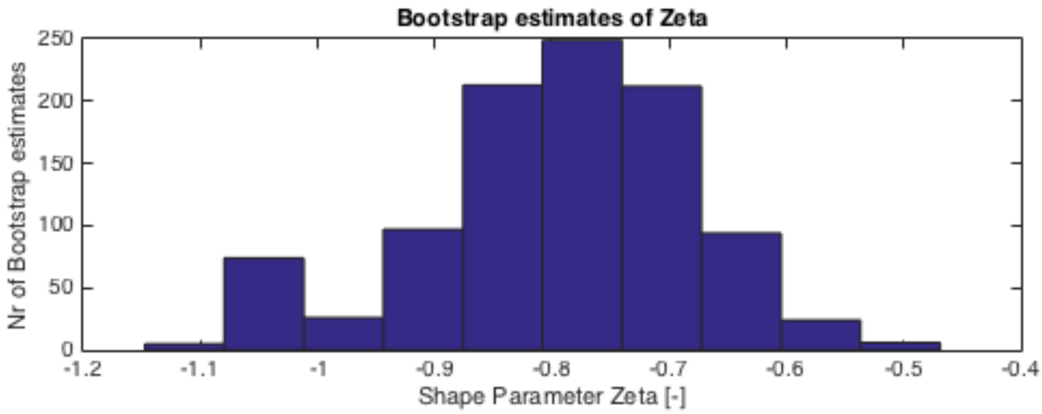
Bootstrap estimates of Zeta
Nr of Bootstrap estimates
Shape Parameter Zeta [-]
0
50
100
150
200
250
-1.2
-1.1
-1
-0.9
-0.8
-0.7
-0.6
-0.5
-0.4

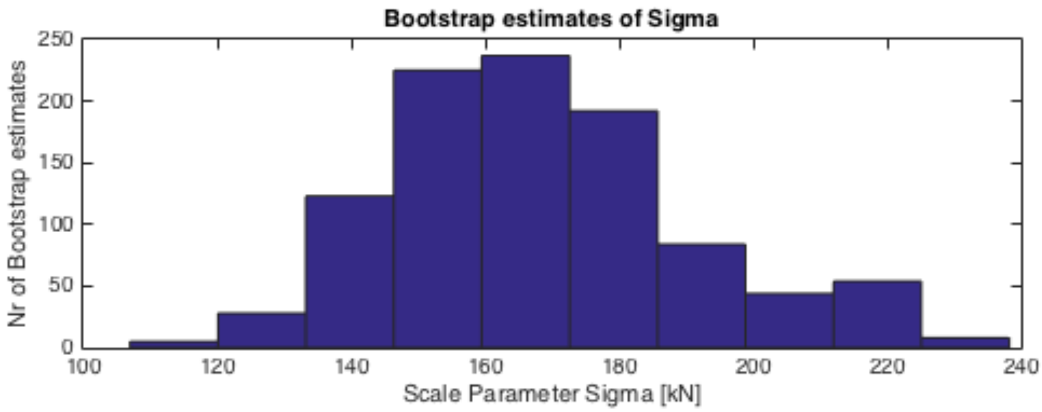
Bootstrap estimates of Sigma
Nr of Bootstrap estimates
Scale Parameter Sigma [kN]
0
50
100
150
200
250
100
120
140
160
180
200
220
240

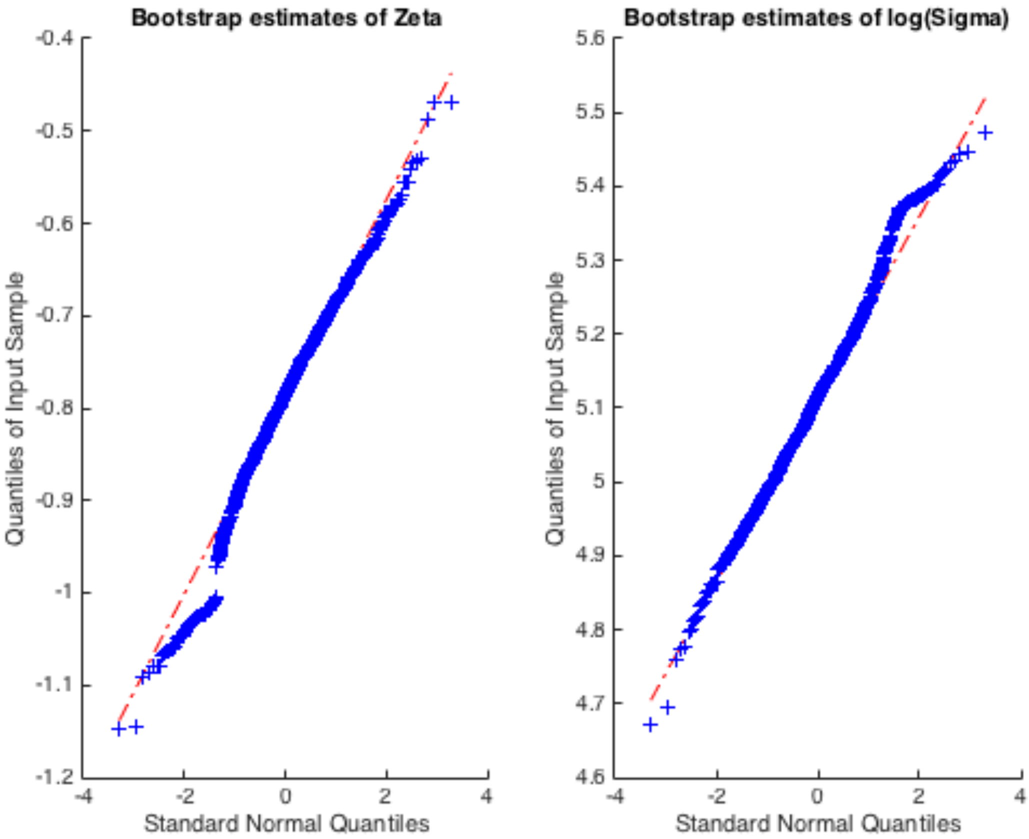
Bootstrap estimates of Zeta
Quantiles of Input Sample
Standard Normal Quantiles
Bootstrap estimates of log(Sigma)
Quantiles of Input Sample
Standard Normal Quantiles

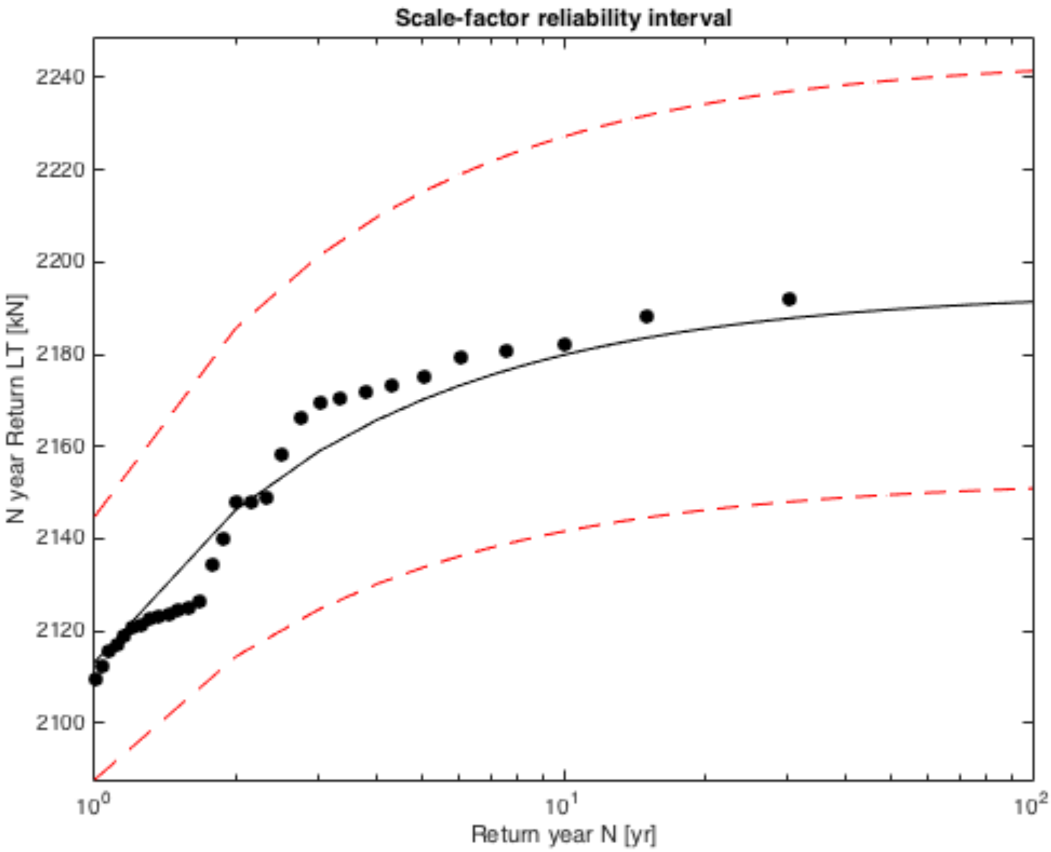
Scale-factor reliability interval
N year Return LT [kN]
Return year N [yr]

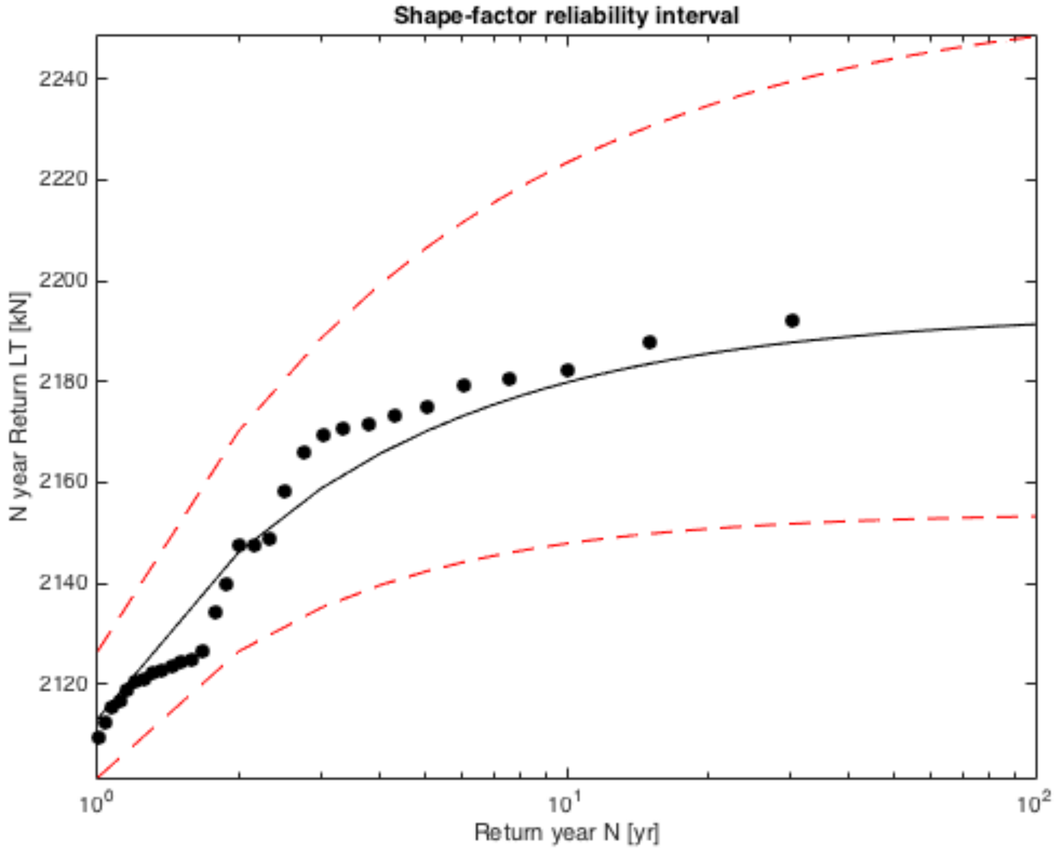

Shape-factor reliability interval
2240
2220
2200
2180
2160
2140
2120
N year Return LT [kN]
10^0
10^1
10^2
Return year N [yr]

Appendix IV Monthly maxima GEV fits

IV.I Monthly maximum wave height

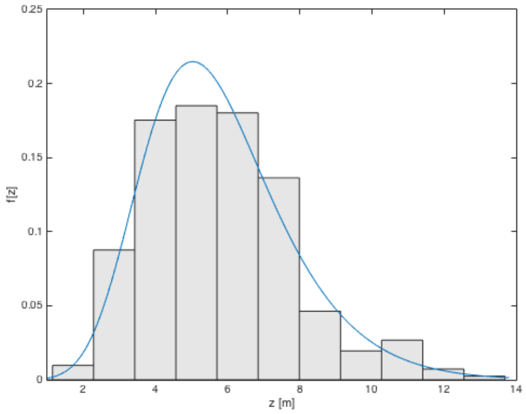

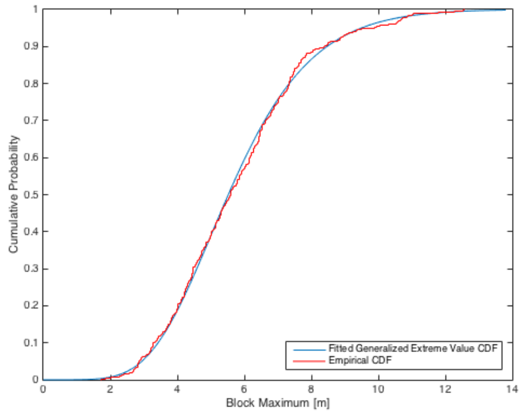

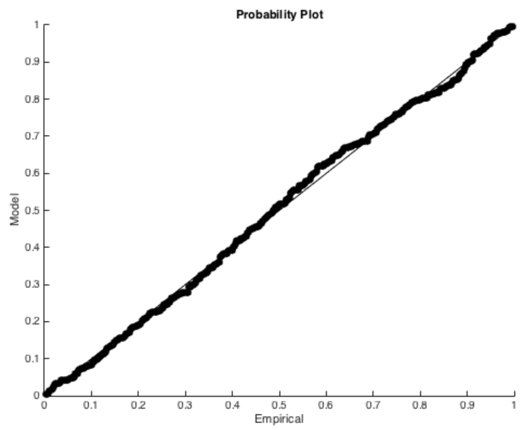

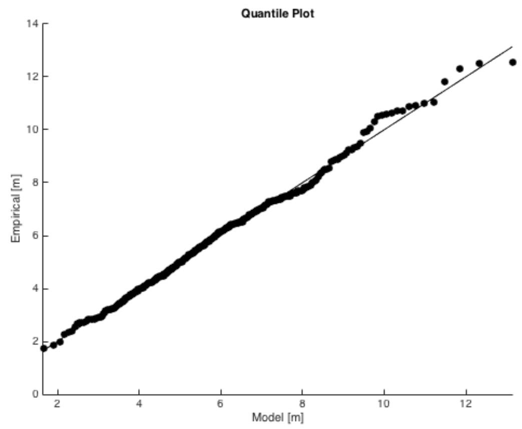

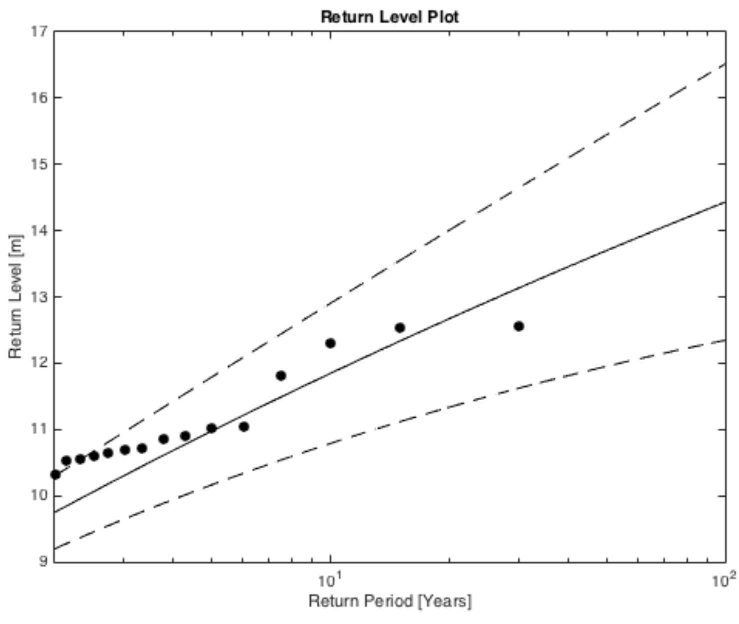

IV.II Absolute monthly maximum line tension

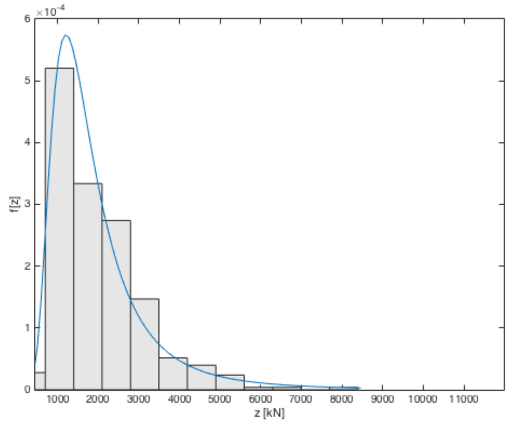

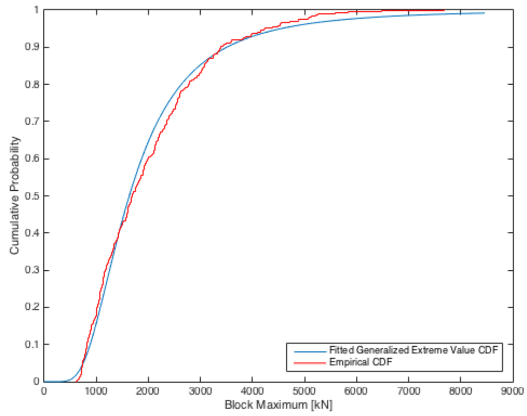

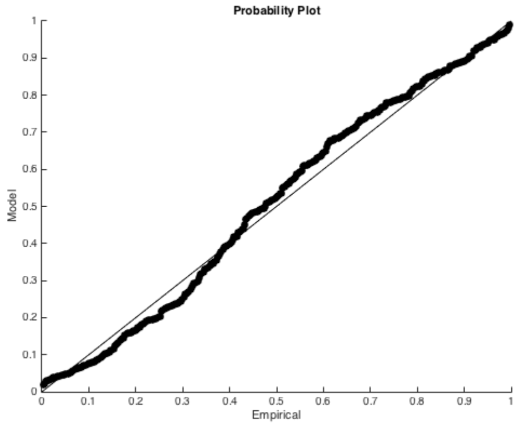

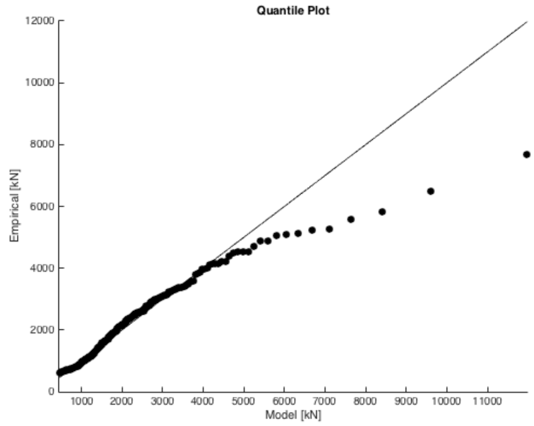

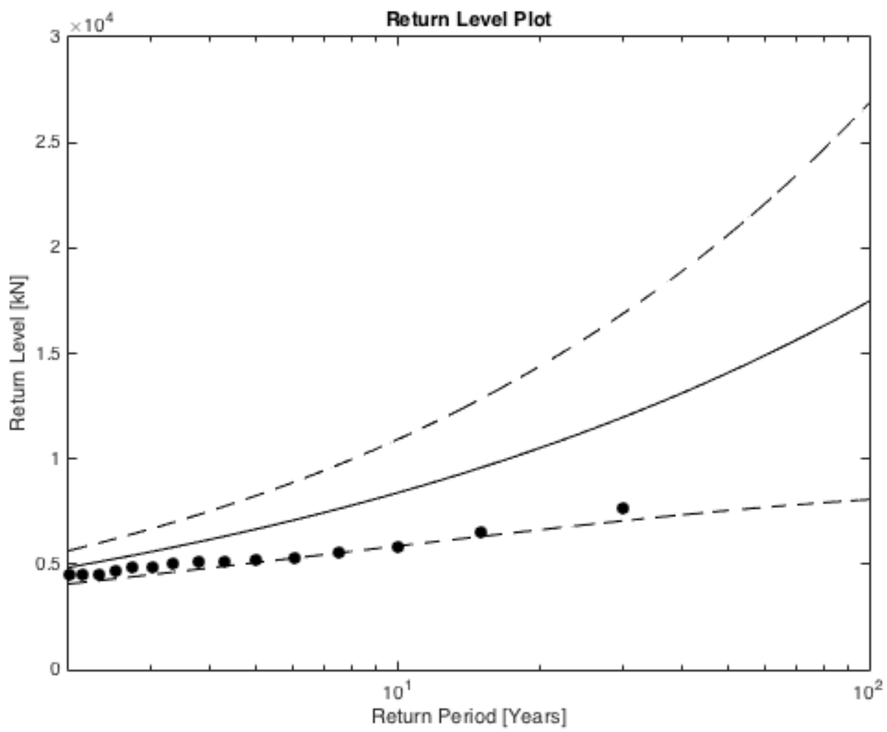

Appendix V Seasonal GEV distributions

V.I winter

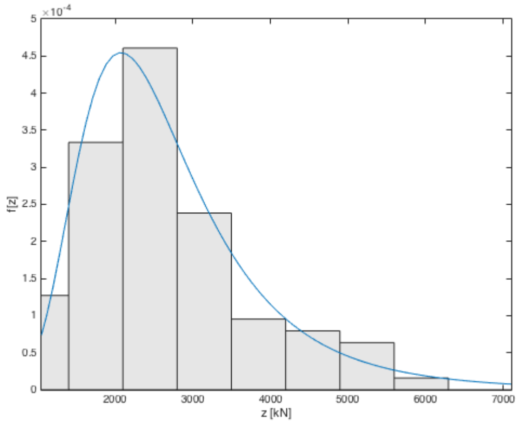

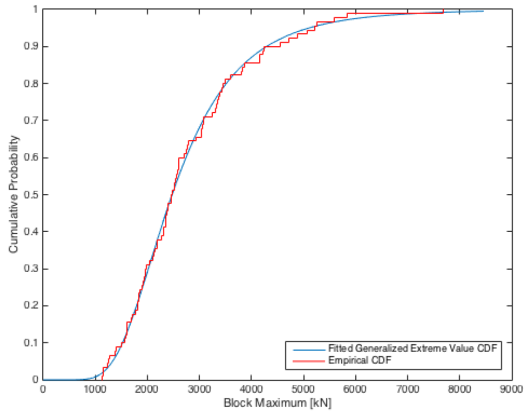

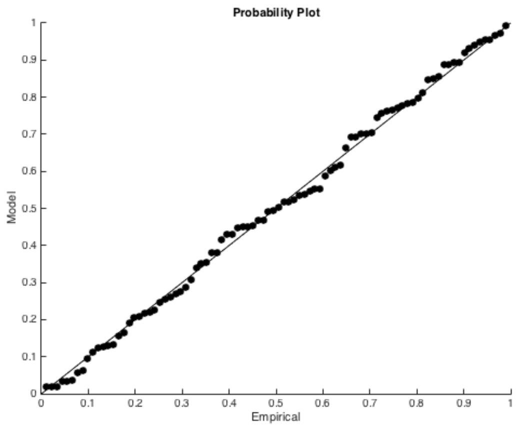

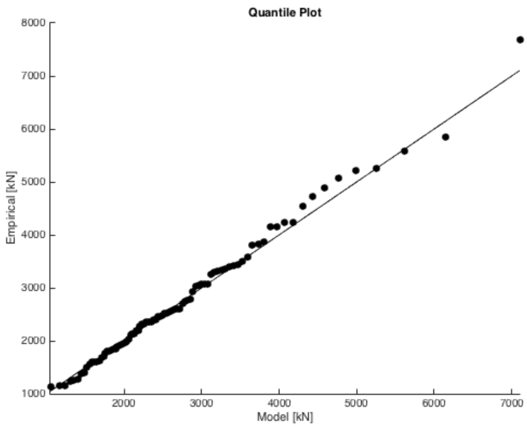

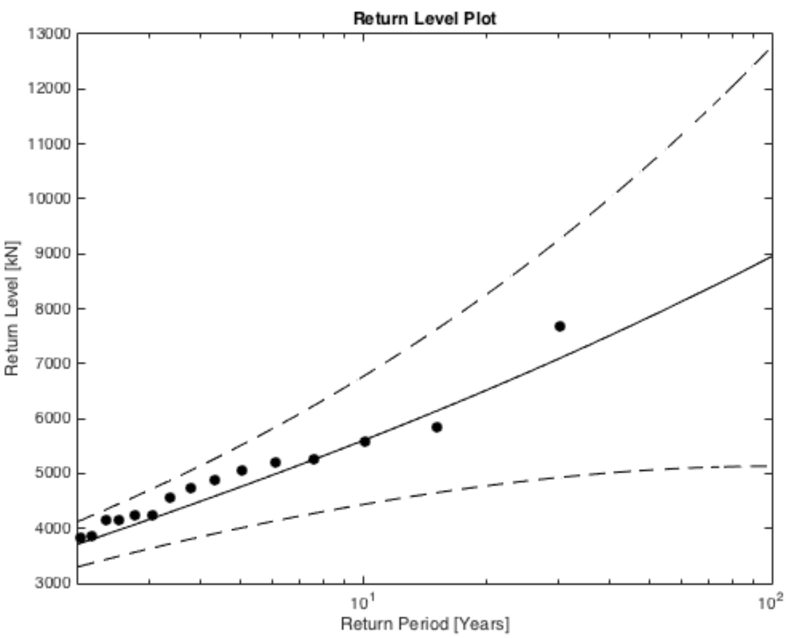

V.II spring

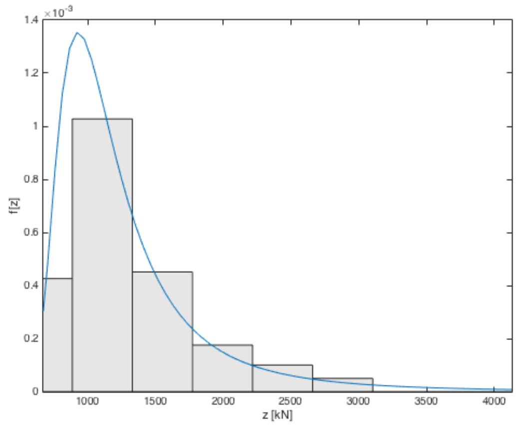
×10⁻³
f[z]
z [kN]

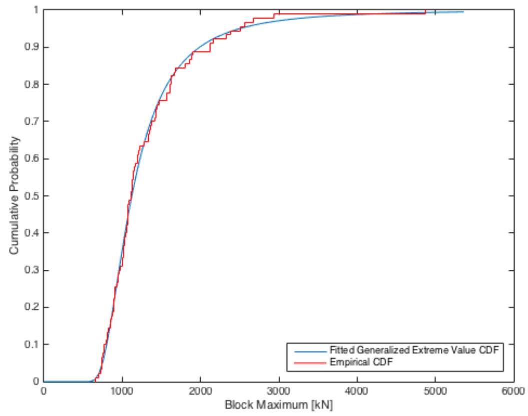
Cumulative Probability
Block Maximum [kN]
Fitted Generalized Extreme Value CDF
Empirical CDF

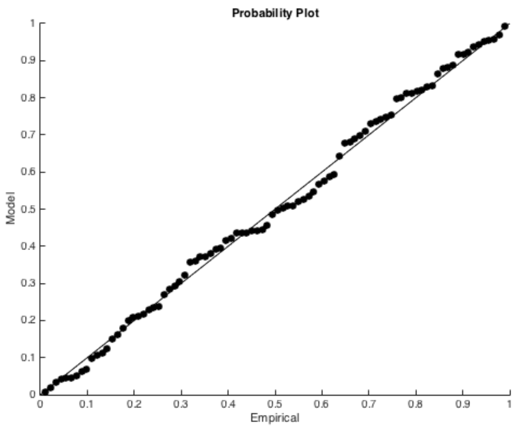
Probability Plot
Model
Empirical

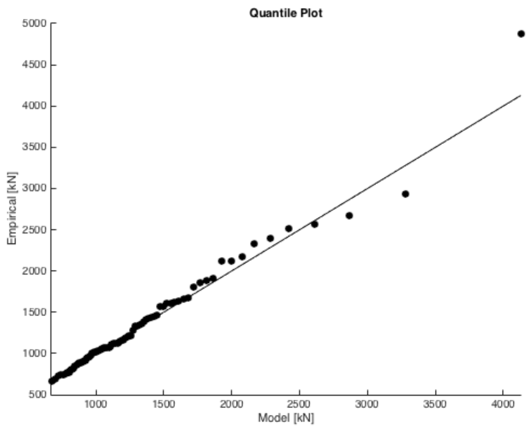
Quantile Plot
Empirical [kN]
Model [kN]

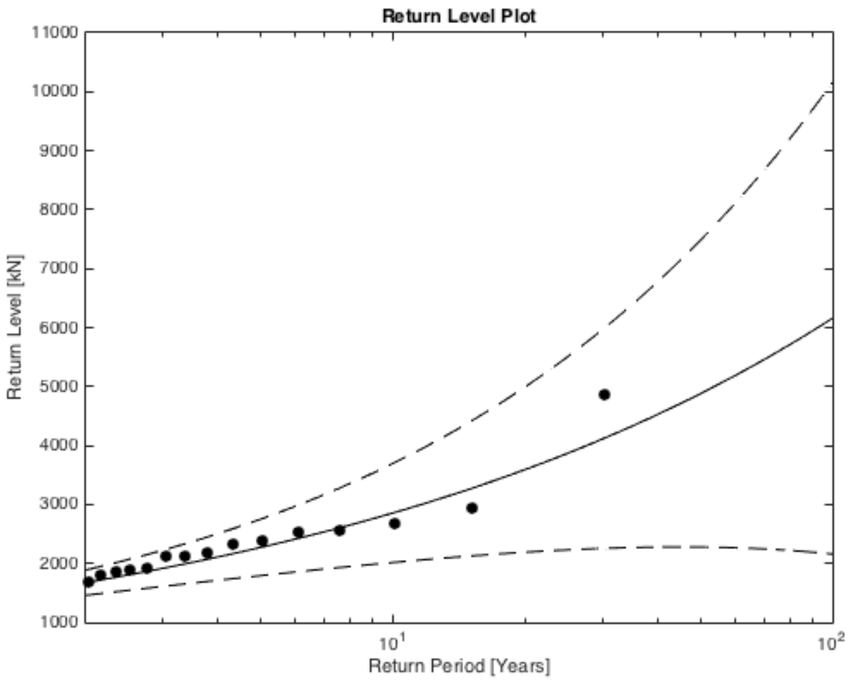
Return Level Plot
Return Level [kN]
Return Period [Years]

V.III summer

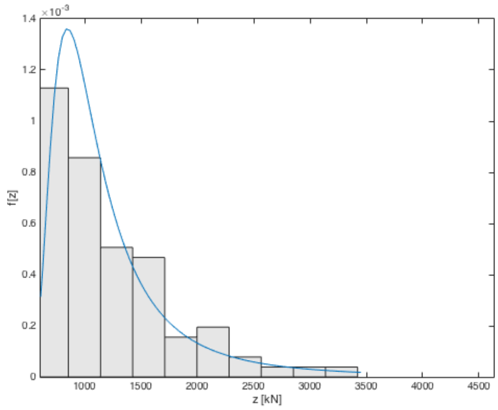

f[z]
z [kN]

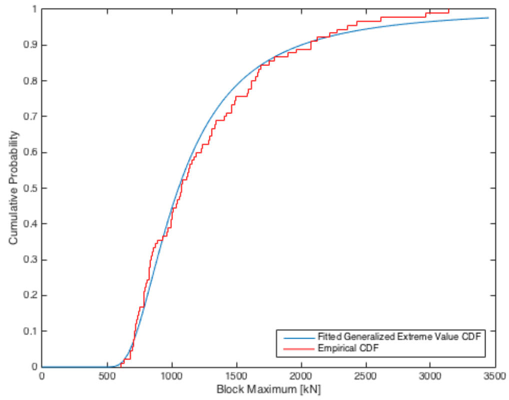

Cumulative Probability
Block Maximum [kN]
Fitted Generalized Extreme Value CDF
Empirical CDF

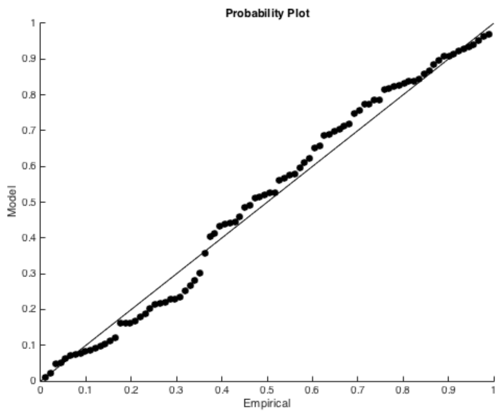

Probability Plot
Model
Empirical

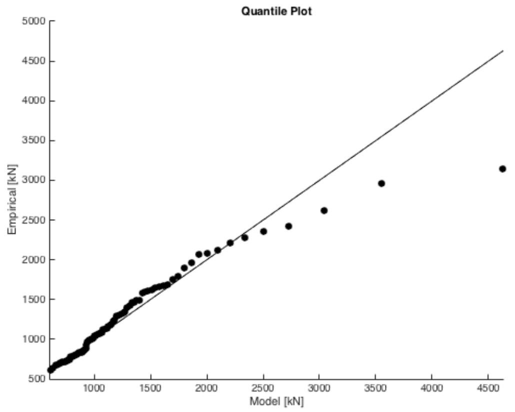

Quantile Plot
Empirical [kN]
Model [kN]

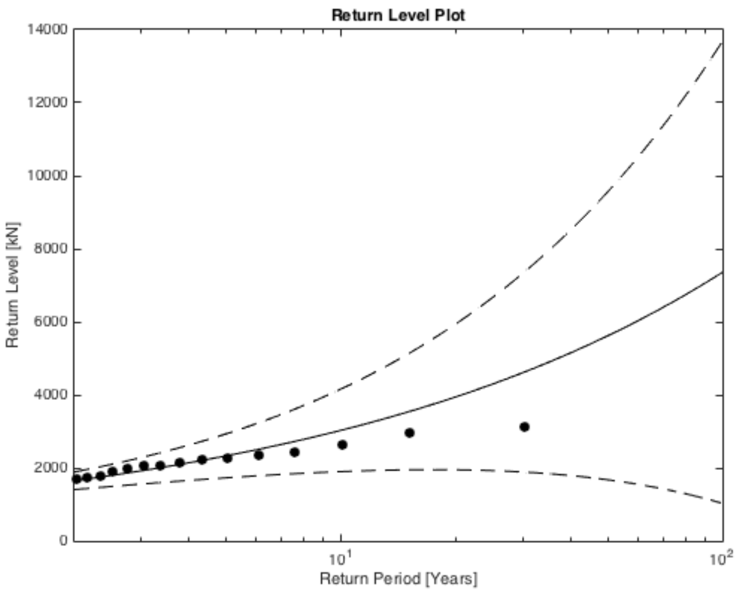

Return Level Plot
Return Level [kN]
Return Period [Years]

V.IV autumn

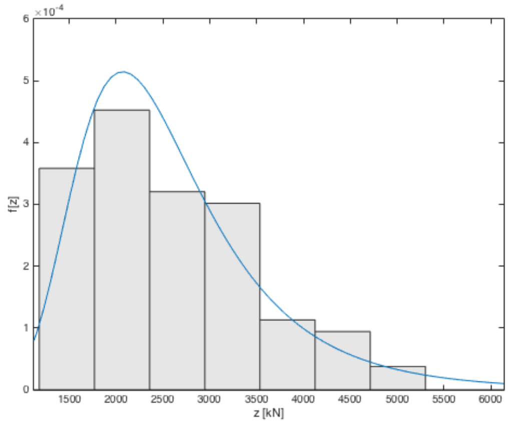

×10⁻⁴
f(z)
z [kN]

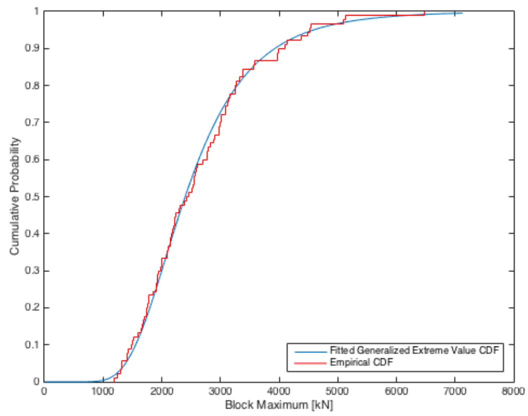

Cumulative Probability
Block Maximum [kN]
Fitted Generalized Extreme Value CDF
Empirical CDF

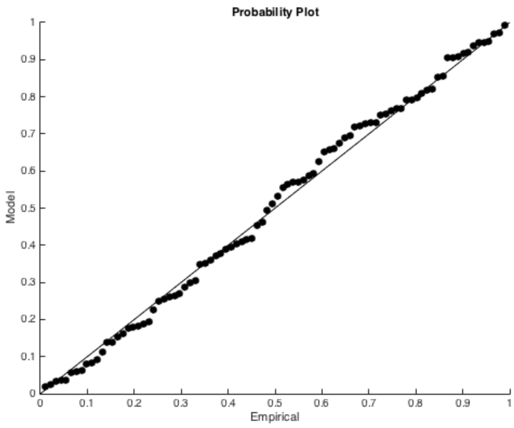

Probability Plot
Model
Empirical

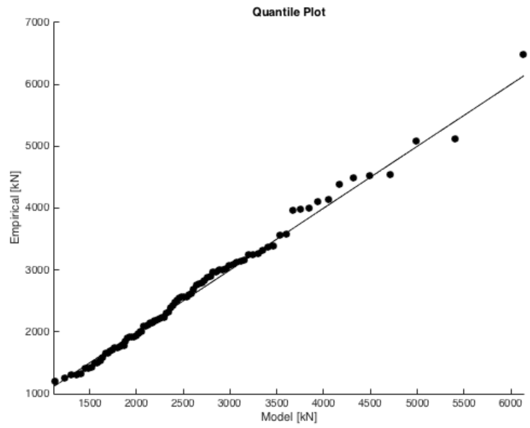

Quantile Plot
Empirical [kN]
Model [kN]

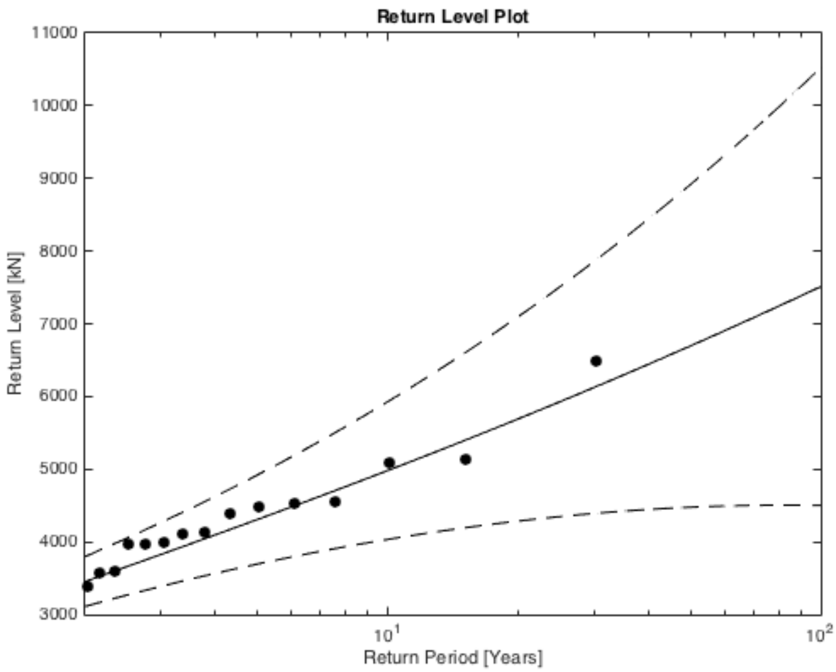

Return Level Plot
Return Level [kN]
Return Period [Years]